UNIVERSITÄT
BERN

Graduate School for Cellular and Biomedical Sciences

University of Bern

Bone Augmentation for Cancellous Bone Using Variable Injectable Composites as Biomimetic Agents

PhD Thesis submitted by

Karina Klein

from **Germany**

Thesis advisor

Prof. Dr. med. vet. Brigitte von Rechenberg, Dipl. ECVS
Musculoskeletal Research Unit
Vetsuisse Faculty of the University of Zurich

Accepted by the Faculty of Medicine, the Faculty of Science, and the Vetsuisse Faculty of the University of Bern at the request of the Graduate School for Cellular and Biomedical Sciences

Bern, Dean of the Faculty of Medicine

Bern, Dean of the Faculty of Science

Bern, Dean of the Vetsuisse Faculty Bern

Acknowledgements

Completing this PhD was truly a marathon event for me. I wouldn't have been able to complete this journey without the support of many people over the last years.

First of all, my deepest thanks go to my thesis advisor, Professor Brigitte von Rechenberg for giving me the chance to perform the studies and to complete the thesis, for her continuous support throughout these years, for giving me the opportunity to profit from her outstanding knowledge and this, not only in research, but also professionally and socially. She always believed in my capabilities, especially in times when I had given up and supported me to develop my scientific as well surgical skills.

My great gratitude goes to Professor Thomas Steffen, the co-referee of this PhD thesis for stimulating discussions, openness and support.

Furthermore, I would like to thank Professor Klaus Siebenrock and PD Dr. Richard Nyffeler, who were my mentors during Graduate School in Cellular and Biomedical Science at the University of Bern.

My gratitude goes to the anesthetists Dr. Peter Kronen, Dr. Michèle Sidler and Dr. Nathalie Fouché, who took care of the animals during surgery.

I also wholeheartedly thank Peter for his unwavering support, both professionally and personally, being the anchor and best friend, who is always there for support and help.

These studies would never have been possible without the help of all my colleagues at the MSRU including Dr. Sabine Koch, Dr. Katja Nuss, PD Dr. Stefan Stübinger, the histology personnel Käthi Kämpf, Kati Zlinski, Ladina Ettinger-Fergusson, Sabina Wunderlin and all the doctoral students over the last years, who tended and cared for the animals.

I express my deepest gratitude to the animals operated in this study, without whom we would never gain these insights into new and improved and often life-saving therapies and treatments.

I thank my industrial partner Kuros Biosurgery AG for financing the studies.

Our computer specialist and good friend, Rainer Egle, certainly deserves an award for never getting tired to help out with computer problems, to solve emergency crises and to help me with formatting the final version of this thesis.

Many thanks to Salim Darwiche, PhD for being this one friend - the advisor for all circumstances - helping me to dissolve every problem while supplying me with the best coffee ever – you are right Salim, no more jackets, only shoes.

I wholeheartedly thank PD Dr. Zsolt Kulçsar for providing me with insightful information concerning percutaneous vertebroplasty in humans.

My thanks also to Professor Michael Blauth and Dr. Simon Euler (University Hospital of Innsbruck) for providing me with helpful clinical information concerning currently used augmentation procedures in humans.

A warm thank you to all my friends in Zurich and abroad for the good times and their never-ending support.

Last but not least, a special thank you to my parents Elke and Winfried Klein as well as my sister Franziska and my brother Matthias for their support, patience and their love.

Abstract

With increasing life expectancy, the rising incidence for osteoporosis-induced fragility fractures such as vertebral compression fractures has become a major public health problem. Prophylactic local treatment has emerged as a new treatment strategy involving percutaneous injections of biodegradable and osteoconductive augmentation materials into bones at risk for osteoporotic fractures.

The work herein details the successful development of two *in vivo* animal models for augmentation of cancellous bone in sheep to evaluate the biocompatibility, osteoconductivity and degradation properties of new injectable composites.

Using fluoroscopy and a customized aiming device for each animal model, the biomaterials were successfully injected with high accuracy and repeatability within the inter-trabecular space of the intact femoral condyle and proximal tibia metaphysis (first animal model) or the cervical vertebral bodies (second animal model). The suitability of various biomaterial formulations was investigated using specialized evaluation procedures. In vivo florescent staining at 6 and 12 weeks as well as 16 weeks post surgery for the cervical augmentation model was performed to detect enhanced bone activity in the region of interest at each time point. After a 12-week follow up for the tibia and femur augmentation and a 16-week follow up for the cervical augmentation, the sheep were sacrificed and the injected bones harvested and evaluated. For evidence of new bone formation, radiographs were taken after sacrifice using a Faxitron. Micro-Computed Tomography measurements of the regions of interest were taken to qualitatively assess bone volume density and trabecular thickness. Qualitative and quantitative histological evaluations were performed to assess bone structure, bone remodeling, percentage of new bone formation and remaining material as well as cellular reactions to the material.

Both animal models revealed to be suitable for the evaluation of new biomaterials for prophylactic augmentation of cancellous bone in sheep. While the tibia and femur augmentation model showed to be particularly suitable for screening studies to evaluate new biomaterial formulations, the cervical augmentation model revealed to be more challenging due to a high rate of clinical relevant pulmonary emboli with subsequent cardiovascular alterations.

Therefore, this animal model could be chosen to particularly study the development of a pulmonary embolism and its consequences following augmentation of cancellous bone, as these complications also occur in humans.

1 Introduction

1.1 Overview of osteoporosis and bone augmentation

Bone augmentation of cancellous bone is a developing field in orthopedic surgery and represents a treatment option for various disease states in conjunction with loss of bone mass and stability.

Such loss of bone integrity may be observed in a range of clinical diseases caused by osteolytic tumors, osteoporosis and bone deformities. The affected patients can be grouped by etiology into: the high-energy trauma patient, the patients with tumors, the elderly, and the patients with osteoporosis. Depending on the underlying disease, different forms or applications of bone augmentation are clinically used. In acute trauma patients with structural bone loss such as the one found in joint depression fractures, bone augmentation is commonly performed using autologous bone graft.

Bone augmentation, as applied to the latter three patient groups, instead often uses injectable synthetic augmentation materials.

In the elderly patient, lack of physical activity as well as decreased cellular regeneration capacity may lead to a disturbance of the natural balance of bone resorption and remodeling. Hence, bone mass decreases, stability is reduced and fracture healing is delayed. Tumors may be benign (hemangioma) or include malignant lesions (metastatic cancers, myeloma). Loss of bone mass in tumor patients is the primary factor leading to instability, pathological fractures as well as bone cysts. Finally, osteoporosis patients represent the single largest patient group undergoing augmentation procedures using synthetic bone cements. Osteoporosis may be classified as primary osteoporosis, affecting juvenile, postmenopausal or senile patients. It may also be classified as secondary osteoporosis, being the result of another underlying disease (e.g., congenital, hypogonadal, endocrine, inflammatory, cancer), various deficiency states (e.g., calcium, magnesium, protein, Vit.D, malabsorption, gastrectomy), drug-induced alterations in bone metabolism (e.g., antipsychotic, antiretroviral, and anticonvulsant drugs) or an altered metabolism due to alcohol abuse. By far, the most common form of osteoporosis encountered today is primary osteoporosis in postmenopausal and senile patients; a patient group frequently burdened also with other diseases and comorbidities and

therefore must be seen as a high-risk patient group. Better treatment modalities through bone augmentation with biomimetic injectable composites are urgently required to enhance bone mineral density (BMD) and prophylactically stabilize bones at risk for fracture.

1.2 Fragility fractures and fracture fixation failures in osteoporotic bone

Fragility fractures are a major public health problem, particularly in the elderly population due to increased life expectancy, affecting up to 9 million people worldwide each year [1]. While in younger patients the main fracture etiology is high-energy trauma [2], in the geriatric population the largest proportion of fractures occurs after falls from a standing or sitting position and/or other low-energy trauma. This could be attributed to the aging skeleton and/or osteoporosis, where compromised bone regeneration capacity is increasing the fracture risk. [3-7].

Osteoporosis is a systemic skeletal disease, characterized by an overall loss of bone density [8] and a reduction in bone quality by microarchitectural deterioration such as reduction, thinning and disconnection of the trabeculae from each other and from the surrounding cortical bone (Figure 1.1). These alterations increase bone fragility and susceptibility to fractures. An imbalance of osteoblast and osteoclast activity shifts bone remodeling towards resorption. The metaphyseal regions with high amounts of cancellous bone - especially the proximal femur, distal radius, proximal humerus and vertebrae - are primarily affected and are particularly at risk for fractures [9].

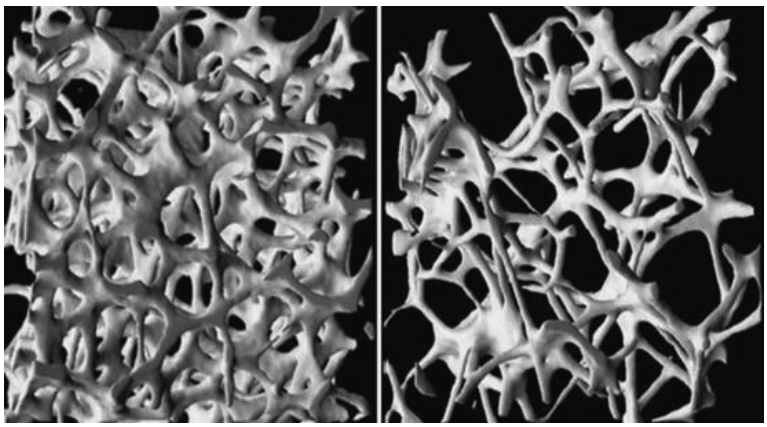

Figure 1.1: Micro-CT images of healthy (left) and osteoporotic (right) human trabecular bone. Reduction, thinning and disconnection of trabeculae characterize the osteoporotic bone.

As a consequence of the osteoporotic, weakened bone and the compromised bone regeneration at the cellular and molecular level, also fracture fixation failures occur more often in the elderly. Reduced stability of fixation screws leads to screw cut-out and implant migration, especially in hip [5,10], vertebral [11-13], and humerus fractures [14,15].

Additionally, comorbidities in geriatric patients contribute to the cause of fracture, but also provoke significant post interventional complications (e.g. delirium, infection, kidney failure) and high mortality rates [16-18]. For example, hip fractures, being one of the most common osteoporotic fractures, are caused by low-energy trauma in 90% of the cases and are associated with a first year mortality up to 30%, as well as very high disability and poor functional outcome [17,19,20].

Therefore, the surgical and overall management of multimorbid geriatric patients suffering from fragility fractures is highly demanding. Co-management by geriatricians and orthopedic surgeons, combined with standardized care, reduced waiting time for surgery, reduced surgery time and technical innovations will lead to improved overall outcomes. New implants featuring conduits to add cement for supplemental fixation for *standardized* cement augmentation [16,17] represent a new class of instruments used to treat fragility fractures.

1.3 Indications for augmentation of cancellous bone

Cancellous bone augmentation is commonly used to mechanically enhance bone structure and/or implant fixation in weakened and osteolytic bone with low BMD. It is proven effective in stabilizing deteriorated or fractured bone for filling bone voids and enhancing anchorage for implants at risk for loosening. Different augmentation techniques and materials (e.g., autograft, allograft, polymethyl-metacrylate (PMMA) bone cement, tricalciumphosphate, hydroxyapatite) are used at various anatomical locations for therapeutic or prophylactic indications, or a combination of both.

1.3.1 Therapeutic indications for cancellous bone augmentation

1.3.1.1 Implant augmentation

Reduced bone mass due to osteoporosis or cancer induced osteolysis leads to implant failures, affecting mainly metaphyseal regions, the head-neck fragment of the hip and the vertebral bodies. Changes in the cancellous bone due to osteoporosis (see chapter 1.2) lead to a smaller bone-implant contact area and, subsequently, to a decrease of holding power for implants. In order to alleviate these problems, implant augmentation with PMMA bone cement can be performed. This expands the bone-implant interface and provides enhanced implant anchorage with higher stability [17,21]. Especially in cases of revision surgery after previous implant failure, implant augmentation has shown good results with enhanced implant anchorage and reduced risk for refracture or other complications [22].

The indication for implant augmentation is based on multiple relevant criteria: preoperative radiographic findings, the age of the patient (e.g., guiding principle that all hip fractures in patients older than 80 years should be augmented) and intraoperative subjective assessment of bone softness. The ad-hoc intraoperative use of a newly developed densitometer (DensiProbe®) to measure the peak breakaway torque of trabecular bone may provide the surgeon with biomechanical information on local bone strength [23-25]. Despite supportive evidence however, DensiProbe® has not achieved yet a clinical breakthrough.

Different *ex-vivo* studies have demonstrated superior biomechanics (higher failure loads, higher number of load cycles to failure) following implant augmentation using PMMA cements for osteoporotic regions at risk for implant loosening. In these studies, in situ augmented cannulated implants were used for vertebrae [26,27], proximal humerus [28], and proximal femur [29,30].

In a biomechanical study of Sermon *et al.* using human cadaveric femoral heads, the implants sustained on average 51% more load cycles following cement augmentation [30]. No correlation was found between BMD and the number of load cycles to failure when using augmented implants. These results support the hypothesis that augmentation reduces the adverse effects of low bone quality and hence reduces the negative impact of osteoporosis on implant anchorage. However, with increasing bone

quality, a reduced augmentation effect was observed, suggesting that PMMA augmentation is primarily useful in weakened osteoporotic bone. This was illustrated by an inversely related impact of cement augmentation with respect to the BMD [28,30]. Therefore, augmentation with PMMA-cement should only be performed after thorough risk-benefit-analysis in weakened bone with low BMD values.

Implant augmentation is categorized in *standardized* and *non-standardized* techniques. For *standardized* augmentation, implants featuring conduits to add cement for supplemental fixation have been specifically developed. The standardization often includes the development of guiding instruments for reproducible implantation and subsequent augmentation.

Standardized implants are available for treatment of hip fractures [22,29-32], proximal humerus fractures [33] and for spinal instrumentations [13,34-36]. Three examples are listed here:

1. Proximal Femur Nail Antirotation™ Augmentation (PFNA™ Augmentation, DePuy Synthes Companies Trama, Zuchwil, Switzerland): This intramedullary nail with a helical blade (including augmentation option) was designed for better rotational stability and resistance to cut-out within the femoral head [37]. The injected cement surrounding the tip of the helical blade results in a greater load-bearing surface with improved initial stability and the possibility of immediate full weight-bearing [32]. The improved anchorage is most effective in osteoporotic bone and could prevent further clinical interventions within the geriatric patient group. A maximum cement volume of 3 mL should be used for augmentation.

Figure 1.2: Schematic illustration of an implanted augmented PFNA™. The injected cement surrounds the tip of the helical plate in a cloud-like shape. (http://www.synthes.com/MediaBin/International%20DATA/036.001.143.pdf)

2. Proximal Humeral Internal Locking System (PHILOS AUGMENTATION, DePuy Synthes Trauma): It was developed for internal fixation of proximal humerus fractures using locking screws with perforations at their tip for screw augmentation in combination with a locking compression plate. Biomechanical studies have shown enhanced anchorage in low-density bone after augmentation of the fixation screws placed in the head [28,38]. Every screw is augmented with maximally 0.5 mL of cement with a maximum of 3 mL cement for all augmented screws.

Figure 1.3: Schematic fluoroscopy image of a PHILOS locking plate in combination with two augmented perforated locking screws.

(http://www.synthes.com/sites/intl/IntlContent/Files/016.001.576.pdf)

3. MATRIX spine system (DePuy Synthes Spine): Posterior pedicle screw and hook fixation system for precise and segmental stabilization of the spine. Perforated pedicle screws for augmentation feature six radial openings for 360° cement distribution (in a cloud like shape) applied only after final screw positioning. Each screw is augmented approximately 2-3 mL of cement.

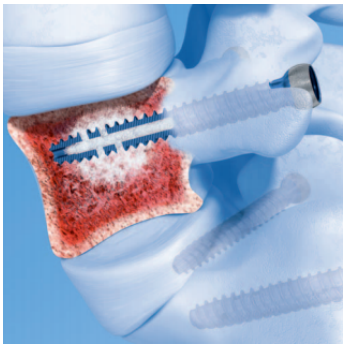

Figure 1.4: Schematic illustration of a bisected vertebra and perforated pedicle screw showing the cloud like distribution of the bone cement.

(http://www.synthes.com/MediaBin/International%20DATA/036.001.197.pdf)

If *standardized* implants and guiding instruments are not available for a specific anatomical site and/or type of fracture, *non standardized* augmentation techniques are used. Especially for tumor surgeries, involving osteolytic bone, *non standardized* implant augmentation and void filling techniques are performed. Implantation and augmentation steps are then switched such that after drilling and thread cutting, the bone is first augmented and then only conventional non canulated/perforated screws are implanted in the cement prefilled site. Such procedures could also be performed for intramedullary nails and other *non-standardized* implants.

1.3.1.2 Void filling

Currently, void filling is used in spine and trauma surgery.

In *trauma surgery*, bone voids are frequently seen as a result of an acute metaphyseal and joint depression fracture with impaction of the underlying cancellous bone, or as the result of an acute dislocation and depression of the articular surface (e.g., proximal tibia, distal femur, calcaneus). Whether acutely traumatic or surgically created after fracture reduction and fixation, bone voids need to be filled to prevent long-term complications such as posttraumatic arthritis, pain and limited range of motion due to joint surface depression [39]. The gold standard for this type of fractures remains autologous bone graft (cancellous or corticocancellous) because of its combined osteoinductive, osteoconductive and osteogenic properties [40]. It can be used to replace regions of bone loss caused by comminution or crushing, thus enhancing fracture construct stability.

The iliac crest is the most common donor site for autografts. However, in elderly osteoporotic patients, the quantity and quality of bone available from the iliac crest is often inferior. This usually requires a larger exposure, leading to an increased risk at the donor site and other morbidities, such as chronic pain and wound dehiscence [41,42]. Allograft bone and synthetic bone void fillers could be used as alternative graft materials for fracture void filling. Bone allografts avoid donor site morbidity, but still provide most of the beneficial properties. However, it can lead to other serious complications, including histoincompatibility, disease transmission and more frequently non-unions. To avoid the above complications, synthetic bone void fillers

(e.g., calcium phosphate cements) have lately used. Ideally, these synthetic fillers should contain bioactive and biocompatible components and offer compressive strength to achieve immediate load bearing, thus decreasing the risk of secondary fracture dislocation causing long-term complications. Rapidly degrading synthetic bone filler is likely to induce rapid new bone formation at the resorption site.

Calcium phosphate based bone cements have already been used successfully for bone void filling following tibial plateau [43-45] and calcaneus [46,47] fracture reduction and internal fixation. For both fracture types, bone void filling following surgical reduction allows early load bearing, without radiological evidence of loss of reduction.

In *spine surgery*, percutaneous vertebroplasty (PVP) and balloon kyphoplasty (BKP) are both popular minimally invasive augmentation procedures for the treatment of painful vertebral compression fractures caused by osteoporosis, benign (hemangioma) or malignant lesions (metastatic cancer, myeloma) [48-55]. These minimally invasive techniques can provide immediate pain relief and in case of BKP also reduce kyphotic deformity and realign the spine. Both techniques are particularly indicated in patients, where internal fixation techniques (like instrumented long posterior or posterolateral spinal fusion) is contraindicated due to bone fragility.

The PVP technique was introduced in 1984 by Galibert and Deramond [56] and is a fluoroscopy-guided procedure, involving percutaneous injection of PMMA bone cement into a fractured vertebral body. Using PVP to stabilize the fracture, pain relief is achieved by fracture stabilization and decompression in 80% - 90% of the patients [57]. However, existing kyphotic deformity or reduced vertebral body height cannot be restored. Cement distribution from endplate to endplate is important to achieve pain relief. An angulated unipedicular approach is sufficient as long as the cement crosses the vertebras midline [58]. The unipedicular approach leads to a reduced surgery time and decreased risk for venous or epidural cement extravasation [59]. The entire injection procedure, however, has to be performed under high quality fluoroscopy to monitor the expanding cement cloud. If extravasation occurs, the injection has to be stopped immediately and the needle repositioned to prevent pulmonary cement embolism or cement leakage into the spinal canal.

Depending on the clinical situation (vertebra size, fracture type, progression of osteoporosis) an average of 3-6 mL bone cement is commonly injected per lumbar vertebra. For multiple level augmentations a maximum of 25 mL (less in patients with severe compromised heart and lung function) and six augmented vertebrae per session are advocated to avoid possible fat and cement embolism [60]. Both, the use of high viscosity cement and limiting the injected cement volume to the minimum required reduce the risk of cement extravasation and leakage [61,62]. The minimum required amount of cement is somewhat subjective and dependent on a surgeon's experience.

In 1998, balloon kyphoplasty (BKP) was introduced, adding an additional step prior to cement injection, rendering BKP a slightly more invasive procedure than PVP. The surgical procedure takes much longer and thus has to be performed always under general anesthesia. An inflatable balloon tamp is placed in the fractured vertebral body creating a cavity within the vertebral body [50,63]. Guided over bipedicular cannulas, two ballons are inserted using fluoroscopy, then inflated to a maximum pressure monitored with a digital manometer. A cavity is created and the fractured vertebra's height is restored. Subsequently, the balloons are deflated and removed. Low cement pressure is used to fill the cavities [64] with 2-6 mL of high viscosity cement per side.

Using bilateral balloons, correction of a kyphotic deformity (defined as a segmental kyphosis of > 6°) is achieved with 70% restoration of the vertebras original height [18,50,65-67]. Treatment of acute vertebral compression fractures with associated kyphotic deformity using BKP may relief pain in 90% of the patients [50], stabilizes the fracture, restores vertebral body height and avoids pulmonary and gastrointestinal complications usually associated with severe kyphosis.

1.3.2 Prophylactic indications for cancellous bone augmentation

Prophylactic augmentation is typically a minimally invasive mechanical augmentation procedure to stabilize weakened, osteoporotic or osteolytic bone at risk for fracture. If possible the procedure is performed percutaneously via injection of an adequate augmentation material into the intertrabecular space. To date, prophylactic augmentation is only used in two anatomical locations: spine and hip.

In spine surgery, prophylactic percutaneous vertebroplasty of unaffected vertebral bodies adjacent to fractured and already augmented vertebra is thought to prevent additional fractures [68,69] and thereby avoiding deterioration of the patient's quality of life due to chronic pain [70] and kyphosis progression. Prophylactic augmentation may be performed in combination with implant augmentation (pedicle screw augmentation), or in combination with multi-segmental posterior spinal instrumentation, this to prevent fractures at the upper most vertebra included in the construct and the adjacent un-instrumented vertebra. Combined treatment may decrease the risk of adjacent segment disease next to a rigid fixation, especially in patients that already have an established osteoporosis [71].

In some hospitals, prophylactic augmentation of the contralateral hip is performed concurrently with fixation of prosthetic replacement of a primary hip fracture. (Personal communication with Prof. M. Blauth; University hospital Innsbruck). This prophylactic procedure reduces the risk of a contralateral primary hip fracture, which otherwise is about 10% in the first five years following the initial fracture.

Currently, prophylactic augmentation is performed using exclusively non-resorbable PMMA bone cement.

1.4 Injectable augmentation materials

An adequate injectable augmentation material should feature the following properties: High radiopacity for visibility during injection, low curing temperature, no cytotoxicity and adequate mechanical properties (tensile strength, bending modulus, compressive strength). Additionally, the cured material should have microporosity (mean pore diameter <10 γm; to allow circulation of body fluid) as well as macroporosity (mean pore diameter >100 γm; to provide a scaffold for blood-cell colonization). The latter are mandatory features for sufficient bone ingrowth, for osteoinductivity, osteoconductivity, and bioactivity [72].

Injectable bone cements used for augmentation are classified based on their chemistry as acrylic bone cements, as ceramic bone cements (calcium phosphate and calcium sulfate based), and as filamentary composite materials [73].

To date, only acrylic bone cements and acrylic based composites offer the required mechanical strength for high load-bearing applications (e.g., implant augmentation, anchoring of total joint replacements). Calcium phosphate and calcium sulfate based cements are typically used as bone void fillers or bone graft substitutes in low load-bearing applications. In medium load-bearing applications (e.g., PVP, BKP) mainly acrylic cements are used, but rarely also calcium phosphate based bone cements.

1.4.1 Acrylic bone cements and their composites

Currently, the most widely used injectable acrylic bone cement is polymethylmethacrylate (PMMA). It has been used in orthopedics since the 1940s for open joint replacements [74]. The first commercially available PMMA cement was introduced in 1966 and specifically designed for joint replacements. Much later it was used as injectable material to augment and stabilize osteoporotic bone. For decades PMMA was the only available injectable polymer usually combined with a contrast agent (e.g., barium sulfate, zirconium oxide) to allow for radiographic cement visualization during injection.

PMMA is composed of a prepolymerized powder and a liquid monomer, initiating an exothermic polymerization reaction when combined. The curing process is divided into four phases: mixing, adhering, working, and hardening. Commercially available PMMA cements can be categorized as low or high viscosity cements depending on which phase predominates during the curing process. Low viscosity cements typically have a longer sticky phase and a shorter working phase, high viscosity cements behave opposite. The mechanical properties of PMMA are between that of cancellous and cortical bone, having a high compressive strength [74], a 4 - 40 times higher bending (Young's) modulus than cancellous bone [75,76] and a relatively low tensile strength [77] (Table 1.1).

	PMMA	Cancellous Bone	Cortical Bone
Compressive strength (MPa)	85 - 110		133 - 193
Bending (Young's) modulus (GPa)	2 - 3	0.05 – 0.8	10 - 20
Tensile strength (MPa)	30 - 51		51 - 133

Table 1.1: Compressive strength, bending modulus and tensile strength of PMMA, cancellous bone and cortical bone.

Cured PMMA is bioinert with good long-term biocompatibility [78]. However, PMMA has several disadvantages: Because it is neither integrated nor remodeled, it stays in the bone like a placeholder. At higher strain rates PMMA cement becomes stiffer, leading to an increased risk of adjacent vertebral fractures [79,80]. The high polymerization temperature may cause thermal damage and subsequent necrosis to surrounding bone or cartilage tissue [81,82]. Incomplete polymerization may cause monomer toxicity [83].

To address the disadvantages of PMMA, composites of acrylic bone cements in conjunction with ceramics are currently favored for PVP, BKP and for implant augmentation. Cement composites containing PMMA and various ceramic components, e.g. Traumacem® (DePuy Synthes Companies, Zuchwil, Switzerland) with 45% w/v PMMA and 55% w/v ceramic components (40% zirconium dioxide, 15% hydroxyapatite), have shown in various medium to high load bearing applications improved handling and clinical outcomes compared to PMMA alone [29-32]. These composites are ready to use immediately after mixing and show enhanced viscosity for controlled injections with improved flow properties and increased working time (27min at room temperature, 15min at body temperature). Due to a decrease of polymerization temperature (60°C), no thermal damage to surrounding tissue may be observed. However, the bending modulus as well as the yield strength of Vertecem® (DePuy Synthes Companies, Zuchwil, Switzerland), used for PVP, is still much higher than that of cancellous bone, which could lead to a load shift to the adjacent vertebra with an increase of the risk for fracture.

In an *in vitro* study of Boger *et al.* the mechanical properties of a low modulus PMMA bone cement were investigated for augmentation of osteoporotic bone. They produced porous PMMA bone cements, thereby mixing commercial PMMA cement (Vertecom®, DePuy Synthes) with various volume fractions (15-50%) of an aqueous sodium hyaluronate solution. Mechanical properties for composites with 35-45% w/v sodium hyaluronate solution were promising. Bending modulus and yield strength were similar to those of cancellous bone, the polymerization temperature much lower (< 41°C), but injectability, viscosity and monomer release were unaffected [76]. All tests were performed using only non fractured vertebra, leading to the conclusion that the

application of porous PMMA cement for prophylactic vertebroplasty may successfully reinforce non-fractured osteoporotic bone without modifying the stress distribution und physiological loading significantly [84].

In studies of Hernandez *et al.* the main focus was to improve the biocompatibility and osseointegration of PMMA bone cement combined with a bioactive component (20% w/v strontium-hydroxyapatite). The newly developed cements demonstrated enhanced handling properties, optimum injectability and could withstand wear conditions [85]. They presented homogenous radiopacity and an excellent *in vitro* and *in vivo* bioactivity [86]. Future studies are required for preclinical tests of this promising composite as alternative to the currently available cements for minimal invasive augmentation surgery (PVP, KB).

1.4.2 Ceramic bone cements

Ceramic bone substitutes have been successfully used in various orthopedic and cranio-maxillofacial applications. Substitutes are available pre-shaped (e.g., cylinders, blocks, wedges) to precisely fit into variably shaped, critical size bony defects, but also as granules or powder for injection in bone augmentation procedures. Ceramics are remodelled and integrated into the surrounding bone while acting as a synthetic osteoconductive scaffold, thus being degraded and building new bone concurrently. Therefore, when used in combination with internal or external fixation methods, they are able to fill bone voids or restore fractures.

1.4.2.1 Calcium phosphate based cements

Calcium phosphate based, synthetic bone grafts have osteointegrative and ostoconductive properties. They are known to be biocompatible without systemic toxicity or foreign body reactions. Calcium phosphate cements based on hydroxyapatite, β-tricalcium phosphate and mixtures thereof are reportedly bioactive and osteoconductive.

They consist of two components, calcium orthophosphate (solid phase) and a liquid phase, forming a paste, which hardens through dissolution and precipitation without extensive exothermal heat generation. The compressive strength of the hardened material is 25-45 MPa, comparable or even higher than that of cancellous bone, but a

very low tensile strength (3-5MPa) limit the use of calcium phosphate cements to virtually non load-bearing applications. Low mechanical strength in shear, bending and tension led to development of fiber reinforced calcium phosphate composites. Various studies have demonstrated improved strength using different bioresorbable fibers for reinforcement (e.g., polyglactin fibres [87], polypropylene fibres [88]). Norian SRS (DePuy Synthes) is a commercially available, fiber-reinforced bone void filler. It consists of a calcium phosphate powder, bioresorbable fibers (lactide-glycolide co-polymer, to provide an increase in toughness and allow the material to be drilled and tapped) and a liquid component to increase viscosity leading to improved mixing and flow properties. Various clinical applications show favorite outcomes [45,89].

Most common clinical use of calcium phosphate bone cements and composites is filling of bone defects and subchondral voids in metaphyseal fractures (distal radius [89], proximal humerus [90], calcaneus [46], tibial plateau [43]), acting thereby as osteoconductive scaffold and structural support.

1.4.2.2 Calcium sulfates-based cements

Calcium sulfate, known also as "plaster of Paris" was first documented being used by the Arabs in the 10th century for external fracture treatment, surrounding the affected limb with a tube of plaster. In 1852 it was integrated in bandage material used externally to brace the fractured limb. In 1892 it was first used internally for the treatment of tuberculosis osteomyelitis in long bones [91].

Plaster of Paris implanted adjacent to periosteum or endosteum act as osteoconductive matrix for vessel ingrowth and cell migration [92], degradates fast by dissolution within 5-7 weeks [93]. In comparison to cancellous bone it has a higher compressive strength, but a lower tensile strength. However, because *in vivo* it softens and cracks when exposed to moisture and degradates fast, it lacks extended structural properties and therefore should only be used as bone void filler in non load-bearing applications [40].

Successful non load-bearing applications include filling stable cavity defects resulting from curettage of benign bone tumors [94], metaphyseal traumatic fractures impacting underlying cancellous bone or periprosthetic bone loss [95,96].

1.5 Complications of augmentation procedures

Although augmentation of cancellous bone is effective to enhance fracture stability, reduce fracture incidence and relief pain, its indication has to be balanced against the potential risk for various complications. Especially PMMA bone cement and composites thereof, used for medium and high load-bearing applications may lead to cement leakage, fat embolism, toxic effects and thermal damage. In vertebral augmentation it may increase the risk for adjacent fractures. Complication rate and severity are related to cement volume, cement viscosity and cement distribution as well as to the type of augmentation procedure and the anatomical site.

Cement leakage or extravasation into joints, the fracture site, surrounding tissue or into the blood system is one of the most common complications, which could lead to severe consequences.

From knowledge gained in a theoretical and experimental model used by Bohner *et al.*, the authors conducted that cement extravasation is influenced by several parameters: Bone permeability, bone marrow and cement viscosity, bone porosity and pore size, size of injection cavity, diameter of extravasation path, and injected cement volume. Among all these parameters, only cement viscosity and cement volume do not depend on bone structure [61]. Seemingly only an increase in cement viscosity and a decrease of injected cement volume [97] are parameters under control of the surgeon to reduce the risk of extravasation, which is in agreement with surgical observations [98].

Breusch *et al.* demonstrated in a sheep model using bilateral, simultaneous cement injection under pressure into femoral heads that low viscosity cement follows the path of least resistance into the venous system before deeper cement penetration into the cancellous bone can occur [62]. Cement flow into the venous system may lead to pulmonary infarction and death [74]. Contrary, for injections of high viscosity cement, an improved cement penetration was observed, eventually leading to fat embolism by the cement forcing bone marrow and fat cells instead into the blood circulation [62].

While the maximum PMMA cement volume used for implant augmentation is rather low (0.5 mL per screw up 2-4 mL total if more screws are augmented), the volumes are commonly higher for vertebral augmentation and void filling procedures

in general (3-6 mL per lumbar vertebra up to 25 mL total). Extravasation of cement into the blood system is therefore extremely rare during implant augmentation.

Nevertheless, to reduce the risk of cement leakage during implant augmentation into the joint, fracture gap or venous system, contrast fluid (0.5-10 mL) is injected under fluoroscopic control prior to cement application. If the contrast fluid stays in the injected bone, it is washed out using saline solution (6-10mL). Only if no leakage of contrast fluid is observed, augmentation should be performed. If cement leakage occurs the injection has to be stopped immediately. Cement leakage into the joint always requires immediate open joint surgery to remove the cement from the joint.

Many studies have demonstrated that lower infiltration volumes decrease the risk for complications such as cement extravasation, cement or fat embolism of the lungs and fractures of adjacent vertebrae [99].

Although, cement leakage is often asymptomatic, severe consequences may exist [100] and depend on the type of leakage. Three main types of leakages exist for vertebral augmentation [101]:

(1) Leaks through a cortical defect into surrounding tissue are relatively unpredictable and may invade areas like the disc space, spinal canal, neural foramen or even leak into surrounding muscles.

(2) Leaks into the segmental vein may lead to respiratory (pulmonary embolism) and cardiovascular deterioration [102,103].

(3) Leaks into the basivertebral veins invade the spinal canal and may lead to spinal cord or nerve root compression, or rarely to pulmonary embolism [104,105].

If spinal cord or nerve root compression is diagnosed by CT and comprises severe neurological deficiencies, immediate surgical decompression has to be performed.

Most cases of pulmonary cement embolism seem to be without clinical symptoms, although some symptoms like chest pain, dyspnea, acute respiratory distress syndrome and also death may occur.

Hulme *et al.* indicated that leakage in surrounding tissue occurs in 41% of augmented vertebrae, with 2% of these belonging to pulmonary emboli and a total occurrence of pulmonary embolism during PVP of 0.6% [106]. These numbers, however, are challenged by others [100,101] as they argue that omission of CTs or chest

radiographs after vertebroplasty on asymptomatic human patients may lead to an underestimation of cement leakage and pulmonary emboli occurrence secondary to vertebroplasty.

Embolization of bone marrow and fat occurs in a large proportion of patients undergoing major orthopedic surgery such as total hip [107] and knee [108] arthroplasty, intramedullary nailing for stabilization of fractured long bones [109], instrumented spine surgery [110], PVP and BKB [111,112]. However, it remains asymptomatic in most patients.

In case of vertebral augmentation procedures (PVP/BKB) it is hypothesized that the injection of PMMA bone cement causes an increase of the intramedullary pressure leading to a dislodge of bone marrow and fat cells. These follow the path of least resistance into the venous circulation [111]. This may occur with and without evidence of additional cement leakage. Subsequently, the capillaries of the end organs are obstructed mechanically. If the emboli are flushed out into the pulmonary vasculature, a biochemical and inflammatory cascade is initiated including a reflex vasoconstriction of the pulmonary vessels, a release of vasoactive mediators (endothelin) and activated coagulation. Actual cement embolism may result in an allergic reaction to the foreign material. The inflammatory cascade may prompt an increase of pulmonary arterial pressure [113,114]. If persistent, the high pulmonary arterial pressure will cause a clinically evident pulmonary embolism with severe cardiovascular effects, such as acute heart failure with a decrease in cardiac output causing systemic arterial hypotension. Increased dead space ventilation will cause ventilation-perfusion mismatch ultimately leading to hypercapnia and hypoxemia. While in most cases the cardiovascular effects are mild and transient, cardiac arrest and death have also been reported [111,112,115].

The exothermic polymerization reaction of PMMA cement initiates high temperatures up to 70°C in the center of the material [116]. This likely causes thermal damage and ultimately cell necrosis of osteocytes and chondrocytes [8,81,82]. The resulting disturbance of subchondral bone supply may trigger joint cartilage degeneration [8,117]. Therefore, subchondral cement injection should maintain a

minimal distance to the joint surface of 6-10 mm. The injected volume should be reduced to a minimum needed for sufficient stabilization of the bone [97].

In addition to thermal damage due to the exothermal chemical reaction of curing PMMA, many in vitro studies have shown severe local or systemic cytotoxicity (tissue irritation, inflammation) to the liquid monomer [118]. Local toxic tissue reactions are reported such as fibrous tissue formation at the interface between bone and PMMA [119], especially if injected early in of the polymerization phase, with a still higher percentage of residual, not yet bonded, toxic monomer. Systemic toxic reactions (e.g., hypoxia, hypotension, anaphylaxis, death) due to extravasation of small quantities of unbound liquid monomer into the venous circulation [120] have been reported and may affect lungs, kidneys and the liver. Therefore, research efforts ought to be invested to develop new composites of PMMA bone cements with enhanced biocompatibility and reduced toxicity[121].

Several studies have shown that following a first vertebral compression fracture the risk of additional fractures is increased, particularly in adjacent vertebrae [80,106,122]. A retrospective study of Kulçsar *et al.* estimated "that almost every fifth patient is at risk for developing a new fracture after PVP, but only every tenth fracture is likely to be related to the previous vertebral augmentation. Female patients with severe osteoporosis are probably facing the highest risk for developing new fractures" [123].

Baroud *et al.* demonstrated in ex vivo studies an increase in stiffness of the augmented vertebrae of up to 36 times when compared to normal spinal cancellous bone [99,124]. The cement acts in augmented vertebrae like an "upright pillar", reducing the physiologic inward bulging of the endplates. This increases the pressure measured in the adjacent intervertebral disc by approximately 19%. The induced load shift to the adjacent vertebra may cause an increased risk of fracture and possibly, in the long run degenerative changes. The stiffness of the augmented vertebra is unnecessarily high. The authors hypothesized that injecting a reduced amount of PMMA cement or using a softer augmentation material would still provide sufficient augmentation strength, but the lower stiffness would significantly reduce the risk of adjacent vertebral fractures [99,125].

Barr *et al.* commented in 2001 that kyphotic deformity caused by osteoporosis results in increased stress on adjacent vertebrae and thus puts them at high risk for additional fractures. Hence, in these cases prophylactic augmentation is indicated [48]. A change in local biomechanics may be provoked by either progressive spine deformity, by previous vertebroplasties [57,79,80], by natural progression of the underlying disease (osteoporosis, metastasis induced osteolysis) or by a combination of the above. Whether that increases the fracture risk of adjacent or distant vertebrae remains unclear.

1.6 Animal models in literature

Major research efforts are under way to improve the currently available treatment options for osteoporosis and to develop new strategies for the surgical treatment of fragility fractures and implant loosening. They include new implants for osteosynthesis with augmentation options, as well as biological approaches including new biocompatible materials. Although new implants and biomaterials could be mechanically tested in fresh cadaveric specimen, in vivo experiments are required for proof of principle and safety reasons. Therefore, animal models are important to test new strategies.

Davidson *et al.* defined already in 1987 that "an appropriate animal model for research should be based on the following considerations: 1) appropriateness as an analog, 2) transferability of information, 3) genetic uniformity of organisms where applicable, 4) background knowledge of biological properties, 5) cost and availability, 6) generalizability of the results, 7) ease and adaptability to experimental manipulation, 8) ecological considerations, and 9) ethical and societal implications" [126]. Animal models used for research of human diseases meet some, but certainly not all of these criteria.

Rodents, especially mice and rats, are widely used as animal models for research of osteoporosis in humans. Numerous genetically well-characterized mouse strains and transgenic-mice with deficiencies in bone metabolism (e.g., knock-out mice) are available and used for studying the genetic contribution to peak bone mass and age-related bone loss [127]. Therefore, the mouse seems to be a good model for basic research of age-, disuse-, or postmenopausal-related osteoporosis.

Rats, as well as mice, have proven to provide excellent models to study etiology of osteoporosis including pathophysiological changes of the skeleton (e.g., bone fragility), histomorphometric changes and the validity of biochemical markers for osteoporosis [128]. Mice are small-sized and inexpensive to purchase and maintain. They also grow rapidly with a relatively short lifespan, which enables studying of age-related bone loss. Mice also have well-characterized skeletal bone parameters (e.g., BMD, trabecular thickness) [129]. Rodents do not experience a natural menopause, as humans do. Therefore, the ovariectomized, skeletally mature rat is widely used as a model for postmenopausal osteoporosis in humans and has been validated as a clinically relevant model for human postmenopausal bone loss [130-132]. Estrogen deficiencies using an estrogen receptor antagonist induced similar loss of cancellous and endocortical bone, but the changes were reversible when medication was ceased [133]. Other models have been used to study the etiology of disuse osteoporosis induced by lack of physical activity, as well as the efficacy of potential interventions. As animal models for disuse osteoporosis unloading a limb was forced using different methods (e.g., unilateral sciatic nerve section, tenotomy, unilateral limb casting, internal or external joint fixation and spaceflight) [134-136]. These methods led to similar skeletal changes with significant reduction of mineralization and changes in histomorphometric parameters. The induced changes towards osteoporosis, however, are related primarily to unloading of bone and thus are observed locally, but never systemically. Alcohol-dependent rats are used to study etiology and severity of alcohol-induced bone loss [137].

Contrasting advantages of using rats and mice, there are also limitations and disadvantages to their use. The small blood volume of rodents limits the amount of sampling for multiple biochemical measurements. Rats have a different bone structure than humans with no Haversian system in the cortical bone and no remodeling via the basic multicellular unit in trabecular bone [138]. The small size and total overall amount of bone is another limiting factor. Resulting in difficulties to harvest adequate sample sizes for biomechanical testing and limitations for surgical procedures such as fracture fixation. Trabecular thickness and separation both are three times smaller in comparison to humans. These obvious differences in the trabecular bone structure

reduce the comparability of rodent osteoporotic bone to human osteoporotic bone as the trabecular structure plays the primary role in fragility fractures. The translational problem is further exacerbated because trabecular bone mass represents more than half of total bone mass in the proximal femur and lumbar vertebrae, the two bones most frequently affected by osteoporotic fractures.

Therefore, large animals such as sheep, pigs, goats, calves, and dogs may be more suitable to test new implants or biomaterials evaluated for osteoporosis treatment in humans. Although some large animals show a decrease in BMD due to ovariectomy induced osteopenia, the structure and BMD of osteoporotic human vertebral bodies seems unique. A study of Aerssens *et al.* [139] found marked interspecies differences between healthy human, dog, pig, cow, and sheep lumbar vertebrae regarding bone composition, bone density, and bone mechanical competence. Indeed, human vertebrae reveal much lower values for bone mineral content and density compared to that of the other species. The study conducted that dogs have the most similar bone structure compared to humans, but porcine bone is most similar in BMD and bone mineral content (BMC) when compared to human bone. Nevertheless, possible differences in bone loading with the quadruped gait of animals in comparison to humans should be investigated and taken into account.

For many years, dogs have been used for studies on the human skeleton (e.g., fracture healing, effects of immobilization, long-term effects of bone-active agents, allografts) as well as for studies on bone ingrowth and joint replacement [140,141]. However, due to a higher bone-remodeling rate in dogs compared to humans, results may not be transferable [140]. Ovariectomy-induced osteopenia models for osteoporosis in dogs are not suitable, because dogs do not develop estrogen deficiency-related bone loss. This may be explained by the infrequent estrus cycle of dogs resulting in extremely low estrogen levels throughout most of the year [142]. In addition to the above limitation, the use of dogs in medical research is further hindered by the rise in negative perception and increasing ethical concerns.

In that regard, farm animals (e.g. sheep, pigs, goats) are preferable because of a higher public acceptance. Indeed, the latter models may be used to study

postmenopausal osteoporosis, fragility fractures, as well as new treatment options including surgical techniques and biomaterials.

Over the last decades, an increasing number of sheep has been used for orthopedic research [143]. As farm and flock animals, they suffer the least stress when housed in groups of two or more animals, which makes handling easier and reduces costs [144]. In comparison to pigs, sheep are usually docile and compliant. They show a high acceptance for bandages and suspension systems. Due to their comparable size to humans, implants and surgical equipment for human use does not need to be downsized before testing. Therefore, various animal models using mature sheep have been successfully established by our group for studying orthopedic research questions in different anatomical locations. Some examples are: aseptic loosening model of hip prosthesis [145], drill hole model for biocompatibility testing of biomaterials in cancellous bone [146], pelvic model for testing of osseointegration and biocompatibility of different implants [147,148], tibiaosteotomy models for testing new biomaterials or newly developed implants [149], impingement model in the hip [150], or a chronically retracted rotator cuff model [151,152].

Other research groups have reported using the sheep as a suitable model for research of osteoporosis. Ovariectomy [153], glucocorticoid treatment [154], and highly anionic diet inducing metabolic acidosis [155] have been used alone or in combination [156-159] to induce bone loss in sheep. Different studies have demonstrated that ovariectomy alone may not be sufficient to provoke perceptible bone loss [154]. The BMD even may return to baseline after an initial decrease including a rebound effect [160]. However, the combination of ovarioectomy followed by six months of glucocorticoid treatment has produced a significant loss of trabecular bone in the proximal tibia. Compared to control animals a significantly reduced bone mineral density, bone volume, and elastic modulus was assessed using densitometry, histomorphometry, and biomechanical testing, respectively. Even six months later without glucocorticoid treatment, the changes in trabecular bone were still similar [154]. In a study of Ding *et al.* [159] significant loss of cancellous bone was induced using the combination of glucocorticoid treatment and deficient diet (i.e., low calcium and phosphorus). After seven months, significant changes in microarchitecture and

mechanical properties in the lumbar vertebrae, distal femur and proximal tibia were detected. However, three months later without glucocorticoids and diet microarchitecture and bone strength have recovered. A combination of ovariectomy, glucocorticoid treatment and calcium/vitamin D-restricted diet seems an effective method to induce and retain a decrease of bone mineral density and deterioration of trabecular bone [156]. However, for both the glucocorticoid treatment (adverse effects, especially for immune system) and for the deficiency diet, ethical considerations need to be taken into account when using these models. In addition, this combined treatment does not mimic the pathogenesis of osteoporosis in postmenopausal women, because glucocorticoid induced osteopenia presents with a different underlying cell mechanism.

Another important fact is that seasonal changes of bone mass are a potential variable when using sheep in studies of osteopenia [161,162] and, like in dogs, related to the periods of anestrus, which in sheep is linked to the environmental photoperiod. Some breeds can continue their cycle almost all year-round and therefore are more sensitive to estrogen deficiency (e.g. merino sheep).

As already discussed in our previous publications, good animal models for vertebral augmentation are rare [163,164]. Sheep has been mainly used in acute studies for augmentation in the lumbar spine for research of cardiovascular complications such as pulmonary fat [165] or cement [114] embolism. Using percutaneous [166], retroperitoneal [167,168] and open approaches [165,169] to the lumbar vertebrae, pulmonary complications similar to those seen in humans have been described in vertebroplasty studies in sheep (immediate sacrifice on the table after augmentation). Turner *et al.* reported using aged-ovariectomized ewes for vertebroplasty of the lumbar spine using histological evaluation for examination of osteoconductivity and remodeling properties of the injected cement [144]. They indicated that a serious complication and major limitation of this model is inadvertent penetration of the floor of the spinal canal with subsequent leakage of material into the dural space even under fluoroscopic guidance [170]. In fact, this complication may lead to paraplegia and early termination of the experiment, although mostly these complications are never reported in the literature and only admitted in personal communications. An adequate surgical

access to the ovine vertebral body of the thoracic and lumbar spine including subsequent injection of augmentation material in a standardized and reproducible fashion is very difficult and almost impossible [171-173]. The limiting factors compared to the human spine are the large muscle mass in this area, the oversized transverse processes, the different orientation of the facet joints and, mainly, the ovine vertebral body size and shape (slim, trapezoid), which is quite different to that of humans (round, solid, almost rectangular).

1.7 Rationale of the study and specific aims of the project

This PhD project was designed to develop new *in vivo* animal models for the augmentation of cancellous bone in a highly standardized and reproducible manner for the evaluation of new biomimetic materials. Using these *in vivo* models, biomaterial composites were tested for their efficacy to induce new bone formation and, therefore, strengthen the cancellous bone. The material's biocompatibility and degradation properties were equally evaluated.

To the best of our knowledge, to date there is still no adequate, bioactive and resorbable material for prophylactic augmentation available. Such material would require the ability to induce new bone formation and normalize pathologically changed trabecular structure of osteoporotic bones at risk for fracture. Research efforts should be made to develop adequate animal models for testing of existing and newly developed augmentation materials.

2 Bone Augmentation for Cancellous Bone- Development of a New Animal Model

2.1 Aim of the study

This study aimed at developing a simple reproducible and standardized bone augmentation model in sheep. The model should preferably reproduce the pulmonary complications seen in human and ovine vertebroplasty. In addition, a standardized and reproducible evaluation method to compare results of different studies should be established. We hypothesized that a tibia and femur augmentation model in sheep would fulfill all these above needs.

2.2 Main conclusions

The tibia and femur augmentation model has proven to be suitable for screening studies of new biomaterials intended for trabecular bone augmentation. It enabled analysis of biodegradable, biocompatible and osteoconductive material properties. The model also has proven to be adequate for the study of the sequelae of material leakage into the circulation, i.e. pulmonary embolism with associated cardiovascular changes.

Overall, we consider the tibia and femur augmentation model to be safe when used by the experienced surgeon, resulting in reduced animal suffering and suitable to serve well for testing of bone inducing or enhancing materials for vertebroplasty.

2.3 Contribution to this publication

I was profoundly involved in all aspects of the study including performing the surgeries, outcomes, evaluation and writing the manuscript.

2.4 Publication reference

Klein K, Zamparo E, Kronen PW, Kämpf K, Makara M, Steffen T, von Rechenberg B. Bone augmentation for cancellous bone- development of a new animal model. BMC Musculoskelet Disord. **2013** Jul 2;12:200. Doi: 10.1186/1471-2474-14-200

Klein *et al. BMC Musculoskeletal Disorders* 2013, **14**:200
http://www.biomedcentral.com/1471-2474/14/200

BMC Musculoskeletal Disorders

RESEARCH ARTICLE Open Access

Bone augmentation for cancellous bone- development of a new animal model

Karina Klein[1,2*], Enrico Zamparo[3], Peter W Kronen[1,4,5], Katharina Kämpf[1], Mariano Makara[6], Thomas Steffen[7] and Brigitte von Rechenberg[1,4]

Abstract

Background: Reproducible and suitable animal models are required for *in vivo* experiments to investigate new biodegradable and osteoinductive biomaterials for augmentation of bones at risk for osteoporotic fractures. Sheep have especially been used as a model for the human spine due to their size and similar bone metabolism. However, although sheep and human vertebral bodies have similar biomechanical characteristics, the shape of the vertebral bodies, the size of the transverse processes, and the different orientation of the facet joints of sheep are quite different from those of humans making the surgical approach complicated and unpredictable. Therefore, an adequate and safe animal model for bone augmentation was developed using a standardized femoral and tibia augmentation site in sheep.

Methods: The cancellous bone of the distal femur and proximal tibia were chosen as injection sites with the surgical approach via the medial aspects of the femoral condyle and proximal tibia metaphysis (n = 4 injection sites). For reproducible drilling and injection in a given direction and length, a custom-made c-shaped aiming device was designed. Exact positioning of the aiming device and needle positioning within the intertrabecular space of the intact bone could be validated in a predictable and standardized fashion using fluoroscopy. After sacrifice, bone cylinders (Ø 32 mm) were harvested throughout the tibia and femur by means of a diamond-coated core drill, which was especially developed to harvest the injected bone area exactly. Thereafter, the extracted bone cylinders were processed as non-decalcified specimens for µCT analysis, histomorphometry, histology, and fluorescence evaluation.

Results: The aiming device could be easily placed in 63 sheep and assured a reproducible, standardized injection area. In four sheep, cardiovascular complications occurred during surgery and pulmonary embolism was detected by computed tomography post surgery in all of these animals. The harvesting and evaluative methods assured a standardized analysis of all samples.

Conclusions: This experimental animal model provides an excellent basis for testing new biomaterials for their suitability as bone augmentation materials. Concomitantly, similar cardiovascular changes occur during vertebroplasties as in humans, thus making it a suitable animal model for studies related to vertebroplasty.

Background

Handling and injective properties of new biomaterials for vertebral bone augmentation can be tested in fresh cadaveric specimens, but *in vivo* experiments are required for proof of principle and safety reasons as the presence of blood flow could significantly alter the risk of leakage. Animals such as sheep, pigs, goats, calves, and dogs have been reported as models for several medical problems associated with the human spine [1], including bone defects [2] and kyphoplasty [3] in the lumbar area, although with a high complication rate. For vertebroplasty in sheep, mostly acute studies (euthanasia during anesthesia without recovery) were reported with the focus on cardiovascular complications such as pulmonary embolus formation. Cement leakage was followed within the systemic circulation, but not

* Correspondence: kklein@vetclinics.uzh.ch
[1]Musculoskeletal Research Unit (MSRU), Equine Department, University of Zurich, Winterthurerstrasse 260, Zurich CH-8057, Switzerland
[2]Graduate School for Cellular and Biomedical Sciences, University of Bern, Bern, Switzerland
Full list of author information is available at the end of the article

Klein et al. BMC Musculoskeletal Disorders 2013, 14:200
http://www.biomedcentral.com/1471-2474/14/200

documented within the spinal canal as reported also in humans [4].

Pulmonary complications similar to those seen in humans have been described in vertebroplasty studies in sheep, where percutaneous [5], retroperitoneal [6,7] and open approaches [8-11] to the lumbar vertebrae were used. However, the minimally invasive surgical technique of percutaneous augmentation as commonly used for treatment of symptomatic vertebral compression fractures in humans, occurring secondary to osteoporosis or neoplasia [12-19], proved to be difficult to reproduce in the lumbar vertebrae of sheep. This is primarily due to the shape of the ovine vertebral body which is quite different and much more difficult to surgically access than in humans [3,20,21]. Even the standard surgical open approach to the lumbar area is complicated due to the large muscle mass in this area, the size of the transverse processes, the different orientation of the facet joints and mainly the slim, hour-glass shaped vertebral bodies. Even under fluoroscopic guidance, inadvertent penetration of the floor of the spinal canal with subsequent leakage of material into the dural space are serious complications and major limitations of this model [22]. In fact, this complication often leads to paraplegia and early termination of the experiment, although mostly these complications are never reported in the literature and only admitted in personal communications. A high percentage of the animals have to be euthanized immediately after recovery due to severe pain and clinical symptoms often require immediate termination of the experiments.

Apart from animal welfare reasons (suffering, numbers of animals used in the experiment), increased costs, high efforts, and unpredictable outcome necessitate a novel, simply reproducible and standardized animal model in sheep. In addition, the animal model preferably should reproduce the pulmonary complications ranging from no clinical signs to severe cardiac distress symptoms as seen in human and ovine vertebroplasty [10,16]. Moreover, a standardized and reproducible evaluation method to compare results of different studies should be available. We hypothesized that a femoral and tibial bone augmentation model in sheep would fulfill all these criteria.

Methods

Study design and experimental animals

For this novel experimental animal model the relatively dense cancellous bone of the distal femoral condyle and proximal tibia metaphysis was chosen as location for the application of radiopaque augmentation materials. A customized aiming device was developed that allowed repeatable, safe and standardized injections under fluoroscopic guidance.

For proof of this animal model 63 adult, female, Swiss alpine sheep with an average age of 2.7 years (2–5 years) and a body mass of 70.4 kg (49–99 kg) were used from consecutive studies focusing on different biomaterial formulations for augmentation (see Table 1). In all sheep, the same material was injected into the femoral condyle and proximal tibia of the same limb. Various radiopaque formulations of biomimetic materials based on a fibrin-scaffold were tested in comparison to sham controls. Since this manuscript is dedicated to the description of the animal model including evaluative procedures, the details of materials and results of bone enhancement will be published elsewhere (publication in preparation). Overall, 12 groups of materials were tested with 5–7 animals/group (Table 1). As controls sham surgeries were conducted in 5 sheep.

Due to the low morbidity and invasiveness of the surgical procedure, both hind limbs could be chosen, resulting in a total of four augmentation sites per sheep to inject material (n = 252 augmentation sites). For animal protection and welfare issues, a vertebral augmentation group as comparison to the new animal model was omitted due to the expected complications. (In a previous study in collaboration with an associated research group using an open and retroperitoneal approach to the lumbar spine, >80% of the animals had to be euthanized due to complications such as leakage into the spinal canal and fracture of the vertebral body).

All experiments were conducted according to the Swiss regulations of Animal Welfare and permission was granted by the local federal authorities (application # 7/2008).

The animals were acclimatized to the new environment approximately 2 weeks before surgery. A preanesthetic examination was performed including general clinical examination, hematology and chemscreen. Food was withdrawn 24 h before induction of anesthesia, while water was available ad libitum.

Animal model

Instruments/equipment

In addition to the routinely used surgical instruments, a custom-made-aiming device was developed in order to increase reproducibility of surgical access and to standardize the injected area. The C-shaped aiming device allows exact positioning at the medial and lateral aspects of the tibia or femur including drilling in a given direction and at a predictable length (Figure 1). The aiming device consisted of two arms. The distance between the arms could be adjusted in order to fit the lateromedial axis of the stifle. A sharp tip is mounted axially on one arm while a concentric outer tube with sharp teeth is positioned on the other arm. The aiming device has to be placed with the tube for the drill hole at

Klein et al. BMC Musculoskeletal Disorders 2013, 14:200
http://www.biomedcentral.com/1471-2474/14/200

Table 1 Group distribution and CT analysis

Group	Number of animals	Material	CT	Clinical signs of pulmonary embolism
1	6	FS + MP1 + CA, with/without BM4	1	1
2	7	FS + CA, with/without BM4		
3	5	control/sham	2	
4	6	FS + MP2 + CA, with/without BM4		
5	6	FS + MP2 + CA, with/without BM4		
6	6	FS + CA, with/without BM4		
7	5	FS + MP2 + BM1	5	
8	5	FS + MP2 + BM2	4	
9	5	FS + MP2 + BM3	4	1
10	2	FS + MP2 + BM4		
11	5	FS + MP2 + BM5	2	1
12	5	FS + MP2 + BM6	1	1

Legend:
FS: Fibrin-scaffold.
MP1 or 2: Mineral powder 1 or 2.
CA: Contrast agent.
BM1-6: Biomimetic agent concentration 1-6.
with/without: One leg with and one leg without BM4.
This table shows the group distribution of all animals including the numbers of CT's performed in each treatment group as well as the numbers of animals with cardiovascular complications occurring during surgery.

the medial aspect and the sharp tip fixed on the lateral aspect of the tibia or femur (Figure 2a). This positioning of the aiming device allows the insertion of the drill and ultimately the needle relatively parallel to the articular surface of the femoro-tibial joint. With the concentric tube and the distal sharp tip being in line, the suggested insertion trajectory for the needle can be validated using fluoroscopy in mediolateral and craniocaudal view (Figure 2b).

For the injection of augmentation material, a 10G (3.2 mm diameter) 100 mm-long special vertebroplasty needle (1394–1010, Optimed Medizinische Instrumente GmbH, Ettlingen, Germany) and an Optimed CementoRE gun (1392–0000, Optimed Medizinische Instrumente GmbH, Ettlingen, Germany) were used. The vertebroplasty needle consisted of three parts, needle, handle, and stylet (Figure 1).

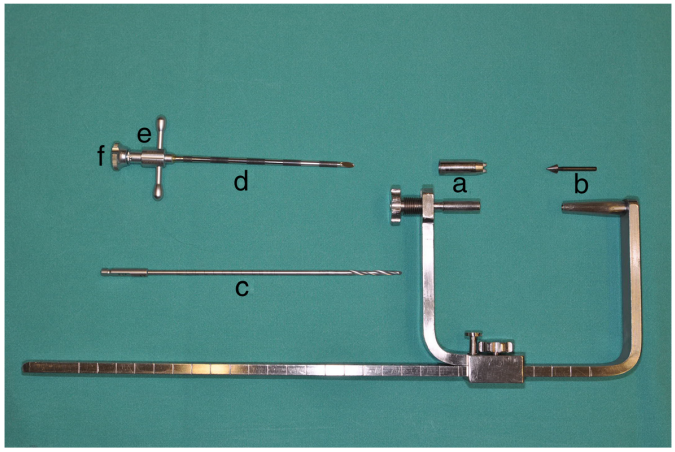

Figure 1 C-shaped aiming device. This photograph shows the c-shaped aiming device consisting of two adjustable arms with a mountable concentric outer tube with sharp teeth **(a)** and a mountable sharp tip **(b)** for device fixation. For application of biomaterial, a drill **(c)** and subsequently a 10G-vertebroplasty needle (needle **(d)**, handle **(e)**, and stylet **(f)**) were applied through the arm with the concentric tube **(a)**.

Klein et al. BMC Musculoskeletal Disorders 2013, 14:200
http://www.biomedcentral.com/1471-2474/14/200

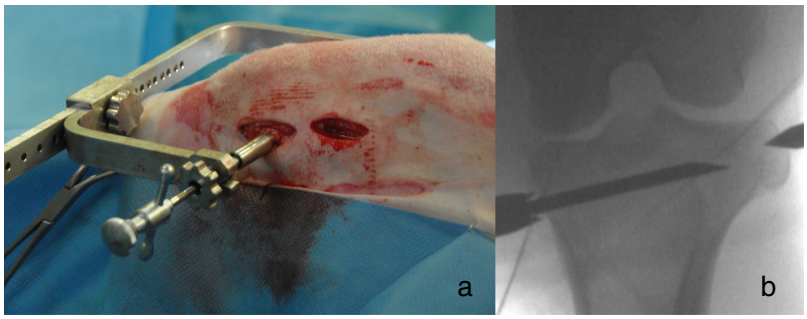

Figure 2 Correct placement of the aiming device. The aiming device was placed with the tube for the needle at the medial aspect and the sharp tip fixed on the lateral aspect of the tibia **(a)**. Fluoroscopy pictures were used to validate correct placement of aiming device and needle as well as subsequent material injections **(b)**.

Anesthesia and analgesia

Animals were premedicated intramuscularly with buprenorphine (Temgesic®, 0.01 mg/kg, Essex Chemie AG, Lucerne, Switzerland) and xylazine (Rompun® 2%, 0.1 mg/kg im, Streuli Pharma, Uznach, Switzerland). After approximately 30 minutes, a catheter (Vygonyle S® G14, Vygon GmbH, Aachen, Germany) was placed into one jugular vein and prophylactic antibiotics (Penicillin Natrium® 35´000 IU/kg i.v.; G. Streuli Pharma, Uznach Switzerland; gentamicin, Vetagent®, 4 mg/kg i.v., Veterinaria AG, Zurich, Switzerland) as well as a pre-emptive analgesic (Rimadyl®, 4 mg/kg i.v.; Pfizer SA, Zurich, Switzerland) were given intravenously. A booster for tetanus (tetanus serum Intervet, 3000 IU/sheep s.c.; Veterinaria AG, Zurich, Switzerland) was administered subcutaneously. Anesthesia was induced with diazepam (Valium®, 0.1 mg/kg i.v., Roche Pharma AG, Rheinach, Switzerland), ketamine (Narketan 10®, 2 mg/kg i.v., Vetoquinol AG, Belp-Bern, Switzerland) and propofol (Propofol®, 0.4-2 mg/kg iv, Fresenius Kabi, Stans, Switzerland) administered to effect. After laryngeal desensitization with lidocain spray (Xylocaine Spray 10%, 3 pumps of 0.1 mL, Astra Zeneca AG, Zug, Switzerland), the trachea was intubated and correct placement was confirmed by expired carbon dioxide monitoring ($F_{et}CO2$). Anesthesia was maintained with a balanced anesthetic protocol employing administration of isoflurane (1-2%vol) in oxygen via an adult F-circuit (circle system, Intersurgical, Berkshire, UK) and a constant rate infusion of propofol (Propofol®, 0.5-1 mg/kg/h, Fresenius Kabi, Stans, Switzerland). All animals received intravenous fluids throughout the procedure (Ringer solution, 10 mg/kg/h). Cardiovascular monitoring parameters included electrocardiogram (ECG), heart rate, pulse rate and invasively measured blood pressures (systolic, mean and diastolic arterial) via an arterial catheter in an auricular artery.

Surgical procedure

The anesthetized sheep were placed in dorsal recumbency tilted at a 30° angle to the non operated side, with the hind limb slightly flexed and fixed at the surgery table. For the second leg repositioning was required. Aseptic preparation of the surgical field was performed routinely.

Two small incisions (1 cm) were performed at the medial aspect of the femoral condyle (directly above the femoral epicondyle) and at the metaphysis of the proximal tibia (at the distal end of the collateral ligament). Soft tissue was dissected down to the bone and the aiming device was placed with the tube for the drill hole at the medial aspect and the sharp tip fixed on the lateral aspect of the tibia or femur (Figure 2a). For fixation of the sharp tip on the lateral side only two stab incisions of the skin were needed, at the same level as the medial ones. Bleeding was controlled using an electrocautery.

Using fluoroscopy in two projection planes (mediolateral and craniocaudal), the right position of the aiming device and subsequent needle positioning could be validated and inaccurate injections avoided.

A drill hole with a diameter of 2.7 mm was created and followed by placing the special vertebroplasty needle with the tip ending in the trabecular portion of the femoral condyle (in parallel direction to the stifle joint surface) or proximal tibial bone (in slightly oblique direction to the fibula head).

The material injections were done in multiple steps under fluoroscopic guidance. Needle filling with biomimetic material was done slowly with the aid of the Optimed CementoRE gun (Figure 3). Subsequently, the gun was removed and a stylet was used to push the material through the needle into the bone, so as to provide exact quantities of injectate. If necessary a hammer was used to push the stylet and the material into the bone. The filling-clearing procedure was repeated three or four

Klein et al. BMC Musculoskeletal Disorders 2013, 14:200
http://www.biomedcentral.com/1471-2474/14/200

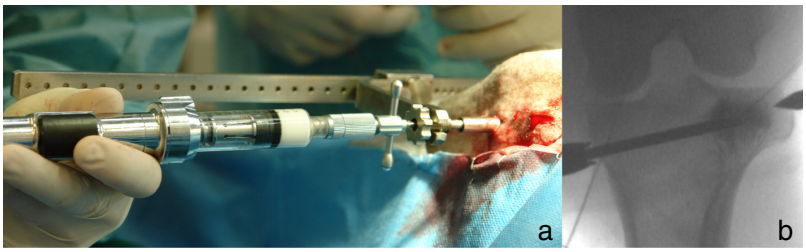

Figure 3 Injection procedure. Injections were performed with an Optimed CementoRE gun **(a)** and made in multiple steps under fluoroscopic control **(b)**.

times, until a target of 2.7 mL was distributed within the intertrabecular space. Using fluoroscopy, leakage of the material into a vessel and thrombus formation was recorded and the amount of that material was estimated and documented.

Sham operations consisted of drilling and placing the needle as described above. The stylet was then inserted and removed three times without material injection.

At completion of the injection procedure, the vertebroplasty needle and the aiming device were removed and the insertion point was closed with a 3.5 mm diameter self-tapping screw (10 mm in length, Synthes, Oberdorf, Switzerland). The screw was used to determine the insertion point and the direction of the needle after sacrifice.

Closure of subcutaneous tissue was routinely done using resorbable suture material (Vicryl® 2–0, Johnson & Johnson Int., Brussles, Belgium) in a continuous fashion, while the skin was closed with a skin stapler (Appose ULV, United States Surgical). No further external stabilization was used.

After repositioning, the augmentation procedure of the contralateral limb was performed in identical manner. Immediately after surgery lateral and craniocaudal fluoroscopy images were taken to document the distribution of the injected material in two projection planes.

Postoperative treatment

After surgery and recovering from anesthesia, the animals were kept in small groups and their health status was checked twice daily. Food and water were offered ad libitum. Antibiosis and analgesia administrations were continued via the jugular catheter for 4 days using the same dosages as perioperatively applied. In addition, buprenorphine injections i.m. were continued every 4 hours for two applications to reduce postoperative pain.

After 21 days the staples were removed and the animals were released to pasture.

Fluorescence labelling

For a dynamic representation of new bone formation and remodeling, different fluorescence markers were subcutaneously injected at different time points. Calcein green (1 ml/kg s.c.; Fluka AG, Buchs, Switzerland) was applied after 4 weeks, xylenolorange (1 ml/kg s.c.; Fluka AG) three days before sacrifice.

Evaluation

Computer Tomography Angiography

Computer Tomography Angiography (CTA) of the thorax was performed in 19 sheep either after cardiovascular complications developed during surgery indicating pulmonary embolism or in selected cases to visualize the potential occurrence of pulmonary embolism caused by bone marrow/fat particles or material deposition. The CT study was performed with a multi-row unit using 40 rows, slice collimation of 0.6 cm and a pitch of 1. The contrast medium dose was 700 mg/kg of an iodinated high-osmolar contrast medium (Telebrix®, 350 mgI/ml, Guebert, Zurich, Switzerland). The volume of embolized material was calculated using an automated region of interest propagation technique with an upper attenuation threshold of 5000 Hounsfield units (HU) and lower threshold of 300 HU.

Specimen preparation for evaluative procedures

After sacrifice, the tibia and femur were extracted for final analysis. Augmentation sites were examined macroscopically and digital pictures were recorded (Nikon Digital Camera D5000, © 2009 Nikon Corporation). Subsequently the bones were radiographed using a Faxitron (Faxitron X-Ray Systems; Hewlett Packard, Mc Minnville Division, OR) to visualize the detailed bone structure and detect remaining augmentation material.

To provide a standardized evaluation process, an appropriate harvesting method was designed to locate the area of interest for histological evaluation.

Klein *et al. BMC Musculoskeletal Disorders* 2013, **14**:200
http://www.biomedcentral.com/1471-2474/14/200

By fitting a custom-made axially lined up metal pin pointer into the head of the screw, the original direction of the injection needle could be established (Figure 4a). The bone was fixed to the drill press table with a custom-made universal joint holder. By manipulating the holder, the appropriate position could be found by ultimately aligning the original direction of the injection needle with the central axis (Figure 4b) of the drill press. After screw and pin pointer removal, the 32 mm diameter, water-cooled diamond core drill was mounted on the drill press and an accurate bone cylinder was cored with the original needle path matching the axis of the cylinder (Figure 4c). A mark was made with a band saw on the cortical bone from the entry point of the needle in distal direction. This allowed consistent positioning of the sample for μCT scanning and served as a reference for the cutting of the histology slices.

All bone samples were fixed in 40% ethanol for 1 week, followed by a series of ethanol dehydration (50-100%) within 6 days. Once the specimens were fixed in 70% ethanol, μ-CT analysis was performed by b-cube AG (Bio-Technopark, Schlieren-Zurich, Switzerland).

After μ-CT analysis and complete dehydration all samples were degreased in xylene and subsequently infiltrated in liquid polymethylmethacrylate (PMMA). Polymerization was carried out in plastic molds closed with a lid and kept at 4°C for 1 week, thereafter in a water bath at room temperature until polymerization occurred. Finally the plastic molds were placed in an incubator (37°C) uncovered to complete hardening of the samples.

Ground sections (300 μm) and *native fluorescence sections* (350 μm) were cut using a special band saw (EXAKT® Band System 300/301, EXAKT® Apparatebau GmbH &Co KG, Norderstedt, Germany). The blocks were cut lengthwise the needle path. The needle path, the tip of the needle, and surrounding tissue defined the region of interest. Before mounting (Cementit® CA 12, Merz + Benteli AG, Niederwangen, Switzerland) the sections on plastic slides (ACROPAL, Maagtechnic, Duebendorf. Switzerland), microradiographs were taken in the Faxitron (27 kV, 11 s; Fuji Photo Film Co Ltd, Tokyo, Japan). Ground sections were polished (Exakt® Mikro- Schleifsystem 400CS, Exakt Apparatebau GmbH,

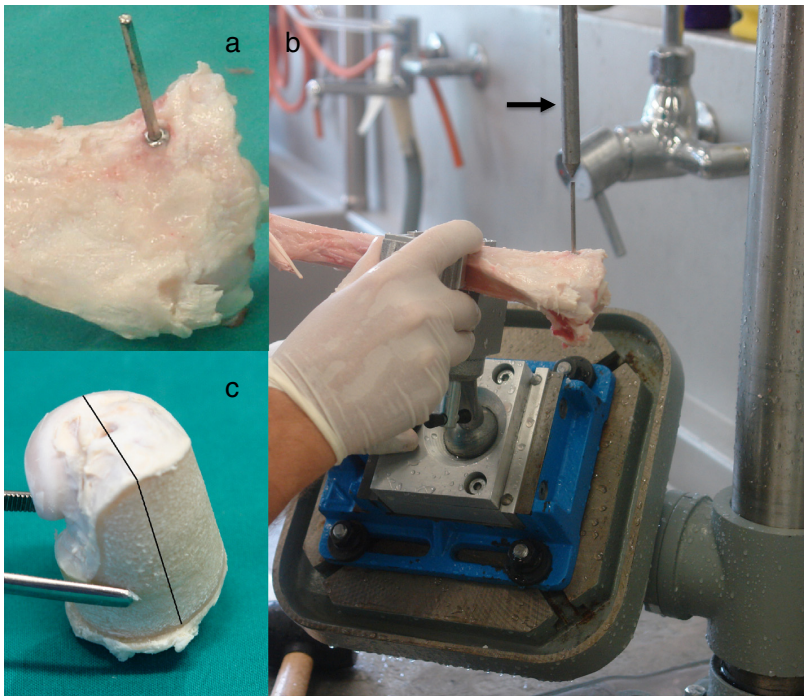

Figure 4 Harvesting method. To provide a standardized evaluation process and locate the area of interest, an appropriate harvesting method was designed: Using a custom-made screw the original direction of the needle could be established **(a)**. A custom-made holder allowed fixation of the bone to a drill press table aligning the original needle path with the axis of a diamond-coated water-cooled core drill **(b)**. The black arrow marks the pin pointer used for defining the drill axis. After screw and pin pointer removal, the core drill was mounted on the drill press and a 32 mm diameter bone cylinder was cut **(c)**. The black line in Figure **c** marks the cutting mark for histology sections with original needle insertion point and needle path in the center.

Klein *et al. BMC Musculoskeletal Disorders* 2013, **14**:200
http://www.biomedcentral.com/1471-2474/14/200

Norderstedt, Germany) and surface stained with toluidine blue. The native sections for fluorescence were mounted on pellucid, acrylic plexiglas slides (Maagtechnic, Duebendorf, Switzerland) and wrapped in aluminium foil to protect slides from bleaching.

For the *thin sections* the area of interest of the remaining bone blocks, comprising the tip of the needle and surrounding tissue, was cut into a smaller segment and polymerized in special customized Teflon forms (D. Nadler, JOSSI AG, Islikon, Switzerland) at room temperature. For hardening, the teflon forms were put in the incubator at 37°C. Thereafter, blocks were mounted on plastic frames and cut using a microtome (Leica® RM 2155, Leica Instruments GmbH, Nussloch, Germany). After placing the sections on glass slides, they were deplastified with Methoxyethyl-acetate (Merck AG, Switzerland) and stained with either toluidine blue or von Kossa/McNeil.

Histological evaluation

The standardized cutting procedure of all samples along the original needle path ensured comparability of the results obtained for the different treatment groups. The area around the tip of the original needle, where most of the augmentation material was injected, was identified as region of interest for analysis.

Ground sections were evaluated histomorphometrically (Leica Qwin®, Leica Quips®, Leica, Glattbrugg, Switzerland) to quantify the percentages of new bone, old bone, granulation tissue, and residual augmentation material within the area of interest.

First, the ground sections were captured with the macroscope (Leica Z6 APOA, Leica DFC 420C, Glattbrugg, Switzerland) as digital images in TIF-format using a 5.6-fold magnification. To standardize the evaluated area four circles of 6 mm in diameter were chosen around the tip of the needle (Figure 5). If the circles contained cortical bone it was excluded from the region of interest, since more old bone with high density is present in the cortex. The rest of the circle was considered as 100%. Circles including the growth plate were excluded from the analysis, since a higher rate of new bone was present independently of the applied material.

Thin sections were semi-quantitative evaluated using a microscope (Leica® DMR, Glattbrugg, Switzerland) in a ten-fold magnification. Scores were given for presence of macrophages, mononuclear cells, osteoclasts, multinucleated foreign body cells, debris of bone, isles of not calcified osteoid, agglomeration of mononuclear cells, percentage of osteoid seam, osteoid thickness, and material in bulk. Three power fields per section were assessed with two peripheral and one central in the injected area. For macrophages, mononuclear cells, and fibroblasts scores were given in percentages of cells per power field (0 = 0%; 1 = 1-25%; 2 = 26-50%; 3 >50%). For multinucleated foreign body cells and osteoclasts absolute numbers were counted per power field (0 = 0; 1 = 1-5; 2 = 6-10; 3= >10 cells).

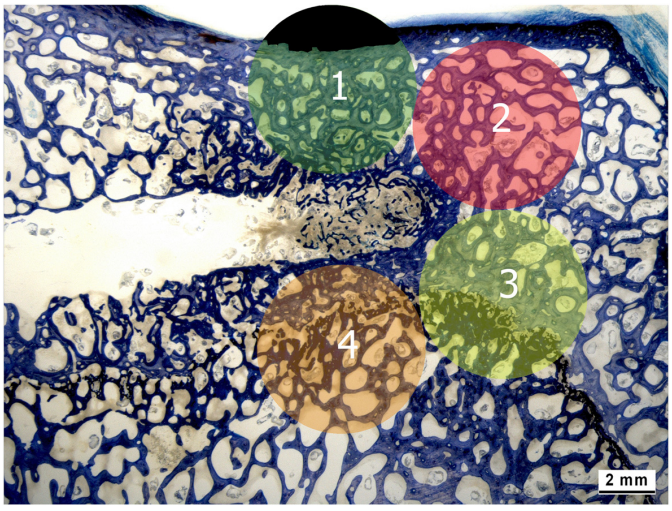

Figure 5 Histomorphometrical evaluation. Histomorphometry was used to quantify the percentage of new bone, old bone, granulation tissue, and residual augmentation material within the area of interest. For standardization of the evaluated area four circles of 6 mm in diameter were chosen around the tip of the needle. Cortical bone area was excluded from the analysis (black area in circle 1). The rest of the circle was considered as 100%. Circles including growth plate were completely excluded from the analysis (circle 3 + 4).

Klein et al. BMC Musculoskeletal Disorders 2013, 14:200
http://www.biomedcentral.com/1471-2474/14/200

Fluorescent sections were evaluated at 1.25× magnification with a special fluorescence microscope equipped with different filters appropriate for the used dyes (Leica® DM 6000B, Leica Microsystems CMS GmbH). To achieve one adequate picture including the whole area of interest centered at the tip of the needle, 30 images had to be taken and merged together to one using a compatible camera (Leica®DFC 350 FX, Leica Microsystems CMS GmbH, Mannheim, Germany) and a specific merging software (Leica® Microsystems CMS GmbH, Mannheim, Germany).

Focus was placed on differences of dye integration between groups as well as at different time points (calcein green at 6 and xylenol orange at 12 weeks).

A semiquantitative evaluation of the recorded images was performed scoring the percentage of each fluorescent dye in the area of interest (considered as 100%) (0 = 0%; 1 = 1-25%, 2 = 26-50%, 3= >50%).

Micro CT evaluation

All samples were measured with a micro-computed tomography system (μCT 40, Scanco Medical AG, Brüttisellen, Switzerland). Semiautomatic masks of sphere shells in different sizes were performed centered at the original position of the tip of the needle to evaluate bone volume density and trabecular thickness of these spheres as well as the residual radiopaque material. To measure only the trabecular bone area, the needle path and the cortical bone were excluded from the analysis.

Results

Animal model

A total of 63 sheep were treated with the tibia and femur augmentation model. Sixty-two sheep completed the 12 weeks follow-up period successfully. One animal had to be euthanized 6 weeks after surgery due to the presence of a malignant lymphoma in the wall of the urinary bladder, unrelated to the study treatment.

Augmentation could be achieved successfully in all 63 animals and after a learning curve initially 245/252 augmentation sites were highly reproducible and without complication. In 7/252 needle positioning problems occurred (see below). The overall surgical procedure for each hind limb was between 30–40 minutes. In addition, the minimally invasive surgical procedure led to immediate recovery and minimal physical stress. After a short recovery period due to anesthesia (e.g. 30 minutes), the sheep rose and moved around without lameness. During the 12 weeks follow up, no signs of inflammation, wound infections, lameness or other discomfort were noticed in any of the 62 remaining sheep. Furthermore, the sheep exhibited no pain response following palpation of the injected sites.

The surgical technique using the aiming device and fluoroscopic imaging were particularly useful to inject the material into a standardized anatomical location. Under fluoroscopic guidance during surgery, it could also be verified that consistent amounts of biomaterials were injected into the trabecular bone and distributed in a sphere-like shape around the tip of the needle. This distribution and needle placement could also be verified using the evaluative procedures. μCT images, microradiographs, indicated very consistent and standardized injection areas (see below).

Due to the high density of the trabecular bone at the injection site, the needle could not be introduced with manual pressure as it is described in human medicine. Instead, a hole was drilled and the needle pushed into the trabecular bone by using a mallet. As mentioned above, needle-positioning problems occurred in only 7/252 injection sites. In two of these cases, the needle direction was slightly different than the original drilling path resulting in a second hole at the tip of the needle, although without associated complications. In the remaining five of these seven cases, the needle positioning was assumed to be in the correct place based on fluoroscopy. However, upon injection a small amount of the biomaterial was identified within the joint space in two cases and within the periarticular soft tissues in three cases. When leakage of material was discovered, the reposition of the needle was attempted in order to inject in the predefined area. In three cases there was no additional leakage during the following injection. In two cases the injection was cancelled due to persistent leakage during the additional attempts.

To inject the augmentation material along the small diameter of the vertebroplasty needle into the dense intertrabecular bony space, high injection pressure was necessary. During the injection procedure the viscosity of the augmentation materials increased depending on the duration of the procedure. For the second and third injection of each augmentation site, a mallet was required to cautiously push the stylet and force the material along the needle into the bone.

The radiopaque materials were visualized without problems during injection in 208 augmentation sites. In 24 injection sites of 6 sheep of the same group, the material could not be identified with fluoroscopy due to inadequate radio-opacity of the augmentation material. This augmentation material was considered not suitable for injections under fluoroscopic control. In the 20 sham control sites (5 sheep) no material was actually injected and thus, could not be visualized. Leakage of augmentation material was observed in 90 out of 208 injections (43.3%). No differences between the various materials could be allocated. Out of those 90 cases, leakage into the venous circulation occurred in 54 injections (26%),

Klein et al. BMC Musculoskeletal Disorders 2013, 14:200
http://www.biomedcentral.com/1471-2474/14/200

whereas leakage into the medullary cavity was observed in 31 injections (14.9%). Leakage into the periarticular soft tissues was detected in 5 additional cases (2.4%). A higher number of leaks during the injection procedure occurred in the tibia (60%) than in the femur (40%), especially for the second and third injections at the injection sites where higher pressure had to be applied for injection. Despite the high number of biomaterial leaks observed with fluoroscopy, no clinical symptoms indicative of cardiovascular and/or pulmonary distress were recorded in 59 sheep (93,7%). In four animals, cardiovascular complications occurred during surgeries including sudden decrease in arterial blood pressure and end-expired CO_2 by approximately 50%. In those four animals, CT angiography of the thorax revealed embolization with augmentation material and bone marrow, and fat particles. All four animals recovered without additional complications and completed the 12-week follow up successfully. Based on this experience, a randomized and prophylactic CT analysis of subsequent 15 sheep was performed, which demonstrated lung embolization in 13/15 animals undergoing augmentation with injection of biomaterial. In the other two animals (2/15), which belonged to the control group, no embolization was found. Out of the 17 sheep treated with augmentation material and demonstrating embolization, 7 sheep (41.2%) showed embolism caused by bone marrow and fat particles as well as material deposition, while 10/17 sheep (58.8%) revealed embolism due to material only. Overall 202 emboli were found in 17 sheep treated with augmentation material. They occurred in the majority of the cases in the subsegmental artery within the lung vasculature, for bone marrow respectively fat particles (12 emboli) and material (156 emboli), but there were emboli in the segmental (6 fat emboli/24 material emboli) as well as in lobar artery (1 fat emboli/3 material emboli), although in lower incidence with the latter.

Another surgical complication was the breaking of the needle during the extraction procedure from the bone. The needle broke, or rather dismantled at the glued junction between needle and handle. In 4 of 14 cases, the broken part of the needle could not be removed and remained in the bone so that the insertion of the self-tapping screw was not possible. However, no further complications resulted from this event, although the absence of the screw made the coring procedure after sacrifice less precise, and all bone cylinders contained the entire area of interest.

Evaluation

The harvesting process of the tibia and femur at sacrifice were uneventful. μCT, microradiography, and histology were excellent tools to verify needle placement and material distribution within the local anatomic sites. On the one hand, material deposition was still visible and on the other hand bone remodeling alongside the original drill hole and the tip of the needle clearly identified the location.

Due to early termination of one sheep, only 248 samples were further processed for evaluation. The harvesting process itself, in terms of drilling the 32 mm bone cylinder and preparing the area of interest for evaluation, proved to be reproducible and guaranteed a highly standardized analysis in 243/248 samples. Three out of 248 samples had to be excluded from the histological evaluation since the tip of the needle was not centered in the cylinder so that the ground sections were cut in the wrong layer. In the other two, no injection was performed due to needle positioning problems. All other samples could be embedded, cut and prepared for analysis without further complications.

Needle placement could be visualized in the μCT images due to the fact that the original needle path was not yet healed. μCT confirmed the suitability of the surgical method with respect to the consistent placement of the needle in the desired trabecular bony space. Due to the presence of an open physis in the proximal tibia in some animals, the injection resulted in deposition of biomimetic material in the trabecular bone within the physis, in the epiphysis or in the metaphysis (Figure 6). In contrast, injections in the femur resulted in consistent deposition of augmentation material within the distal femoral epiphysis. The μCT evaluation of the control animals showed a relatively high bone volume density (Bone volume/total volume) with thick trabeculae for both, the femora and the tibiae with a 10% higher bone volume density for the tibia metaphysis (approx. 35%) than for the femora (approx. 25%).

With the microradiograph images of the ground sections, the stage of calcification of the bone samples within the area of interest and adjacent to remaining biomaterial could be identified as too could the original and standardized needle positioning (Figure 7). While the ground sections were well suited for the assessment of new bone formation, material resorption, and histomorphometrical measurements (Figure 8a), thin sections enabled distinctions to be made between cellular reactions such as osteoblast activation, inflammatory responses or degradation and elimination of biomaterials through macrophages (Figure 8b, c).

The fluorescence sections represented the area of bone activity at six weeks post surgery (Figure 9a, green colours) and at twelve weeks post surgery (Figure 9b, red colors) and demonstrated the sphere-like shape distribution of the biomaterial. A less colored area was observed in the middle of the injected region, corresponding to the biomaterial degradation process followed by a red and a green area towards the periphery. This pattern

Klein *et al. BMC Musculoskeletal Disorders* 2013, **14**:200
http://www.biomedcentral.com/1471-2474/14/200

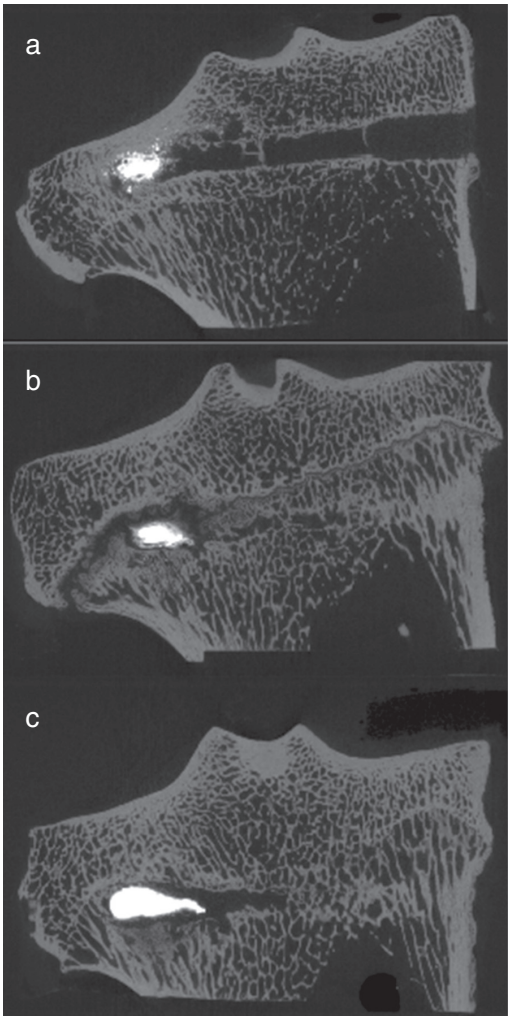

Figure 6 Micro-CT images. Micro-CT images confirmed the suitability of the surgical method with respect to the consistent placement of the needle in the desired trabecular bony space. Due to the presence of an open physis in the proximal tibia in some animals, the injection resulted in deposition of biomimetic material in the trabecular bone within the epiphysis **(a)**, the physis **(b)**, or in the metaphysis **(c)**.

indicated a radial kinetic of new bone formation while biomaterial was being degraded from the periphery towards the center of the injected region (Figure 9).

Discussion

In our study, a femoral and tibial bone augmentation model was successfully established and validated using 63 sheep as an alternative to vertebroplasty in the lumbar area of sheep. In comparison to the lumbar vertebroplasty procedures in sheep, the femoral-tibial

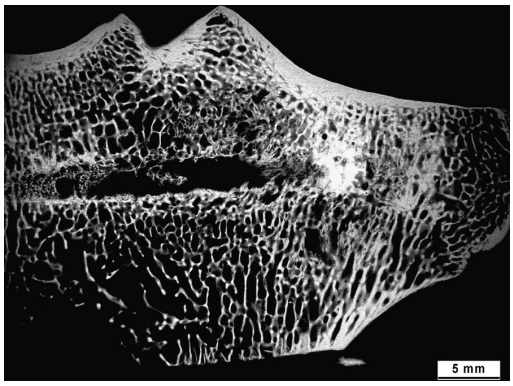

Figure 7 Microradiograph image. This figure shows a microradiograph image of a ground section: Stage of bone calcification in the area of interest and adjacent to remaining biomaterial could be shown.

augmentation model proved to be safe, easy and quick to apply, and additionally showed a high level of standardization including the harvesting of core samples for histology and the histology evaluation. The surgical procedure was limited to 30–40 minutes per side, which was significantly shorter than pilot studies (unpublished data) with lumbar vertebral augmentation in sheep, which lasted for several hours. More importantly, the procedure eliminated severe complications (massive spinal cord injuries) and reduced animal pain and suffering. Moreover, the animal model proved to be adequate to study pulmonary embolism and systemic changes as sequelae to vertebroplasty as they occur in humans.

The animal model presented served well to evaluate new biomimetic materials for their osteoinductive, osteoconductive, and degradation properties as bone augmentation materials. The advantage was that the test-materials could be injected with high accuracy and repeated success within the inter-trabecular spacing of the intact femoral condyle and proximal tibia. This surgical technique required a specially developed aiming device and fluoroscopic imaging. Both are also required for (percutaneous) vertebroplasty in humans. The application and visualization of the injected material in the region of the stifle joint in sheep is much easier compared to the lumbar area, where visualization is impaired by overlying structures (intestines, rumen, transverse processes, etc.). The absence of the third plane using two-dimensional fluoroscopy has to be taken into consideration during needle positioning and injection procedure to avoid injections out of the predefined area, which occurred only in 5/252 needle placements. Solid knowledge of how the trabecular area is distributed within the proximal tibia and experience of the surgeon helps to avoid injections into the bone marrow and/or

Klein *et al. BMC Musculoskeletal Disorders* 2013, **14**:200
http://www.biomedcentral.com/1471-2474/14/200

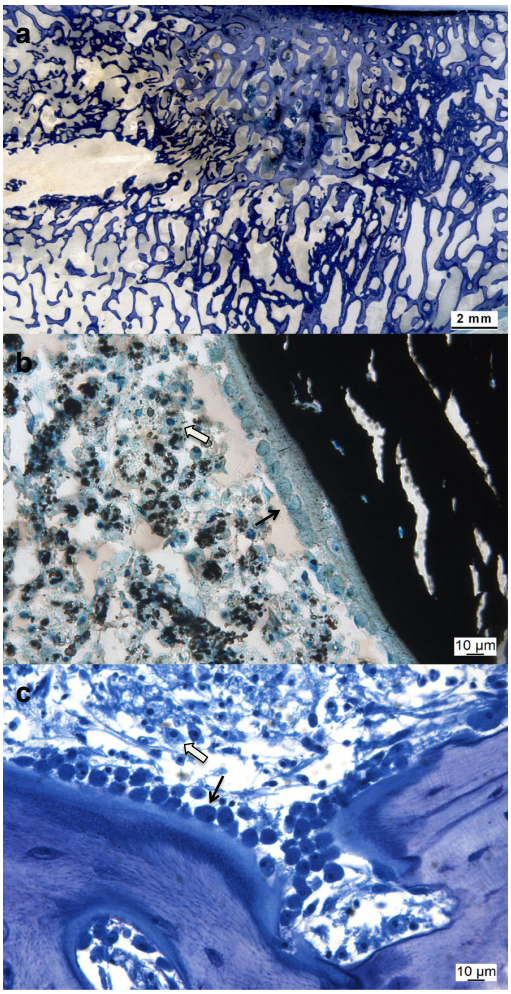

Figure 8 Histology samples. Ground sections (approx. 300 µm, surface stained with toluidine blue) were well suited for assessment of new bone formation, material resorption and histomorphometrical evaluation (Figure **a**), while thin sections allowed assessment of cellular reactions e.g. osteoblast activation (Figure **b**, **c**, thin black arrows) and biomaterial degradation through macrophages (Figure **b, c**, thick white arrows).

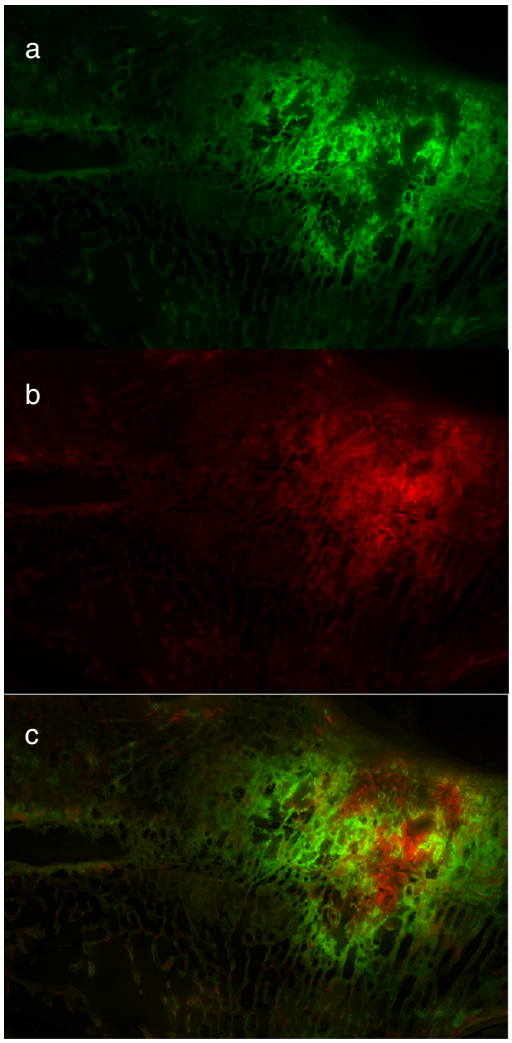

Figure 9 Fluorescence section. These fluorescence images show the bone activity grade at two different time points according to the integrated fluorescent respectively. Figure **a** shows the activity grade at 6 weeks post op (Calcein green), Figure **b** at 12 weeks post op (Xylenol orange), and in Figure **c** both time points are merged together to one image.

penetration of the caudo-lateral cortex of the tibia with the needle.

When comparing the results of Hildebrand *et al.* [23] retrieved from human bone samples with those of Rubin *et al.* [24] from sheep bone, it becomes evident that trabecular bone density is much higher in sheep than in human bone. This comparison of previous findings of other research teams is in alignment with the results of our study presented here. Hildebrand *et al.* measured for samples of lumbar human spine (2. and 4. vertebra) a low bone volume density (8-9%) with small trabeculae, whereas in the current augmentation sheep study bone volume densities between 25-35% for tibiae and femura and even higher values in the study of Rubin *et al.* for medial femoral condyles (49.1 ± 7.1%). This high bone density and thick bone trabecula make the needle placement and the injection procedure more challenging in sheep (personal surgical experience). To place the needle for percutaneous VP in the osteoporotic, brittle human bone, it only has to be tapped with a mallet to engage the cortical bone and afterwards can be pushed forward

Klein *et al. BMC Musculoskeletal Disorders* 2013, **14**:200
http://www.biomedcentral.com/1471-2474/14/200

with manual pressure into the right position [25]. In contrast, in sheep, a hole had to be drilled first to be able to push the needle forward into the trabecular bone with the aid of a mallet. This procedure weakened the needle and caused breakage at the glued junction between needle and it's handle during the extraction procedure of the needle in 14 cases. Due to the fact that the needle could not be extracted in only four cases, and no further complication resulted from this event, the needle type was not changed during this study. For future studies, the use of another type of needle, e.g. with a melted junction (not commercially available at the moment) could be taken into consideration to avoid needle breakage.

During the injection procedure, the viscosity of the augmentation materials increased depending on the duration of the procedure. As such, forced injections under high pressure using a mallet were often necessary for the second and third injections of each injection site along the small diameter of the vertebroplasty needle into the dense intertrabecular bony space of the tibial and femoral bone. This could have led to a higher risk for material extravasation as well as bone marrow and fat particles being forced out into the systemic circulation.

The higher percentage of material leakage detected in the tibia as compared to femur, could be explained by the approximately 10% higher trabecular bone density and thicker trabeculae in the proximal tibia metaphysis than in the femoral condyle, which may have produced higher resistance to the augmentation material. Pulsed jet-lavage of bone marrow and fat was reported to improve injection and lessen the risk of emboli [26]. However, in our hands it did not facilitate injection in a preliminary study and therefore, the fragmented injection technique was invented and applied throughout the study. Although it may not completely mimic vertebroplasty in osteoporotic human bone, it may be considered close enough to test substances in sheep for later use in human bone. During vertebroblasty in humans, leakage of bone cement is also reported as the most common complication [25,27]. Therefore, this animal model could provide important information about the material properties if leakage occurs during the injection procedure. Due to the absence of chest radiographs or CTs after vertebroplasty on asymptomatic human patients, cement leakage and pulmonary emboli occurrence secondary to vertebroplasty may often be underestimated [16]. In the presented study in sheep, CT angiography of 19/63 sheep revealed a high number of asymptomatic pulmonary emboli (13/19 sheep = 68.4%) confirming the opinion of Hulme *et al.* that CT is the best method to detect cement leakage and should be used to report all leaks, including those without clinical signs [16,28,29].

Another consequence of the forced injections of augmentation material was microdamage and microfracture of trabecular bone, which occurred centrally to the injected area, and could be seen in the histology sections as well as in the fluorescence sections. This trabecular damage may be less in human osteoporotic bone due to reduced bone quality and quantitiy (wider trabecular spaces). Alternatively the diminished bone quality may also facilitate microfractures within the trabecular structure, thus resulting in a similar situation as encountered in sheep. Since osteoporotic bone is weaker, but not impaired in proliferation [30], remodeling activities may be similar to those present within our sheep model. As a consequence, a resorption zone around the injected area developed in some cases unrelated to the injected material itself.

Conclusions

This tibia and femur augmentation sheep model proved to be a suitable animal model for screening studies of new biomaterials intended for bone augmentation of trabecular bone and enabled analysis of their biodegradable, biocompatible and osteoconductive properties. It also proved to be adequate for the study of the sequelae of material leakage into the circulation, e.g. pulmonary embolism and following cardiovascular changes.

Overall, we consider it a safe model for the experienced surgeon, resulting in reduced animal suffering and could serve as an excellent basis for testing bone inducing or enhancing materials for vertebroplasty.

Competing interests

The authors declare that they have no competing interests.

Authors' contributions

KKL was the PhD Student and involved in all aspects of the study including writing the manuscript. EZ was involved in developing the model and material. PWK was the anesthetist and was involved in demonstrating embolization. MS was the anesthetist and was involved in demonstrating embolization. KK performed histology and was involved in developing bone sampling. MM was the radiologist and performed all CT including evaluation. TS designed the device and was involved in all aspects of the study. BvR was the head of the experiment, supervisor of PhD Program and was involved in all aspects of the study. All authors read and approved the final manuscript.

Acknowledgements

The authors thank their industrial partners for financing the study.

Disclosure

The study was financed by our industrial partner Kuros Biosurgery AG.

Author details

[1]Musculoskeletal Research Unit (MSRU), Equine Department, University of Zurich, Winterthurerstrasse 260, Zurich CH-8057, Switzerland. [2]Graduate School for Cellular and Biomedical Sciences, University of Bern, Bern, Switzerland. [3]Kuros Biosurgery AG, Technoparkstrasse 1, Zurich 8005, Switzerland. [4]Center for Applied Biotechnology and Molecular Medicine (CABMM), University of Zurich, Winterthurerstrasse 190, Zurich 8057, Switzerland. [5]Veterinary Anaesthesia Services - International (VAS), Zürcherstrasse 39, Winterthur 8400, Switzerland. [6]Division of Diagnostic Imaging, Vetsuisse Faculty, University of Zurich, Winterthurerstrasse 260,

Zurich 8057, Switzerland. [7]Orthopaedic Research Laboratory, McGill University, 687 Pine Avenue West, Montreal, Qc H3A 1A1, Canada.

Received: 15 January 2013 Accepted: 19 June 2013
Published: 2 July 2013

References

1. Turner RT, Maran A, Lotinun S, Hefferan T, Evans GL, Zhang M, Sibonga JD: **Animal models for osteoporosis.** *Rev Endocr Metab Disord* 2001, **2:**117–127.
2. Zhu XS, Zhang ZM, Mao HQ, Geng DC, Zou J, Wang GL, Zhang ZG, Wang JH, Chen L, Yang HL: **A novel sheep vertebral bone defect model for injectable bioactive vertebral augmentation materials.** *J Mater Sci Mater Med* 2011, **22:**159–164.
3. Galovich LA, Perez-Higueras A, Altonaga JR, Orden JM, Barba ML, Morillo MT: **Biomechanical, histological and histomorphometric analyses of calcium phosphate cement compared to PMMA for vertebral augmentation in a validated animal model.** *Eur Spine J* 2011, **20**(Suppl 3)**:**376–382.
4. Cotten A, Boutry N, Cortet B, Assaker R, Demondion X, Leblond D, Chastanet P, Duquesnoy B, Deramond H: **Percutaneous vertebroplasty: state of the art.** *Radiographics* 1998, **18:**311–320. discussion 320–313.
5. Benneker LM, Gisep A, Krebs J, Boger A, Heini PF, Boner V: **Development of an *in vivo* experimental model for percutaneous vertebroplasty in sheep.** *Vet Comp Orthop Traumatol* 2012, **25:**173–177.
6. Krebs J, Ferguson SJ, Hoerstrup SP, Goss BG, Haeberli A, Aebli N: **Influence of bone marrow fat embolism on coagulation activation in an ovine model of vertebroplasty.** *J Bone Joint Surg Am* 2008, **90:**349–356.
7. Krebs J, Ferguson SJ, Nuss K, Leskosek B, Hoerstrup SP, Goss BG, Shaw S, Aebli N: **Plasma levels of endothelin-1 after a pulmonary embolism of bone marrow fat.** *Acta Anaesthesiol Scand* 2007, **51:**1107–1114.
8. Aebli N, Krebs J, Schwenke D, Davis G, Theis JC, Aebli N, Krebs J, Schwenke D, Davis G, Theis JC: **Cardiovascular changes during multiple vertebroplasty with and without vent-hole: an experimental study in sheep.** *Spine (Phila Pa 1976)* 2003, **28:**1504–1511. discussion 1511–1502.
9. Boger A, Benneker LM, Krebs J, Boner V, Heini PF, Gisep A: **The effect of pulsed jet lavage in vertebroplasty on injection forces of PMMA bone cement: an animal study.** *Eur Spine J* 2009, **18:**1957–1962.
10. Aebli N, Krebs J, Davis G, Walton M, Williams MJ, Theis JC: **Fat embolism and acute hypotension during vertebroplasty: an experimental study in sheep.** *Spine (Phila Pa 1976)* 2002, **27:**460–466.
11. Aebli N, Krebs J, Schwenke D, Davis G, Theis JC, Aebli N, Krebs J, Schwenke D, Davis G, Theis JC: **Pressurization of vertebral bodies during vertebroplasty causes cardiovascular complications: an experimental study in sheep.** *Spine (Phila Pa 1976)* 2003, **28:**1513–1519. discussion 1519–1520.
12. Rapado A: **General management of vertebral fractures.** *Bone* 1996, **18:**191S–196S.
13. Old JL, Calvert M: **Vertebral compression fractures in the elderly.** *Am Fam Physician* 2004, **69:**111–116.
14. Lewis G: **Percutaneous vertebroplasty and kyphoplasty for the stand-alone augmentation of osteoporosis-induced vertebral compression fractures: present status and future directions.** *J Biomed Mater Res B Appl Biomater* 2007, **81:**371–386.
15. Lavelle W, Carl A, Lavelle ED, Khaleel MA: **Vertebroplasty and kyphoplasty.** *Anesthesiol Clin* 2007, **25:**913–928.
16. Hulme PA, Krebs J, Ferguson SJ, Berlemann U, Hulme PA, Krebs J, Ferguson SJ, Berlemann U: **Vertebroplasty and kyphoplasty: a systematic review of 69 clinical studies.** *Spine (Phila Pa 1976)* 2006, **31:**1983–2001.
17. Garfin SR, Yuan HA, Reiley MA: **New technologies in spine: kyphoplasty and vertebroplasty for the treatment of painful osteoporotic compression fractures.** *Spine (Phila Pa 1976)* 2001, **26:**1511–1515.
18. Lemke DM: **Vertebroplasty and kyphoplasty for treatment of painful osteoporotic compression fractures.** *J Am Acad Nurse Pract* 2005, **17:**268–276.
19. Phillips FM, Pfeifer BA, Lieberman IH, Kerr EJ 3rd, Choi IS, Pazianos AG: **Minimally invasive treatments of osteoporotic vertebral compression fractures: vertebroplasty and kyphoplasty.** *Instr Course Lect* 2003, **52:**559–567.
20. Wilke HJ, Kettler A, Wenger KH, Claes LE: **Anatomy of the sheep spine and its comparison to the human spine.** *Anat Rec* 1997, **247:**542–555.
21. Wilke HJ, Kettler A, Claes LE: **Are sheep spines a valid biomechanical model for human spines?** *Spine (Phila Pa 1976)* 1997, **22:**2365–2374.
22. Turner AS: **The sheep as a model for osteoporosis in humans.** *Vet J* 2002, **163:**232–239.
23. Hildebrand T, Laib A, Muller R, Dequeker J, Ruegsegger P: **Direct three-dimensional morphometric analysis of human cancellous bone: microstructural data from spine, femur, iliac crest, and calcaneus.** *J Bone Miner Res* 1999, **14:**1167–1174.
24. Rubin C, Turner AS, Muller R, Mittra E, McLeod K, Lin W, Qin YX: **Quantity and quality of trabecular bone in the femur are enhanced by a strongly anabolic, noninvasive mechanical intervention.** *J Bone Miner Res* 2002, **17:**349–357.
25. Moreland DB, Landi MK, Grand W: **Vertebroplasty: techniques to avoid complications.** *Spine J* 2001, **1:**66–71.
26. Benneker LM, Heini PF, Suhm N, Gisep A, Benneker LM, Heini PF, Suhm N, Gisep A: **The effect of pulsed jet lavage in vertebroplasty on injection forces of polymethylmethacrylate bone cement, material distribution, and potential fat embolism: a cadaver study.** *Spine (Phila Pa 1976)* 2008, **33:**E906–E910.
27. Phillips FM, Todd Wetzel F, Lieberman I, Campbell-Hupp M, Phillips FM, Todd Wetzel F, Lieberman I, Campbell-Hupp M: **An *in vivo* comparison of the potential for extravertebral cement leak after vertebroplasty and kyphoplasty.** *Spine (Phila Pa 1976)* 2002, **27:**2173–2178. discussion 2178–2179.
28. Yeom JS, Kim WJ, Choy WS, Lee CK, Chang BS, Kang JW: **Leakage of cement in percutaneous transpedicular vertebroplasty for painful osteoporotic compression fractures.** *J Bone Joint Surg Br* 2003, **85:**83–89.
29. Schmidt R, Cakir B, Mattes T, Wegener M, Puhl W, Richter M: **Cement leakage during vertebroplasty: an underestimated problem?** *Eur Spine J* 2005, **14:**466–473.
30. Rodan GA, Martin TJ: **Therapeutic approaches to bone diseases.** *Science* 2000, **289:**1508–1514.

doi:10.1186/1471-2474-14-200
Cite this article as: Klein *et al.*: Bone augmentation for cancellous bone-development of a new animal model. *BMC Musculoskeletal Disorders* 2013 **14**:200.

3 Feasibility Study of a Standardized Novel Animal Model for Cervical Vertebral Augmentation in Sheep Using a PTH Derivate Bioactive Material

3.1 Aim of the study

(1) Investigation of the scaled effects of a PTH derivate bioactive material for new bone formation in sheep. Different concentrations of TGplPTH$_{1–34}$ were used as bio-enhancers, incorporated in a best performing fibrin matrix formulation tested in previous studies.

(2) Development of a novel, highly standardized model for vertebral augmentation in sheep. Cervical vertebrae were chosen for reasons of the best possible reproducibility and standardization of the model with respect to the surgical techniques and overall evaluation methods implied.

3.2 Main conclusions

Our cervical augmentation model in sheep has proven to be a suitable animal model to evaluate biocompatibility and bone formation of new biomaterials developed for vertebral bone augmentation. Although the model revealed to be more challenging, mainly due to the onset of cardiovascular complications, not previously seen in the femoral and tibia augmentation model, the observation reflected well the human situation.

Nevertheless, bone formation results demonstrated that the TGplPTH$_{1-34}$ was safe to use in sheep, since no signs of inflammation were detected and fast biomaterial degradation took place. All treatment groups were more effective than the sham control. Among these, the medium concentration of TGplPTH$_{1-34}$ induced the best bone enhancing effect. Whether this effect would also be elicited in osteoporotic bone in humans is speculative at this point. Because no suitable true osteoporotic, large animal model exists this could only be verified in a human clinical trial.

3.3 Contribution to this publication

I was profoundly involved in all aspects of the study including performing the surgeries and evaluation as well as writing the manuscript.

3.4 Publication reference

Klein K, Schense J, Kronen PW, Fouche N, Makara M, Kämpf K, Steffen T, von Rechenberg B. Feasibility Study of a Standardized Novel Animal Model for Cervical Vertebral Augmentation in Sheep Using a PTH Derivate Bioactive Material. *Vet.Sci.* **2014**, *1*,96-120; doi: 10.3390/vetsci1020096

Vet. Sci. **2014**, *1*, 96-120; doi:10.3390/vetsci1020096

OPEN ACCESS

veterinary sciences

ISSN 2306-7381

www.mdpi.com/journal/vetsci

Article

Feasibility Study of a Standardized Novel Animal Model for Cervical Vertebral Augmentation in Sheep Using a PTH Derivate Bioactive Material

Karina Klein [1,2,*], Jason Schense [3], Peter W. Kronen [1,4,5], Nathalie Fouche [1], Mariano Makara [6], Katharina Kämpf [1], Thomas Steffen [7] and Brigitte von Rechenberg [1,4]

1 Musculoskeletal Research Unit (MSRU), Equine Department, University of Zurich, Winterthurerstrasse 260, CH-8057 Zurich, Switzerland; E-Mails: nathalie.fouche@web.de (N.F.); kkaempf@vetclinics.uzh.ch (K.K.); bvonrechenberg@vetclinics.uzh.ch (B.R.)

2 Graduate School for Cellular and Biomedical Sciences, University of Bern, CH-3012 Bern, Switzerland

3 Kuros Biosurgery AG, Technoparkstrasse 1, CH-8005 Zurich, Switzerland; E-Mail: jason.schense@kuros.ch

4 Center for Applied Biotechnology and Molecular Medicine (CABMM), University of Zurich, Winterthurerstrasse 190, CH-8057 Zurich, Switzerland

5 Veterinary Anaesthesia Services - International (VAS), Zürcherstrasse 39, CH-8400 Winterthur, Switzerland; E-Mail: peter.kronen@vas-int.com

6 Division of Diagnostic Imaging, Vetsuisse Faculty, University of Zurich, Winterthurerstrasse 258c, CH-8057 Zurich, Switzerland; E-Mail: mariano.makara@gmail.com

7 Orthopaedic Research Laboratory, Department of Surgery, McGill University Hospital Center, 687 Pine Avenue West, Montreal, QC H3A 1A1, Canada; E-Mail: tsteffen@orl.mcgill.ca

* Author to whom correspondence should be addressed; E-Mail: kklein@vetclinics.uzh.ch; Tel.: +41-44-63-58-864.

Received: 29 May 2014; in revised form: 25 July 2014 / Accepted: 30 July 2014 / Published: 4 August 2014

Abstract: Prophylactic local treatment involving percutaneous vertebral augmentation using bioactive materials is a new treatment strategy in spine surgery in humans for vertebral bodies at risk. Standardized animal models for this procedure are almost non-existent. The purpose of this study was to: (i) prove the efficacy of PTH derivate bioactive materials for new bone formation; and (ii) create a new, highly standardized cervical vertebral augmentation model in sheep. Three different concentrations of a modified form of parathyroid hormone (PTH) covalently bound to a fibrin matrix containing strontium carbonate were used. The same matrix without PTH and shams were used as controls. The bioactive materials were

Vet. Sci. **2014**, *1* **97**

locally injected. Using a ventral surgical approach, a pre-set amount of material was injected under fluoroscopic guidance into the intertrabecular space of three vertebral bodies. Intravital fluorescent dyes were used to demonstrate new bone formation. After an observation period of four months, the animals were sacrificed, and vertebral bodies were processed for μCT, histomorphometry, histology and sequential fluorescence evaluation. Enhanced localized bone activity and new bone formation in the injected area could be determined for all experimental groups in comparison to the matrix alone and sham with the highest values detected for the group with a medium concentration of PTH.

Keywords: vertebral augmentation; cervical spine; animal model; fibrin matrix; PTH derivate; sheep

1. Introduction

Symptomatic compression fractures of vertebral bodies occurring secondary to osteoporosis or neoplasia are a major public health problem in our aging society [1–5]. These fractures may cause persistent, often excruciating pain, spinal instability and kyphotic deformity, all of which potentially impair mobility and reduce the patient's quality of life [5–7]. Nowadays, percutaneous vertebroplasty (VP) is the treatment of choice to mechanically augment the spine. It is a successful, minimally invasive surgical procedure [8–10], which seems to be significantly better than non-surgical treatment in terms of pain relief, reduced hospital stay and recovery period [11]. The VP technique is performed through needle-injection of polymethylmethacrylate (PMMA) bone cement into a collapsed or weakened vertebra, this to stabilize, decompress or avoid further compression fractures (prophylactic VP). Common complications during the surgical procedure are bleeding at the puncture site, local infection and cement leakage into the spinal canal, the paravertebral tissues or the perivertebral venous system [12]. Cement extravasation, as well as bone marrow or fat cells forced out of the vertebra into the systemic circulation may lead to pulmonary embolism (PE), either without clinical signs or with severe cardiac distress symptoms, including death [5].

It is well known that PMMA increases the strength and stiffness of the injected vertebral bodies, but in the absence of osteoinductive properties and the inability to be degraded and replaced by new bone, it will remain just a placeholder. It may also lead to long-term complications, such as damage to neurons, toxicity or fracture of adjacent vertebral bodies [3,13]. Therefore, the search for new, preferably resorbable biomaterials, containing locally-released bioactive agents with osteoinductive properties to strengthen and regenerate weakened vertebral bodies is ongoing. Especially adjacent to the index level that was augmented with PMMA for immediate stability, enhancing local bone formation may in the future avoid in systemically-ill osteoporotic patients a domino effect of adjacent vertebral compression fractures [14].

A truncated form of the human parathyroid hormone (PTH_{1-34}) is already used as a registered pharmaceutical product for osteoporosis treatment. Intermittent systemic injections of PTH_{1-34} have shown anabolic effects on cancellous bone, resulting in increased bone mineral density [15]. PTH is able to bind directly to a cell surface receptor on osteoblasts, regulating the production of various

cytokines (insulin-like growth factor 1, transforming growth factor β1, interleukin 1 (IL-1) and IL-6) and, thus, represents a strong anabolic agent for osteoblast precursors and an indirect anabolic factor for osteoclasts (IL-1 and IL-6) [15–17]. It regulates the balance between osteoblasts and osteoclasts, as well, thereby exerting a direct effect on bone turnover [15], and plays a primary role in calcium homeostasis [18]. In contrast to systemic use, a novel recent strategy is to use an engineered peptide variant of the active fragment of parathyroid hormone ($PTH_{1–34}$) that is enzymatically incorporated within a fibrin matrix via the coagulation transglutaminase (TG) factor XIIIa to translate the systemically used molecule into a local bone-inducing therapeutic agent [19]. The incorporation of a plasmin substrate sequence linker (pl) enables the cleavage of the peptide by endogenous plasmin. Via cell migration and infiltration, the peptide is activated and released only into the surrounding tissue for the local increase of bone formation. In previous *in vivo* studies using a tibia and femur augmentation model in sheep, various concentrations of this engineered parathyroid hormone ($TGplPTH_{1–34}$), incorporated in different formulations of fibrin matrices, has already shown good results [20]. However, it was unknown whether these results could actually be reproduced in the vertebral bodies, this due to its different anatomical structure, including high vascularity and sinus formations.

Safety aspects concerning the augmentation procedure must be considered, such that good visibility of the material during injection is key to avoid leakage into the spinal canal and damage to the spinal cord. Furthermore, the rheological properties of the material during injection are critical to avoid leakage into the vascular system, possibly causing pulmonary embolism or death. The radiopaque inorganic salt powder strontium carbonate has proven to be a good contrast agent. Strontium is also known to have positive effects on bone formation and for its capability to decrease bone resorption [21,22]. Different studies have shown that strontium could induce the replication of osteoblasts [23] and, concurrently, the apoptosis of osteoclasts [24] using a pathway involving the extracellular calcium-sensing receptor (CaR). An *in vivo* study of Yang *et al*. using a calvarial defect model in rats showed that locally-delivered strontium was able to act as a bone anabolic agent and could activate the Wnt/*β*-catenin signaling pathway, resulting in an accumulation of extracellular matrix, as well as enhanced osteogenesis and bone remodeling [25].

Good animal models for vertebral augmentation are rare. The sheep has been used as an experimental animal model for augmentation in the lumbar spine, although mainly for studying acute cardiovascular changes and embolization with immediate sacrifice on the table after augmentation [26–30]. Due to the different morphology of ovine vertebral bodies with a more trapezoid and slim vertebral body format compared to a round, solid and almost rectangular human vertebral body, a transpedicular approach for vertebral augmentation is highly hazardous and difficult to standardize in the lumbar area in sheep. Therefore, a new, highly standardized augmentation model in the cervical spine of sheep was developed for these experiments, where a ventral approach and customized instrumentation guaranteed the high reproducibility of the augmentation procedure. Apart from the safe deposition of the augmentation material, this model also involved a risk of pulmonary embolism similar to that found with human vertebral augmentation. Therefore, the study results may be better transferable to the human vertebral bone structure.

The aim of this study was to: (i) investigate the scaled effects of PTH derivate bioactive material as an enhancer for new bone formation in sheep; and (ii) create a novel, highly standardized animal model for vertebral augmentation in sheep. To reach aim (i), different concentrations of $TGplPTH_{1–34}$, incorporated in the best performing fibrin matrix formulation from previous studies, were used as

bioenhancers. For aim (2), cervical vertebrae in sheep were targeted focusing on the reproducibility and standardization of the model, including the surgical technique and overall evaluation. To the knowledge of the authors, this is the first report for both using the local application of an engineered peptide variant ($TGplPTH_{1–34}$) as a bioactive agent and reporting a standardized animal model in the cervical spine of sheep.

2. Material and Methods

2.1. Study Design and Experimental Animals

Seventeen adult female Swiss alpine sheep with a mean age of 3.2 years (range from 2 to 5 years) and a mean weight of 72.6 kg (54–89 kg) were used for this study, conducted adhering to the Swiss regulations of Animal Welfare (TSchG 455), with a specific permission granted by the federal authorities (Application No. 151/2009).

Using a cervical vertebral augmentation model in sheep, three different concentrations of a modified form of parathyroid hormone ($TGplPTH_{1-34}$) covalently bound to a fibrin matrix containing strontium carbonate, the same matrix without any $TGplPTH_{1-34}$, as well as sham controls were tested and compared. Three vertebrae per sheep were augmented. Each group consisted of three sheep, with the exception of Group 2, where two sheep died during surgery, and therefore, two additional sheep were used (for the group distribution, see Table 1).

Table 1. Group distribution and clinical signs of pulmonary embolism. PTH, parathyroid hormone; PE, pulmonary embolism.

Group	Material	Number of animals	Number of evaluated vertebra	Clinical signs of pulmonary embolism
Matrix alone	FS+SrCO3	3	8	2× mild clinical signs
Low	FS+SrCO3+PTH low conc.	5	9	2× severe clinical signs led to death, 1× mild clinical signs
Medium	FS+SrCO3+PTH low conc.	3	8	1× mild clinical signs
High	FS+SrCO3+PTH low conc.	3	9	1× mild clinical signs
Sham	No materials	3	9	

FS: Fibrin scaffold; SrCO3: Strontium carbonate; PTH low-high: TGplPTH1-34 concentration low-high; Mild clinical signs of PE: intermittend bradycardia, Hypercapnia and mild oxygen desaturation

Using a ventral surgical approach and a customized aiming device, a fixed amount of biomaterial per vertebra (1–1.5 mL) was injected under fluoroscopic guidance in a standardized trajectory and to a standardized depth into the intertrabecular space of three vertebral bodies per sheep (between C2–C6). For the sham controls, the same procedure was performed without material injection. To detect pulmonary emboli, non-invasive airway dead space measurements were performed during surgery, as well as CT angiography of the thorax in all sheep prior to and after surgery [31]. After 16 weeks of follow-up, the sheep were sacrificed, and the harvested vertebral bodies were further processed for macroscopic assessment (signs of inflammation and irritation), μCT analysis and histology, including histomorphometry and evaluation of fluorescent dye incorporation.

2.2. Test Material

Three different concentrations (low, medium, high) of a modified inactivated form of PTH_{1-34} ($TGplPTH_{1-34}$) with a transglutaminase hook (TG-Hook) were evaluated (pending patent application) [19]. Using the TG-hook, the peptide was covalently bound and immobilized onto a fibrin matrix during the coagulation process and later locally released *in vivo* and activated by plasmin-induced proteolytic cleavage (via a plasmin substrate sequence linker (pl)) after cellular infiltration and replacement of the fibrin matrix with a newly secreted extra-cellular matrix. As a contrast agent for better radio-opacity and to improve the rheological properties during the injection procedure, 40% weight volume (w/v) strontium carbonate was added to the formulation. In one of the test groups, only the fibrin matrix including the strontium carbonate was used without PTH_{1-34}.

2.3. Instruments/Equipment

In addition to the routine surgical instruments, a customized aiming device was developed to guarantee the reproducibility of surgical access and to standardize the access point on the bone surface for injection into the trabecular bone of the vertebral body (Figure 1a–c). Using a ventral surgical approach, the aiming device allows an exact drilling and subsequent positioning of the injection needle. This can be achieved via a central drill guide that is positioned on the promontorium of the caudal aspect of the vertebral body (Figure 1a), an aiming targeting tip lined up with the vertebra midline and two sharp long fixation dents (beside the midline) resting on the cranial deeper part of the vertebral body. An oval hole allows monitoring the drill guide tip placed on the promontorium while the drill guide remains positioned (Figure 1b).

Figure 1. This figure shows the aiming device in a correct position using a ventral approach to the vertebral body. (**a**) The lateral view represents the central drill guide in the correct position on the promontorium of the caudal aspect of the vertebral body. (**b**) The craniocaudal view shows the drill guide positioned on the promontorium, with an aiming targeting tip lined up with the vertebra midline and two sharp long dents, arranged symmetrically lateral of the midline, resting on the cranial deeper part of the vertebral body. In (**c**), the aiming device is shown as a whole with the handle, central drill guide and fixation dents.

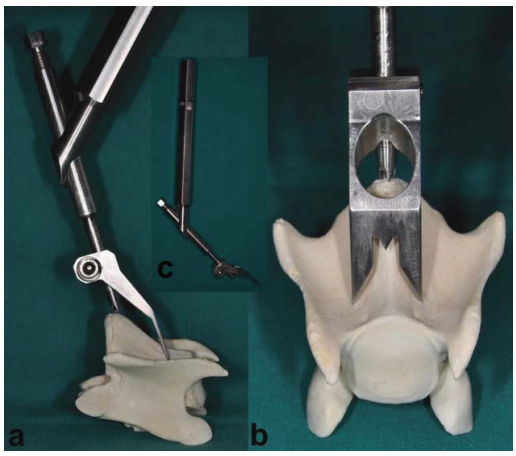

For injection of augmentation material, a 10 G (3.2-mm diameter) 100 mm-long special vertebroplasty needle (1394-1010, Optimed Medizinische Instrumente GmbH, Ettlingen, Germany) (Figure 2b) and an Optimed CementoRE gun (1392-0000, Optimed Medizinische Instrumente GmbH, Ettlingen, Germany) were used (Figure 2c).

Figure 2. The images (**a**–**e**) show the different steps of the surgical procedure: (**a**) an aiming device was used for repeatable and standardized drilling; (**b**) the vertebroplasty needle was correctly positioned; (**c**) material injection was performed in multiple steps using the Optimed CementoRE gun. Fluoroscopic imaging was used for repeatable and standardized drilling (**d**) and to detect material leakage during injection, as seen in (**e**), where leakage into vertebral vessels was detected at the caudal part of the two injected vertebrae (see the →).

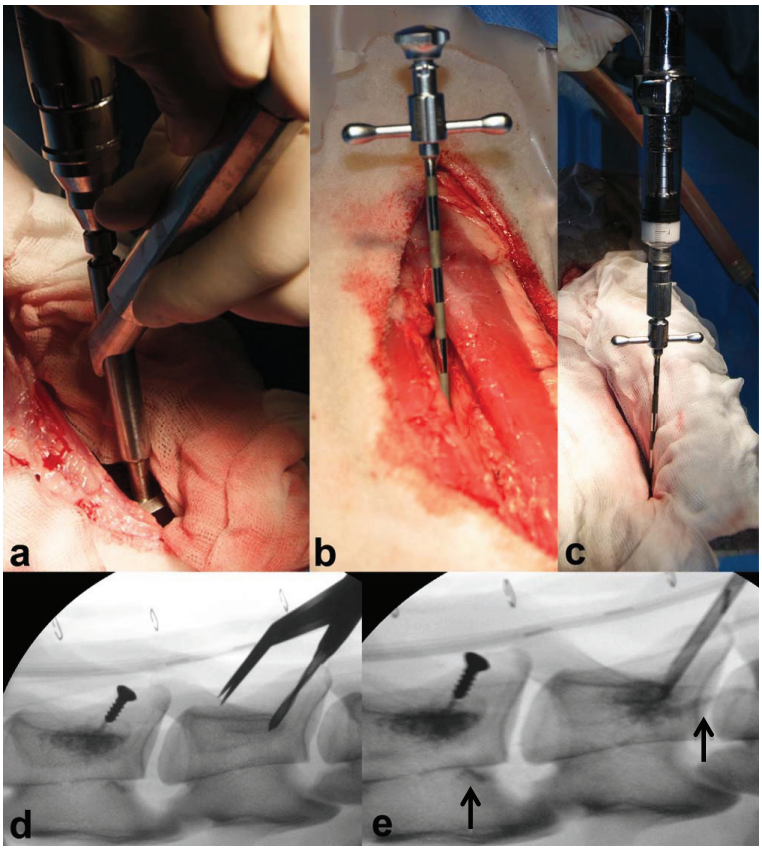

2.4. Anesthesia

A standard anesthetic protocol was used. After 24 hours of fasting and 30 minutes before induction of anesthesia, the animals were premedicated with buprenorphine (Temgesic®, 0.01 mg/kg i.m., Essex Chemie AG, Lucerne, Switzerland) and xylazine (Rompun® 2%, 0.1 mg/kg i.m., Streuli Pharma, Uznach, Switzerland). A catheter was placed into the vena cephalica antebrachii of one of the front legs and prophylactic antibiotics (Penicillin Natrium® 35,000 IU/kg i.v., G. Streuli Pharma, Uznach,

Switzerland; gentamicin, Vetagent®, 4 mg/kg i.v., Veterinaria AG, Zurich, Switzerland), as well as a pre-emptive analgesic drug, carprofen (Rimadyl®, 4 mg/kg i.v., Pfizer SA, Zurich, Switzerland), were given intravenously. A booster for tetanus (Tetanus Serum Intervet, 3,000 IU/sheep s.c., Veterinaria AG Zurich, Switzerland) was administered subcutaneously.

Anesthesia was induced with diazepam (Valium®, 0.1 mg/kg i.v., Roche Pharma AG, Rheinach, Switzerland), ketamine (Narketan 10®, 3 mg/kg i.v., Vetoquinol AG, Belp-Bern, Switzerland) and propofol (Propofol®, 0.4–2 mg/kg i.v., Fresenius Kabi, Stans, Switzerland), the latter administered to effect. After laryngeal desensitization with lidocaine spray (xylocaine spray 10%, 3 pumps of 0.1 mL each, Astra Zeneca AG, Zug, Switzerland), the trachea was intubated and correct placement was confirmed by expired carbon dioxide monitoring ($F_{et}CO_2$). Anesthesia was maintained with a balanced anesthetic protocol employing the administration of isoflurane (1%–2%) in oxygen via an adult F-circuit (circle system, Intersurgical, Berkshire, U.K.), a variable rate infusion of propofol (Propofol®, 0.5–1 mg/kg/h, Fresenius Kabi, Stans, Switzerland), as well as lidocaine given at the beginning of the surgical procedure as bolus (1 mg/kg) and afterwards as constant rate infusion (Lidocaine®, 40 μg/kg/min, Kantonsapotheke, Zurich, Switzerland).

Monitoring parameters included electrocardiogram (ECG), heart rate, pulse rate and invasively measured blood pressures (systolic, mean and diastolic arterial) via an arterial catheter in an auricular artery. Furthermore, inspired and expired concentrations of carbon dioxide, oxygen and isoflurane, as well as esophageal temperature and saturation of arterial blood (SpO_2) were monitored. All parameters were constantly measured and recorded in 10-minute intervals. Intraoperatively, fluids Ringer's lactate solution (Ringer Lactat®, Bichsel, Interlaken, Switzerland) was administered at a rate of 10 mL/kg/h, and heat was applied using a forced-air warming device (Bair Hugger® 505, Augustine Healthcare, Eden Prairie, MN, USA).

Intermittent positive pressure ventilation was applied (if needed) to maintain normocapnia. A Swan-Ganz-catheter was inserted via the jugular vein into the pulmonary artery to allow invasive measurements of pulmonary artery pressure and cardiac output. Physiologic airway dead space measurements were performed with the non-invasive cardiac output monitor, NICO® (Respironics Novametrix, Inc., Wallingford, CT, USA). The results of this comparison between invasive and non-invasive measurements are not included in this paper and will be described elsewhere.

2.5. Surgical Procedure

The anesthetized sheep were placed in dorsal recumbency with the forelimbs retracted caudally and fixed to the surgery table. The neck was bent slightly upwards for an easier approach to the vertebral bodies. The correct position of the sheep was further supported with an inflatable surgery mat, rubber foam rolls and wedges. To prevent bloating and regurgitation, a stomach tube was placed prior to surgery. The tube was maintained throughout the entire surgery until recovery in sternal recumbency. The ventral aspect of the neck was shaved and surgically scrubbed and cleansed. The animals were draped according to routine. A midline skin incision was performed from the pharyngeal region extending caudally to the level of the thoracic inlet. The subcutis and superficial facial planes were bluntly dissected to expose sternohyoid and pharyngeal muscles. A blunt and careful dissection was made in the midline in between the left and right sternohyoid muscles. The jugular vein, carotid artery,

vagal nerve, trachea and oesophagus were carefully retracted using a blunt retractor wrapped in gauze. Exposure of the ventral aspect of the vertebral bodies was maintained by securing the retractors in place. The desired vertebra was identified by palpating the transverse processes and the intervertebral spaces. The identification of the area of interest was performed using two anatomical landmarks: the promontorium caudal to the desired vertebral body and the deeper laying cranial aspect of the vertebra. The muscles covering the caudal aspect of the vertebral body were bluntly divided to expose the area of interest. Hemostasis was meticulously kept using electrocautery. The aiming device was placed with the tip of the drill guide at the promontorium in the cranial drill direction (Figure 1a–c).

Under fluoroscopic control, the correct placement of the aiming device and subsequent needle positioning was validated to avoid inaccurate injections. A drill hole with a diameter of 2.8 mm was created in the vertebral body (Figure 2a) followed by placing the special vertebroplasty needle using a Kirschner wire as guide for the correct direction of the needle path. Afterwards, the needle was pushed forward, till its tip was firmly seated and surrounded by bone (Figure 2b).

Material injections were done in multiple steps under fluoroscopic guidance (Figure 2e). Needle filling with augmentation material was done slowly with the aid of the Optimed CementoRE gun (Figure 2c). Subsequently, the gun was removed, and the stylet was used to push the material into the bone, so as to provide exact quantities of injectate. The filling-clearing procedure was repeated one or two times, until a target between 1.5 and 1.8 mL was injected within the intertrabecular space. Using fluoroscopy, the leakage of material into a vessel and thrombus formation was recorded, the injection needle slightly advanced and injection continued. At completion of the procedure, the vertebroplasty needle was removed and the insertion point closed with a 3.5-mm diameter self-tapping screw (8 mm in length, Synthes, Oberdorf, Switzerland) (Figure 2d and 2e). The screw was used to later determine the direction of the needle and insertion point at the time of sacrifice.

Afterwards, the muscles were repositioned, and the closure of the soft tissue was routinely done using resorbable suture material (Vicryl® polyglactin, 2-0, Johnson & Johnson Int., Brussels, Belgium) in a simple continuous fashion, while the skin was closed with a skin stapler (Appose ULV, United States Surgical). The Swan-Ganz catheter was removed, and a normal catheter (Vygonyle S® G14, Vygon GmbH, Aachen, Germany) was placed in the other jugular vein. Intra-operative fluoroscopy images were taken in right lateral view throughout the surgery to document the surgical technique and the injection steps. Immediately after surgery, fluoroscopy images in latero-lateral and ventrodorsal view were taken to document the distribution of the injected material in two projection plans.

2.6. Postoperative Treatment

The animals were supervised during recovery from anesthesia until they could stand on their own, walk around and eat without further complications. They were kept in small groups, and their health status was checked twice daily. Antibiotic and analgesia administrations were continued for 4 days intravenously using the same dosage as perioperatively applied.

Additional analgesia treatment was provided to reduce postoperative pain using intramuscular injections of buprenorphine (Temgesic®, 0.01 mg/kg, Essex Chemie AG, Luzern, Switzerland) every 4 hours for a total of three applications.

2.7. In Vivo Fluorescence Labeling

Different fluorescence markers were subcutaneously injected at 6 weeks (calcein green, 5 mg/kg BW s.c., Fluka AG, Buchs, Switzerland), 12 weeks (xylenol orange, 90 mg/kg BW s.c., Fluka AG) and three days prior to sacrifice (oxytetracycline, 20 mg/kg BW s.c., Engemycin® 10%, MSD Animal health GmbH, Lucerne, Switzerland) to dynamically represent new bone formation and remodeling.

2.8. Sacrifice and Specimen Preparation for Evaluative Procedures

All animals were sacrificed after a follow up period of 16 weeks, and the three treated cervical vertebrae were harvested for final analysis. Augmentation sites were examined macroscopically, and digital photographs were taken to document tissue reaction at the surgical site (Nikon Digital Camera D5000, 2009 Nikon Corporation©). Radiographs were taken using a Faxitron (Faxitron X-Ray Systems, Hewlett Packard, Mc Minnville Division, OR, USA) to visualize the detailed bone structure and detect remaining augmentation material. Subsequently, each vertebra was cut in a smaller segment containing only the injected vertebral body for evaluative procedures. An additional radiograph was performed to qualitatively assess new bone formation in the vertebral bodies. The bone samples were fixed in 40% ethanol for one week, followed by a series of ethanol dehydration steps (50%–100%) within 6 days. μ-CT analysis of the specimen was performed in 70% ethanol fixation (b-cube AG, Bio-Technopark, Schlieren-Zurich, Switzerland). After complete dehydration, the samples were degreased in xylene and subsequently infiltrated in liquid methymethacrylate (MMA) until polymerization occurred [20]. Using a special band saw (EXAKT® Band System 300/301, EXAKT® Apparatebau GmbH &Co KG, Norderstedt, Germany), cutting of the ground sections (300 μm) and native fluorescence sections (350 μm) were performed. The sections were oriented along the original needle path in the midline of the vertebral body, with the needle path itself, the tip of the needle and the surrounding tissue defined as the region of interest. Before mounting (Cementit® CA 12, Merz + Benteli AG, Niederwangen, Switzerland) the sections on plastic slides (ACROPAL, Maagtechnic, Duebendorf, Switzerland), microradiographs were taken with the Faxitron (27 kV, 11 s; Fuji Photo Film Co Ltd, Tokyo, Japan). Ground sections were polished (Exakt® Mikro- Schleifsystem 400CS, Exakt Apparatebau GmbH, Norderstedt, Germany) and surface stained with toluidine blue. The native sections for fluorescence were mounted on pellucid, acrylic Plexiglas slides (Maagtechnic, Duebendorf, Switzerland) and wrapped in aluminum foil to protect slides from bleaching. For thin section preparation, the remaining bone blocks were cut in smaller segments comprising only the tip of the needle and surrounding tissue. Polymerization was achieved in special customized Teflon forms (D. Nadler, JOSSI AG, Islikon, Switzerland) [20]. Afterwards, the small blocks were mounted on plastic frames and cut using a microtome (Leica® RM 2155, Leica Instruments GmbH). After mounting on glass slides and pressing for two days in the incubator, the sections were stained with either toluidine blue or van Kossa/McNeal.

2.9. Analysis

2.9.1. Micro-Computed Tomography Analysis

Micro-computed tomography (μCT) analysis of the vertebral bodies was performed to qualitatively assess the bone volume density and trabecular thickness, as well as the location and amount of residual augmentation material within the treated levels. The samples were scanned by a micro-computed tomography system (μCT 40, Scanco Medical AG, Brüttisellen, Switzerland). The measured data were filtered and then segmented to separate the bone and the potentially present residual biomaterial from the background using a global thresholding procedure. For samples with identified residual biomaterial, a multi-level segmentation technique was used to segment bone and residual material in two separate phases, whereas for samples without residual material, a simple segmentation procedure was applied to separate bone from background. For all samples, the same thresholds were used. The measurements were performed using semiautomatic masks of nine overlapping hollow sphere shells in different sizes centered at the tip of the needle, used to calculate average bone volume density and trabecular thickness within each sphere shell (Figure 3).

Figure 3. This figure represents one slice through the nine hollow sphere shells used for the analysis. The needle path and the cortical bone areas were excluded from the analysis.

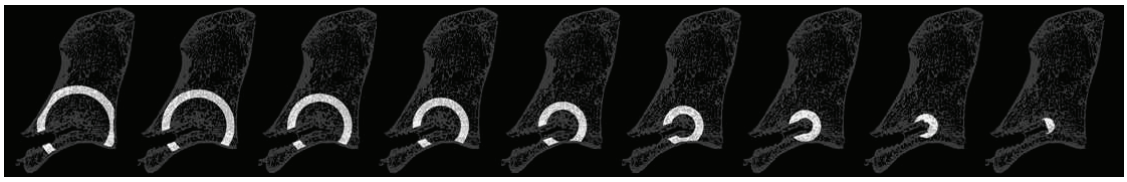

Figure 4. This figure shows the different masks created for density analysis. (**A**) The inner mask to exclude the cortical bone from the analysis. (**B**) The defined cylinder (Ø 3.5 mm) representing the original needle path with two manually determined points "tip" and "base". This cylinder was subtracted from the hollow sphere shells. Furthermore, the part of the sphere shell not lying in the trabecular bone was subtracted from the sphere shell. (**C**) An example of the final sphere shell mask.

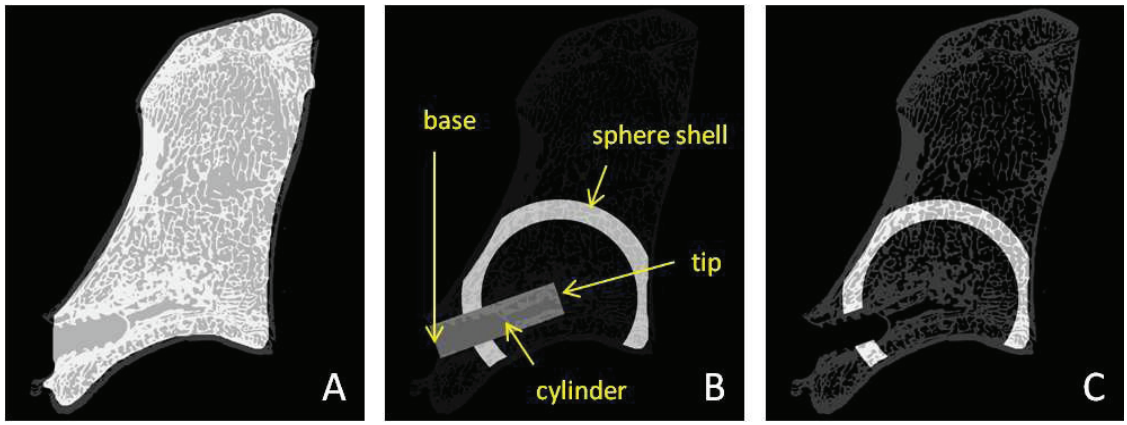

Using these sphere shells, the calculation of average material distribution and bone volume density in correlation to the radial distance from the tip of the needle was possible. To measure only the trabecular bone area, a region correlating to the cylindrical needle path and the cortical bone shell were excluded from the analysis. For the original needle path, a cylinder slightly larger than the original diameter of the needle was chosen, in order to exclude the region of any bone debris produced during the needle insertion procedure (Figure 4).

Integrating the values of the spherical shell data, the bone volume density in full thickness spheres could be computed (Figure 5).

Figure 5. This figure shows one slice with 4 full thickness spheres with 8 mm, 12 mm, 16 mm and 20 mm diameter, respectively.

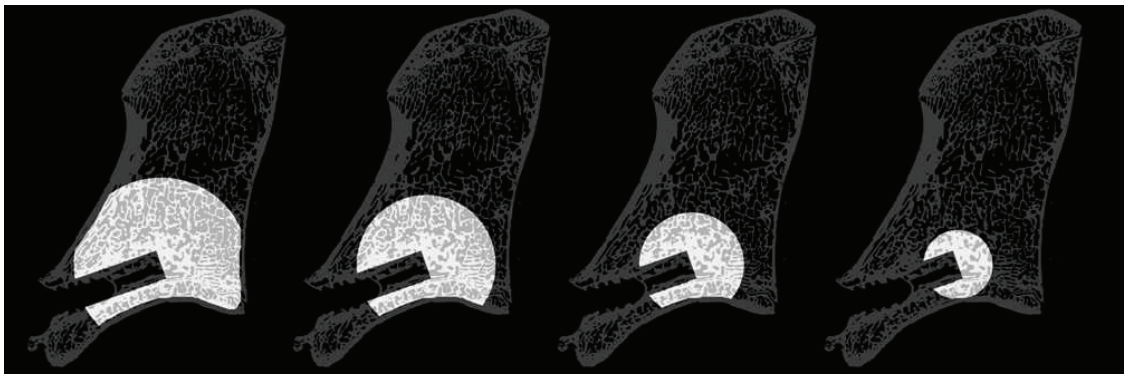

Figure 6. This figure shows a full sphere of 12 mm in diameter and a sphere shell with more than 12 mm in diameter. The inner 'Sphere12' is representative of the injected region of biomaterial, subsequently called 'augmented'. The outer 'Shell12+' is representative of the untreated bone region and used as internal sample reference, subsequently called 'unaugmented'. Needle path and cortical bone regions (grey shaded areas) were excluded from the analysis.

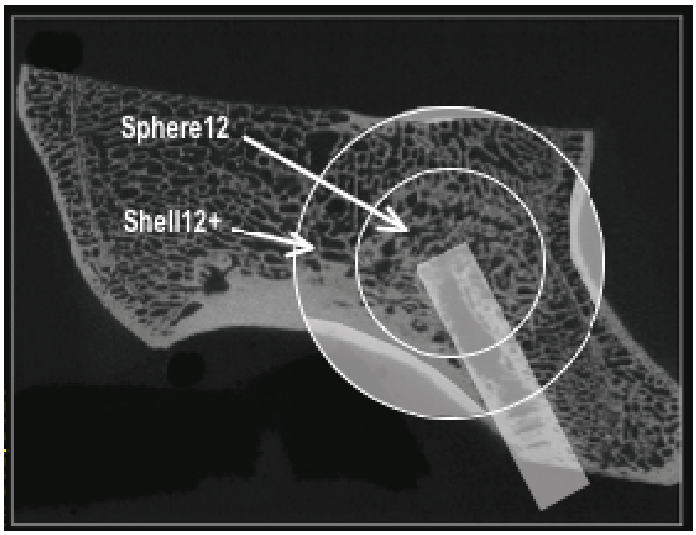

With the injected volume of approximately 1–1.5 mL material, the sum of sphere shells up to 12 mm in diameter were assumed as the injected area (consecutively called the full thickness sphere), whereas the sum of all larger sphere shells were assumed to be non-injected (Figure 6).

2.9.2. Histological Evaluation

Histomorphometry was performed using digitally recorded images of the ground sections (5.6-fold magnification, macroscope Leica Z6 APOA, Leica DFC 420C, Glattbrugg, Switzerland). For standardization of the evaluated area, three circles of 5 mm in diameter were chosen around the tip of the needle (Figure 7). The structures of interest within these circles were manually color-highlighted interactively using Adobe Photoshop Elements 10 (Adobe Systems, San Jose, CA, USA). Old bone was highlighted in blue (R: 0; G: 210; B: 255), newly formed bone in green (R: 34; G: 79; B: 7), granulation tissue in pink (R: 242; G: 40; B: 211) and residual augmentation material in beige (R: 198; G: 156; B: 96) using a standard pixel-detecting tool of Adobe Photoshop. Afterwards, the colored images were analyzed using a special image analysis software (QUIPS/QWIN, Leica standard, V.3.0, 2003, Leica-Microsystems, Heerbrugg, Switzerland), and the colored fractions were automatically detected and measured in pixels using binary segmentation of a standard macro-routine. Afterwards the pixels of each whole circle were set as 100% and the different colored fractions converted into percentages. Circles including the growth plate were excluded from the analysis, to avoid higher rates of new bone present independently of the applied material. Cortical bone in the circles was excluded from the region of interest and the rest of the circle considered as 100%, since disproportional high-density old bone is present in the cortex. The average of all three circles per sample were used for statistical analysis. To reduce any inter-observer variability, only one examiner performed the analysis; certain randomly chosen images were evaluated twice as the control.

Figure 7. Example of a histology ground section for histomorphometric evaluation. Three circles (Ø 5mm) at the tip of the needle were chosen for the evaluation of the percentage of old bone, newly formed bone, total bone and granulation tissue within the area of interest.

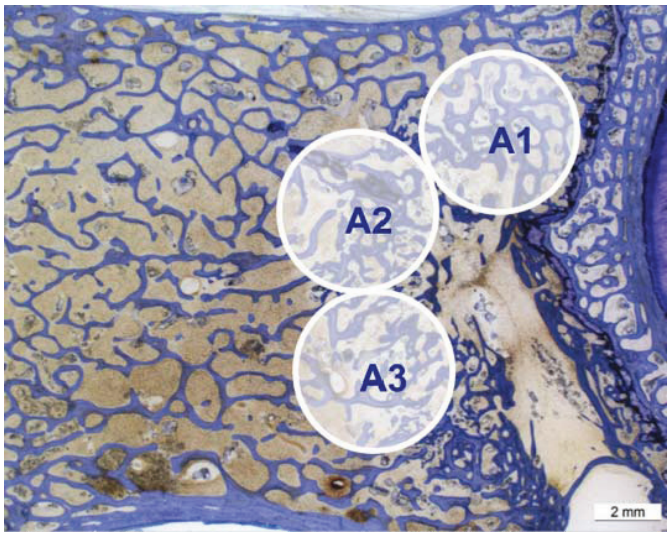

Thin sections were evaluated semi-quantitatively for cellular reactions using a microscope (Leica® DMR, Glattbrugg, Switzerland) in 10- to 20-fold magnification. Scores were given for presence of macrophages, mononuclear cells, osteoclasts, multinucleated foreign body cells, amount of osteoid seam, thickness of osteoid seam and amount of residual material (Table 2). Three power fields per section were assessed with two peripheral and one central in the injected area. The average of all three scoring areas for each augmentation site was statistically evaluated.

Table 2. Indicators for cellular reactions evaluated in the semi-quantitative histology scoring. Low scores indicate low numbers and high scores high numbers of cells, material or osteoid seams.

Indicator	**Observable value** (in the circular scoring area)	**Scoring range** (for each single circular scoring area)
Mononuclear cells	Percentage of mononuclear cells compared to the overall number of cells	0–3
Macrophages	Percentage of macrophages compared to the overall number of cells	0–3
Multinucleated foreign body cells	Absolute number of multinucleated foreign body cells	0–3
Fibroblasts	Percentage of fibroblast compared to the overall number of cells	0–3
Osteoclasts	Absolute number of osteoclasts	0–3
Amount of osteoid seam	Percentage of bone surface covered by osteoid	0–3
Thickness of osteoid seam	Thickness of the osteoid compared to the average size of an osteoblast	0–3
Residual material	Percentage of surface occupied by residual material	0–3

Fluorescent sections were evaluated semi-quantitatively for the differences of dye integration between groups and at different time points (calcein green at 6 weeks, xylenol orange at 12 weeks and oxytetracycline at 16 weeks post-surgery). Digital images of the region of interest at the tip of the needle were recorded. Therefore, 30 single images were taken in a 1.25 magnification and merged together using a special microscope, camera and specific merging software ("Stitching function"; Leica® DM 600B, Leica® DFC 350 FX, Leica® Microsystems CMS GmbH, Mannheim, Germany). Scores were given for the percentage of each fluorescent dye in the region of interest (considered as 100%) with 0% = 0, 1%–25% = 1, 26%–50% = 2, >50% = 3.

2.9.3. Statistical Analysis

Results were analyzed statistically by means of PASWStatistics® software (Base for Mac OS X, Version 21.0, Chicago, IL, USA). Overall differences between groups were assessed using a factorial analysis of variance (ANOVA). Differences between individual groups were calculated with *post hoc* tests according to Scheffe. p-values < 0.05 were considered statistically significant.

3. Results

3.1. Surgery, Postoperative Period and Sacrifice

A total of 17 female adult sheep were treated with the cervical vertebral augmentation model. Out of these 17 animals, two (11.8%) died during surgery after augmentation of the first vertebra. Death was attributed to severe cardiac distress, including a sudden decrease in arterial blood pressure and end-expired CO_2 by approximately 50%, followed by cardiac arrest. The other 15 sheep completed the 16-week follow-up period successfully. Out of these, 5/15 animals (29.4%) developed mild symptoms of pulmonary embolism, but recovered while still in surgery without further complications. No significant difference between treatment groups for the incidence of pulmonary embolism was found. Although only seven animals showed clinical signs of pulmonary embolism, the leakage of biomaterial (0.1–0.5 mL) into the venous circulation was observed in 19/36 (52.7%) material-treated augmentation sites (*i.e.*, sham group excluded) using fluoroscopy during the injection procedure.

In total, 43/45 augmentation sites were treated. Using the aiming device and fluoroscopic imaging for standardized needle placement and material injection, the needle could be positioned successfully during the first attempt in 42/45 augmentation sites (three vertebrae per sheep, 15 remaining sheep). Only in 3/45 augmentation sites (medium and high concentration groups and sham group), needle positioning was unsuccessful in the first attempt. In these cases, the drill guide was repositioned and drilling was repeated due to a misalignment of the first drilling. In one of these injection sites (medium conc. group), no material could be injected in the vertebra, because the first drilling had perforated the opposite cortical bone with a disproportional high risk of leakage outside the vertebral body into the spinal canal. Another unplanned deviation of the surgical procedure occurred in the first sheep of the study, where only two vertebrae were treated due to a very long anesthesia and surgery period. For health and survival reasons, the surgery was stopped after the augmentation into the second vertebra.

Another minor surgical complication at one augmentation site was the breaking of the needle during the extraction procedure from the bone. The small broken part of the needle remained within the bone. However, no further clinical complications resulted from this event, and the augmentation site was evaluated according to the standard protocol.

Under fluoroscopic guidance during surgery, all formulations showed good radio-opacity and a sphere-like shape distribution around the tip of the needle with an injected amount between 1 and 1.5 mL of augmentation material.

The overall surgical procedure for each animal lasted between 45 and 60 minutes. After a short recovery period following anesthesia (approximately 30 minutes), the sheep roamed freely in the stables or on pasture without lameness or other visible discomfort. During the 16-week follow-up, no signs of wound infections or inflammation were noticed in any of the 15 remaining sheep.

The en-bloc harvesting process of the cervical spine, including all treated vertebra, was uneventful, and all samples could be prepared for further evaluation. By setting the screw for needle direction after sacrifice and using the customized aiming device during the surgical procedure, the central area of augmentation within the vertebral bodies could be found in all samples with a longitudinal cut through the original needle path.

3.2. Analysis

3.2.1. Micro-Computed Tomography

Results of μCT are given in Table 3. With the μCT images, the suitability of the surgical method could be confirmed with respect to a consistent, standardized needle placement in the desired and predicted trabecular bone space. For all treatment groups, a higher bone volume density and an increased trabecular thickness was found when compared to the sham group, indicating a bone enhancing effect of all material formulations (Table 3, Figure 8). Trabecular thickness was similar in the treated groups and the matrix alone group. This was combined with a radial distribution for both parameters with higher values central in the augmented area (until sphere 12) and decreasing values to the unaugmented area (sphere >12). Residual augmentation material was only detected in the matrix-only treatment group (no TGplPTH$_{1\text{-}34}$, 4/7 samples) and the low concentration group (2/9 samples). No other treatment group had residual material detected.

Table 3. Means and SD of the morphometric μCT measurements for BV/TV (bone volume density) and Tb.Th. (trabecular thickness) for three spheres: 8 mm, 12 mm and 16 mm. Note that the BV/TV in the larger 12 mm sphere is higher for the treated groups, while trabecular thickness is equal to the matrix alone group and only higher compared to the sham.

Group	BV/TV [%] (sphere 8 mm)	BV/TV [%] (sphere 12 mm)	BV/TV [%] (sphere 16 mm)	Tb.Th [mm] (sphere 8 mm)	Tb.Th [mm] (sphere 12 mm)	Tb.Th [mm] (sphere 16 mm)
Matrix alone	52.2 ± 9.0	44.7 ± 11.0	41.0 ± 8.9	0.43 ± 0.07	0.38 ± 0.08	0.34 ± 0.06
Low	52.9 ± 8.6	47.3 ± 6.0	45.6 ± 5.1	0.34 ± 0.07	0.30 ± 0.06	0.31 ± 0.08
Medium	61.5 ± 3.8	55.1 ± 4.8	50.3 ± 4.7	0.40 ± 0.10	0.37 ± 0.08	0.34 ± 0.08
High	50.2 ± 16.6	46.7 ± 15.5	43.8 ± 14.1	0.34 ± 0.11	0.31 ± 0.10	0.28 ± 0.08
Sham	43.6 ± 10.3	45.0 ± 9.1	46.5 ± 8.6	0.27 ± 0.07	0.27 ± 0.07	0.28 ± 0.06

Figure 8. Three representative sagittal sections of the μCT scans: (**a**) a sample of the control group; (**b**) a sample of the group with medium TGplPTH$_{1\text{-}34}$ concentration is illustrated; (**c**) a sample of the group with high TGplPTH$_{1\text{-}34}$ concentration is shown. A denser bone area in the injected region could be distinguished for the samples in (b) and (c), where the augmentation material was injected. Increased trabecular thickness is visible in the circles of the outlined augmentation area.

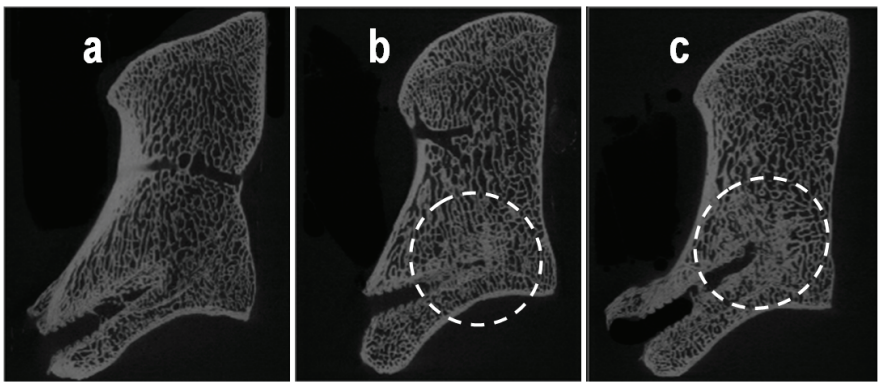

3.2.2. Histomorphometry

Exact percentages of new bone formation, old remaining bone matrix, granulation tissue and total bone are reported in Table 4 and Figure 9.

Table 4. Histomorphometrical measurements of old bone, new bone, total bone and granulation tissue (in percentage of total area measured).

Group	Old bone matrix	New bone matrix	Total bone matrix	Granulation tissue
Matrix alone	22.4 ± 3.4	19.6 ± 8.6	42.0 ± 8.0	58.0 ± 8.0
Low	15.3 ± 2.3	26.3 ± 5.5	41.9 ± 5.2	58.4 ± 5.2
Medium	15.5 ± 3.5	32.0 ± 3.6	47.6 ± 3.6	52.5 ± 3.6
High	9.6 ± 10.5	27.5 ± 9.7	37.1 ± 12.9	62.9 ± 12.9
Sham	34.2 ± 6.9	7.1 ± 8.2	41.4 ± 12.4	58.7 ± 12.4

Figure 9. The bars show the mean and SD values of the histomorphometrical measurements of old bone, new bone and granulation tissue (as a percentage of the total area measured). All treatment groups showed significantly higher percentages of new bone than the control group. In contrast, the sham group had the highest percentage of old bone (significant differences compared to the sham group are highlighted with asterisks; the bracket illustrates the significant difference between the matrix alone group and the group with medium TGplPTH$_{1\text{-}34}$).

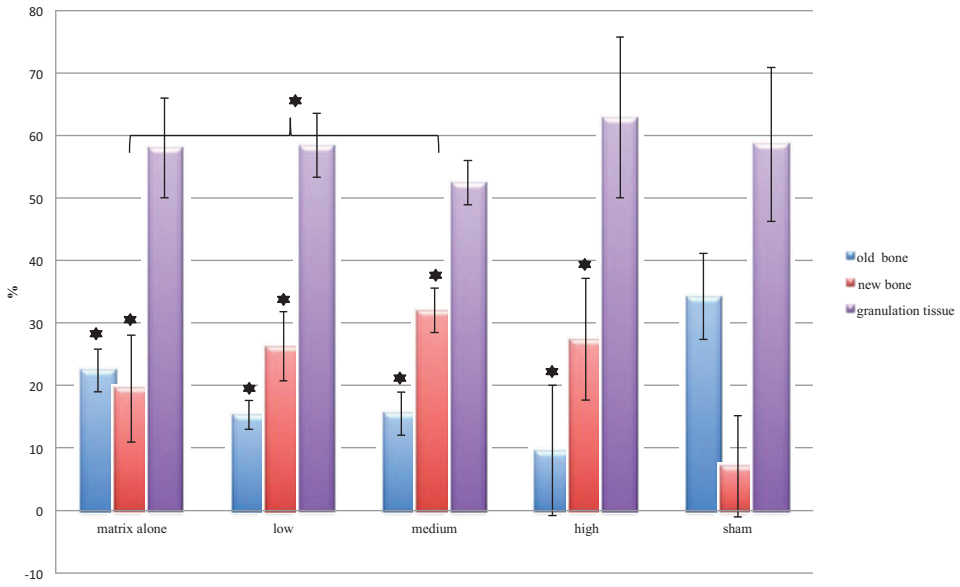

As in the µCTs overall, a high percentage of new bone was found in the augmented region (19.6%–32%) for all treatment groups, whereas in the sham group, new bone was only detected at the border of the needle path (7.1%). In all treatment groups, the area adjacent to the tip of the needle seemed to be mainly filled with new bone, partly due to proliferation and partly to an enhanced remodeling and bone formation process (Figure 10).

Figure 10. Examples of toluidine blue-stained ground sections of all groups; the area at the tip of the needle of all treatment groups showed mainly newly formed bone (indicated by darker blue areas), whereas for the sham group, new bone only was detectable at the border of the needle path. Note the increased trabecular thickness in the augmented area.

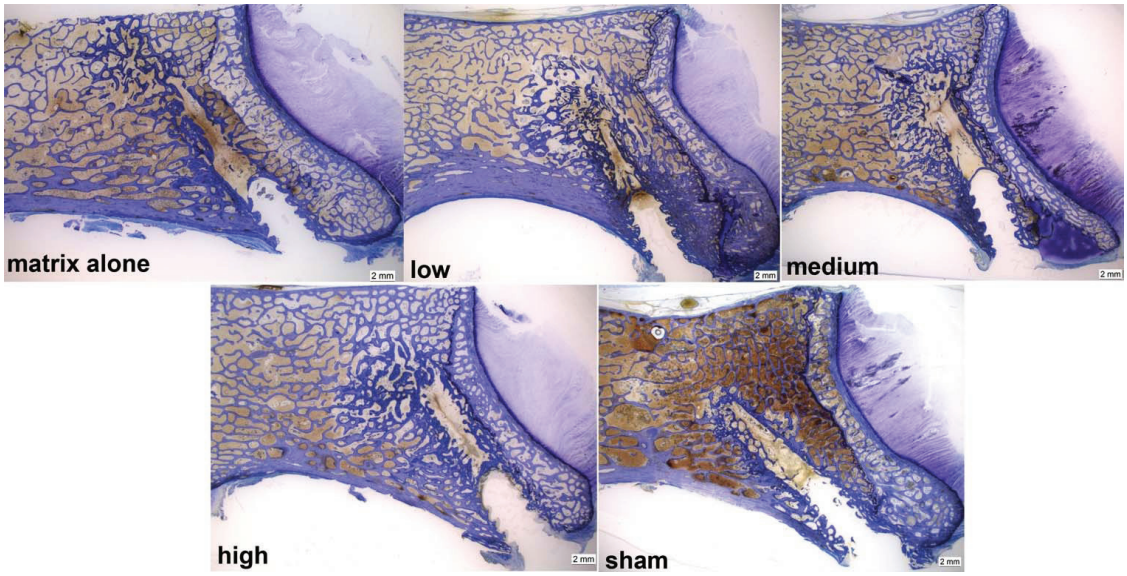

Overall differences between groups in percentage for old and new bone were significant at $p = 0.000$. When compared individually, all treatment groups showed significantly higher percentages of new bone than the sham group (p-value ranging between 0.000 and 0.029). In contrast, the sham group had the highest percentage of old bone compared to all treatment groups (p-value ranging between 0.000 and 0.009). No significant differences between groups were found for the percentages of granulation tissue (52.4%–62.9%) and of total bone (37.1%–47.56%). The bone remodeling process was pronounced in all specimens of the treatment groups, but especially for the groups with higher concentrations of TGplPTH$_{1\text{-}34}$. The highest average for new bone (32%) was found for the group with a medium concentration of TGplPTH$_{1\text{-}34}$. with statistical significant differences also for the group with matrix alone (19.6%) ($p = 0.042$) (Figure 9).

3.2.3. Fluorescence

Means and SD from semi-quantitatively scoring fluorescence sections are reported in Table 5. No fluorescent dye (tetracycline) was detected at 16 weeks, so that it was left out of the table.

The fluorescence images of all treatment groups demonstrated the sphere-like shape distribution of the biomaterial with a red colored area in the middle and a green area towards the periphery. This pattern indicated a radial progression of new bone formation with enhanced bone activity, and precipitation of the fluorescence markers starting in the periphery and the biomaterial being progressively degraded, starting from the periphery towards the middle of the injected region (Figure 11).

Table 5. Means and SD of the semi-quantitative fluorescence scores for all groups and at different time points show that increased new bone formation occurred mainly at the early time point at six weeks in all PTH derivates compared to controls. At 12 weeks, new bone deposition was lower in all groups, except the matrix alone group.

Group	Calcein green (6w.p.OP)	Xylenol orange (12w.p.OP)
Matrix alone	0.8 ± 0.4	0.9 ± 0.9
Low	1.0 ± 0.0	1.1 ± 0.8
Medium	1.5 ± 0.8	0.8 ± 0.7
High	1.4 ± 0.5	0.9 ± 0.9
Sham	0.7 ± 0.5	0.1 ± 0.3

Figure 11. This figure shows representative fluorescence images of all groups at the three different time points, as well as one image merged, respectively overlaid together. At six weeks, enhanced bone activity in the injected region could be detected especially for the treatment groups with a medium and high concentration. This localized bone activity decreased at 12 weeks and, with the degradation of the material, finally disappeared at 16 weeks. In the sham group, only the area next to the needle track was enhanced. Note that the area of bone deposition is broader in its diameter in the treated groups compared to the matrix alone.

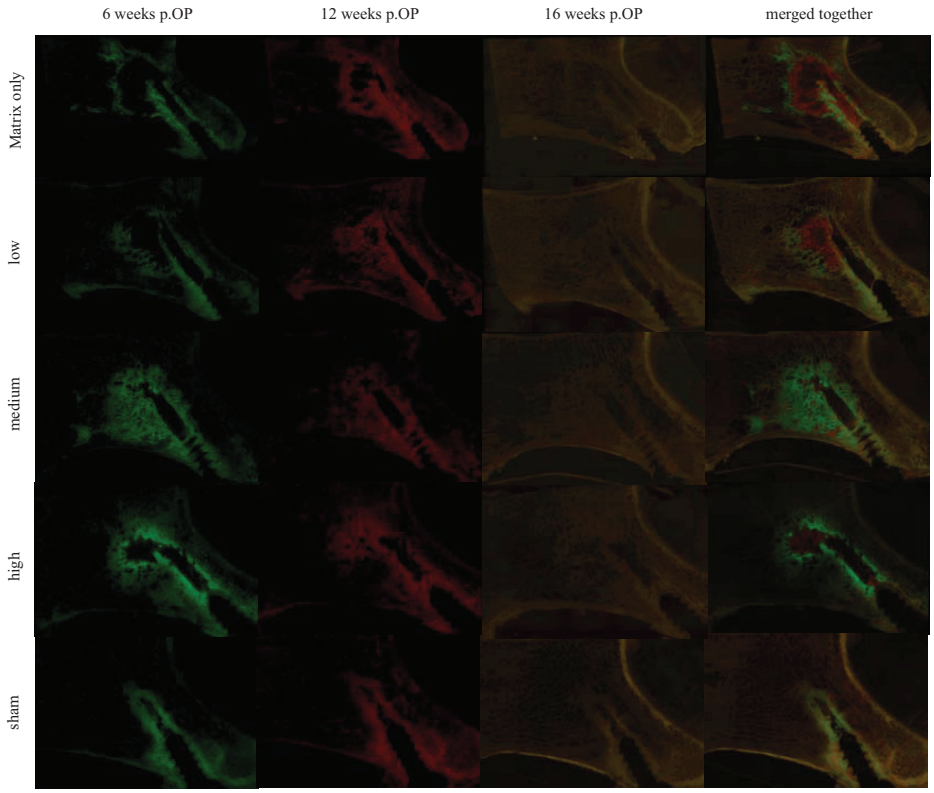

At six weeks, all treatment groups showed enhanced bone activity in the injected area, as indicated by calcein green precipitation. Overall differences between groups in bone activity were significant at $p = 0.003$. Especially in the groups with medium and high TGplPTH$_{1-34}$ concentrations, the bone activity was enhanced with significantly higher values in comparison to the sham group ($p = 0.029$ and $p = 0.040$ for groups with medium and high concentration, respectively). This localized bone activity decreased at 12 weeks (xylenol orange) and finally disappeared at 16 weeks (tetracycline) proportional to the degradation of the material. For the treatment group with matrix only and for the group with a low concentration of TGplPTH$_{1-34}$, higher scores were given at 12 weeks *versus* six weeks, with other treatment groups maintaining stable values during that period. In the sham group, only the area next to the needle track was enhanced for bone activity, which was attributed to the remodeling process of bone debris created by the needle.

3.2.4. Histologic and Cellular Evaluation

Means and SD of the semi-quantitative histology scoring are summarized in Table 6.

Table 6. Means and SD of the semi-quantitative histology scoring are given using the average of the three scoring areas for each augmentation site.

Group	Mononuclear cells	Macro-phages	Multinucleated foreign body cells	Fibro-blasts	Osteo-clasts	Amount of osteoid seam	Thickness of osteoid	Residual material
Matrix alone	1.2 ± 0.4	1.1 ± 0.6	0.0 ± 0.0	0.2 ± 0.3	0.3 ± 0.4	0.7 ± 0.5	0.7 ± 0.5	0.3 ± 0.5
Low	1.3 ± 0.3	1.2 ± 0.5	0.2 ± 0.2	0.0 ± 0.0	0.5 ±0.3	1.2 ± 0.6	1.3 ± 0.6	0.1 ± 0.1
Medium	1.2 ± 0.4	1.0 ± 0.2	0.1 ± 0.2	0.0 ± 0.0	0.5 ± 0.4	1.1± 0.7	1.2 ± 0.7	0.0 ± 0.0
High	1.0 ± 0.2	0.6 ± 0.3	0.0 ± 0.0	0.0 ± 0.0	0.5 ± 0.4	1.2 ± 0.4	1.3 ± 0.3	0.0 ± 0.0
Sham	0.9 ± 0.8	0.2 ± 0.4	0.0 ± 0.0	0.0 ± 0.0	0.5 ± 0.4	0.4 ± 0.3	0.5 ± 0.3	0.0 ± 0.0

The semi-quantitative histology scoring revealed similar values for all groups. Overall differences between groups were only found for scores of macrophages ($p = 0.000$). Due to the degradation process of the biomaterial, the number of macrophages was significantly higher in 3/4 treatment groups compared to the sham group (the *p*-value was 0.003, 0.001 and 0.009 for groups with matrix only, low and medium concentrations, respectively). However, the low scores of all treatment groups in comparison to the sham group for mononuclear cells and multinucleated foreign body cells indicated an excellent biocompatibility for all formulations. Thick osteoid seams and activated round-shaped osteoblasts evidenced an improved bone activity with higher scores found for all material groups containing TGplPTH$_{1-34}$ (Figure 12). Residual biomaterial was found only for the matrix only and low concentration groups.

Figure 12. This figure shows a thin section with many macrophages (→) and a thick osteoid seam with activated round-shaped osteoblasts (→).

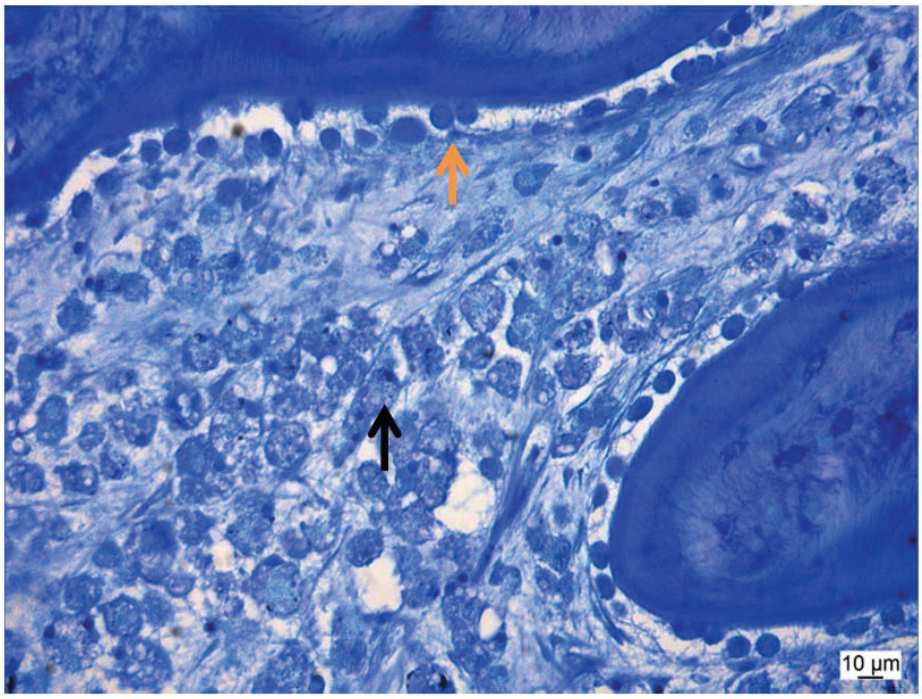

4. Discussion

In this study, a novel animal model in sheep was successfully established by using the cervical vertebrae of 17 sheep for the augmentation of cancellous bone with a biomimetic agent. The surgical and evaluation methods proved to be well standardized and highly reproducible. In addition, the efficacy of locally-delivered TGplPTH$_{1\text{-}34}$ incorporated in a fibrin matrix containing strontium carbonate was demonstrated to be a potentially suitable augmentation material for the cervical vertebra.

The surgical method was straightforward and easy to apply, with the aid of the specially developed aiming device. Using fluoroscopic imaging during the surgical procedure, combined with the various analyses, such as µCT, histomorphometry and sequential fluorescence dye staining, we were able to demonstrate that drilling and subsequent needle placement was accurate and reproducible. Consequently, we were able to inject test materials in 43/45 augmentation sites into the intertrabecular spacing of cervical vertebral bodies again with accuracy and reproducibility. However, as already discussed in a previous study concerning the tibia and femur augmentation in sheep [20], the trabecular bone density, as well as the trabecular thickness is much higher in sheep than in humans, such that the needle placement and material injection is more difficult to achieve in comparison to humans. In osteoporotic, brittle human bone, the injection needle can be placed in position using manual pressure only, whereas in sheep, a hole had to be drilled with a burr first in order to be able to push the needle forward into the healthy and dense trabecular bone. However, in contrast to the tibia and femur augmentation study, where a mallet had to be used after drilling to push the needle forward into the bone, this was not required for cervical bone augmentation. Therefore, the frequently observed surgical complications in

the previous study, where the rather frail needle broke during the extraction procedure, were significantly less frequent in the current study (1/45). The harvesting method of the treated vertebrae was easy, fast and highly reproducible, with no need for an additional aiming device to define the region of interest as needed in the previous study [20].

Cardiovascular emboli are noticed in human patients after vertebral augmentation, even with a reported mortality rate of 2%. Emboli were also reported in our previously established femoral and tibia augmentation model [20]. Nevertheless, this cervical vertebral model presented more challenges regarding cardiovascular complications in comparison. Although the same material was used in both studies, the cervical augmentation model revealed a relatively high rate of pulmonary emboli, with two animals (11.76%) dying immediately on the table with severe signs of PE and five animals (29.4%) still showing mild signs of PE. In the femoral and tibia augmentation model, a higher leakage of material into the vessels was observed. This may be attributed to the different anatomical location, but probably also to the higher volume of material injected in the femoral and tibia augmentation model (3.5 mL per augmentation site). In human patients, reported emboli are less, but then, they are not routinely followed by lung CT after augmentation and, therefore, may often go unnoticed as long as no life threatening complication jeopardizes the patient's life. The higher mortality rate in sheep compared to humans may be related to the fact that injection of a relatively high material volume was performed in healthy cancellous bone of the vertebral body and that the sheep have denser bone compared to humans. Nevertheless, the cervical augmentation model presented the valuable opportunity to study the development of PE and its consequences, as they also occur in humans during vertebroplasty [32].

Mechanical testing of the vertebral bodies was not performed. Apart from technical problems to develop an adequate testing system with highly standardized cubes, it also was not of high priority in this study. One of the main reasons was that we did not treat osteoporotic sheep, since there is no adequate large animal model for this disease. Although we assumed that new bone formation with highly active osteoblast activity on new osteoid seams would be visible, it was not expected to significantly change trabecular thickness in healthy animals, since the mechanical load on the vertebrae had not changed. Trabecular thickness was only measured in μCT, where only calcified tissue is measured. However, in the histology sections, the increased trabecular thickness due to osteoid deposition is clearly visible in the ground and thin sections.

The three different concentrations (low, medium, high) of $TGplPTH_{1-34}$ proved to be suitable for cervical augmentation in sheep and showed indications of enhanced localized bone activity in all groups, especially during the first six weeks after surgery. Micro CT analysis, histomorphometry, as well as the evaluation of fluorescent incorporation indicated an increased bone formation and remodeling activity spatially limited to the injected area. As in the previous study [20], sequential fluorescent dye images indicated a radial propensity for new bone forming gradually over time from the periphery towards the middle of the injected regions. These findings support the hypothesis of Arrighi *et al.* that cell migration and infiltration into the fibrin matrix activate and release $TGplPTH_{1-34}$ into the surrounding tissue [19]. Our results further confirm those of Yang *et al.* showing that locally applied strontium has inherent osteoinductive properties itself [25]. However, combining strontium with high and probably even better medium concentrations of $TGplPTH_{1-34}$ enhanced the overall proliferative effect that was already previously demonstrated by our group in the femoral and tibia

augmentation model [20]. The exact mechanism by which this co-effect is exerted is not fully known. However, we hypothesize that the accumulation of extracellular matrix induced by strontium increases the migration and infiltration of cells into the fibrin matrix and may also reduce osteoclast activity via apoptosis, again enhancing bone formation [25]. PTH, on the other hand, has anabolic activities on osteoblasts, increasing remodeling activity, as clearly shown in our previous study [20]. Taken together, bone forming properties are therefore enhanced by both ways: the increased osteoblastic activity through PTH and the increased population of living cells throughout the extracellular matrix population via strontium. Our evaluation methods did not allow distinguishing between increased remodeling activity and true new bone formation, as would be found in true osteoinduction. However, if in our current study, the different groups are compared to each other, it is obvious that the groups treated with TGplPTH$_{1-34}$ showed considerable increased bone formation compared to the matrix alone group. If the material alone in combination with trabecular microdamage would be the reason for the new bone formation, the matrix alone and with TGplPTH$_{1-34}$-treated groups would be equal in their response. However, the differences in new bone deposition are clearly visible in the fluorescent sections. Therefore, it is safe to assume that the new bone formation is in response to both remodeling activity after material injection and new bone formation after local application of TGplPTH$_{1-34.}$

The broad precipitation of fluorescence markers at six weeks post-surgery for the groups with medium and high concentrations of TGplPTH$_{1-34}$ indicate an enhanced, early and fast bone formation, which could be confirmed by histomorphometry with the highest percentage of new bone formation (32.0%) found for the medium concentration of TGplPTH$_{1-34}$, followed by 27.5% new bone formation found for the high concentration of TGplPTH$_{1-34}$. In comparison, groups with fibrin matrix only or with low concentration of TGplPTH$_{1-34}$ revealed less overall bone activity and at a later time point (12 weeks). This seems connected to the findings in the µCT analysis, where low quantities of residual material for the groups without or with a low dose of TGplPTH$_{1-34}$ could be related to higher amounts of remaining material. We assume that the degradation of these formulations is decelerated and therefore reduces the bone enhancing activity due to the delayed release of activated TGplPTH$_{1-34}$. To prove this theory in a future study, an earlier time point for the first fluorescence injection could be taken into consideration in order to confirm that the enhanced bone activity of medium and high concentrations of TGplPTH$_{1-34}$ shows a faster degradation of material, in correlation with a stronger enhanced bone activity.

In systemic applications of TGplPTH$_{1-34}$, a great concern is that high PTH concentrations may increase osteoclast activity [33]. This may be reflected by a lower percentage of newly formed bone, in addition to increased bone resorption zones and higher numbers of osteoclasts. Due to the mechanism of PTH, the influence on osteoclasts must be evaluated, when PTH is applied as a local peptide. In this study, no increase of osteoclasts and no resorption zones were found for any of the PTH concentrations. These findings were attributed to the use of the peptide covalently bound to the fibrin matrix that is only released and activated via local cell invasion and enzymatic cleavage. We therefore suggest that the osteoclast-enhancing effect of PTH shown by others depends not only on the higher dose, but mainly on the route of administration, which could be avoided by delivering the peptide locally and covalently bound to the fibrin matrix.

5. Conclusion

The cervical augmentation model in sheep described in this study proved to be a suitable animal model to evaluate the biocompatibility and new bone formation properties of new biomaterials, intended for vertebral bone augmentation. Although the model revealed to be more challenging, due to cardiovascular complications compared to the femoral and tibia augmentation model, this reflected well the human situation. Nevertheless, the results demonstrated that the TGplPTH$_{1\text{-}34}$ was safe to use in sheep, since no signs of inflammation were detected and fast biomaterial degradation took place. All treatment groups were more effective than the sham control. Among these, the medium concentration of TGplPTH$_{1\text{-}34}$ induced the best bone enhancing effect. Whether this effect would also be elicited in osteoporotic bone in humans is speculative at this point. Due to the absence of a true osteoporotic large animal model, this could only be verified in a clinical trial study in humans.

Acknowledgments

The authors thank their industrial partners for financing the study.

Author Contributions

K.Kl. was the Ph.D. student and involved in all aspects of the study, including writing the manuscript. J.S. was involved in developing the biomaterial. P.W.K. was the anesthetist and was involved in demonstrating embolization. N.F. was the anesthetist and was involved in demonstrating embolization. K.K. performed histology and was involved in developing bone sampling. M.M. was the radiologist and performed all CT including evaluation. T.S. designed the device and was involved in all aspects of the study. B.R. was the head of the experiment, supervisor of the Ph.D. program and was involved in all aspects of the study.

Disclosure

The study was financed by our industrial partner, Kuros Biosurgery AG, Technoparkstrasse 1, 8005 Zurich, Switzerland.

Conflicts of Interest

The authors declare no conflict of interest.

References and Notes

1. Rapado, A. General management of vertebral fractures. *Bone* **1996**, *18*, 191S–196S.
2. Old, J.L.; Calvert, M. Vertebral compression fractures in the elderly. *Am. Fam. Phys.* **2004**, *69*, 111–116.
3. Lewis, G. Percutaneous vertebroplasty and kyphoplasty for the stand-alone augmentation of osteoporosis-induced vertebral compression fractures: Present status and future directions. *J. Biomed. Mater. Res. B Appl. Biomater.* **2007**, *81*, 371–386.

4. Lavelle, W.; Carl, A.; Lavelle, E.D.; Khaleel, M.A. Vertebroplasty and kyphoplasty. *Anesthesiol. Clin.* **2007**, *25*, 913–928.
5. Hulme, P.A.; Krebs, J.; Ferguson, S.J.; Berlemann, U. Vertebroplasty and kyphoplasty: A systematic review of 69 clinical studies. *Spine (Phila Pa 1976)* **2006**, *31*, 1983–2001.
6. Predey, T.A.; Sewall, L.E.; Smith, S.J. Percutaneous vertebroplasty: New treatment for vertebral compression fractures. *Am. Fam. Phys.* **2002**, *66*, 611–615.
7. Silverman, S.L. The clinical consequences of vertebral compression fracture. *Bone* **1992**, *13* (Suppl 2), S27–S31.
8. Garfin, S.R.; Yuan, H.A.; Reiley, M.A. New technologies in spine: Kyphoplasty and vertebroplasty for the treatment of painful osteoporotic compression fractures. *Spine (Phila Pa 1976)* **2001**, *26*, 1511–1515.
9. Lemke, D.M. Vertebroplasty and kyphoplasty for treatment of painful osteoporotic compression fractures. *J. Am. Acad. Nurse Pract.* **2005**, *17*, 268–276.
10. Phillips, F.M.; Todd Wetzel, F.; Lieberman, I.; Campbell-Hupp, M. An *in vivo* comparison of the potential for extravertebral cement leak after vertebroplasty and kyphoplasty. *Spine (Phila Pa 1976)* **2002**, *27*, 2173–2178; discussion 2178–2179.
11. Jensen, M.E.; Evans, A.J.; Mathis, J.M.; Kallmes, D.F.; Cloft, H.J.; Dion, J.E. Percutaneous polymethylmethacrylate vertebroplasty in the treatment of osteoporotic vertebral body compression fractures: Technical aspects. *AJNR Am. J. Neuroradiol.* **1997**, *18*, 1897–1904.
12. Cotten, A.; Boutry, N.; Cortet, B.; Assaker, R.; Demondion, X.; Leblond, D.; Chastanet, P.; Duquesnoy, B.; Deramond, H. Percutaneous vertebroplasty: State of the art. *Radiographics* **1998**, *18*, 311–320; discussion 320–323.
13. Frankel, B.M.; Monroe, T.; Wang, C. Percutaneous vertebral augmentation: An elevation in adjacent-level fracture risk in kyphoplasty as compared with vertebroplasty. *Spine J.* **2007**, *7*, 575–582.
14. Nardi, A.; Tarantino, U.; Ventura, L.; Armotti, P.; Resmini, G.; Cozzi, L.; Tonini, G.; Ramazzina, E.; Rossini, M. Domino effect: Mechanic factors role. *Clin. Cases Miner. Bone Metab.* **2011**, *8*, 38–42.
15. Poole, K.E.; Reeve, J. Parathyroid hormone—A bone anabolic and catabolic agent. *Curr. Opin. Pharmacol.* **2005**, *5*, 612–617.
16. Carter, P.H.; Schipani, E. The roles of parathyroid hormone and calcitonin in bone remodeling: Prospects for novel therapeutics. *Endocr. Metab. Immune Disord. Drug Targets* **2006**, *6*, 59–76.
17. Pfeilschifter, J.; Laukhuf, F.; Muller-Beckmann, B.; Blum, W.F.; Pfister, T.; Ziegler, R. Parathyroid hormone increases the concentration of insulin-like growth factor-i and transforming growth factor beta 1 in rat bone. *J. Clin. Investig.* **1995**, *96*, 767–774.
18. Whitfield, J.F. Osteoporosis-treating parathyroid hormone peptides: What are they? What do they do? How might they do it? *Curr. Opin. Investig. Drugs* **2006**, *7*, 349–359.
19. Arrighi, I.; Mark, S.; Alvisi, M.; von Rechenberg, B.; Hubbell, J.A.; Schense, J.C. Bone healing induced by local delivery of an engineered parathyroid hormone prodrug. *Biomaterials* **2009**, *30*, 1763–1771.

20. Klein, K.; Zamparo, E.; Kronen, P.W.; Kampf, K.; Makara, M.; Steffen, T.; von Rechenberg, B. Bone augmentation for cancellous bone—Development of a new animal model. *BMC Musculoskelet. Disord.* **2013**, *14*, 200.
21. Ammann, P. Strontium ranelate: A physiological approach for an improved bone quality. *Bone* **2006**, *38*, 15–18.
22. Marie, P.J. Strontium ranelate: A physiological approach for optimizing bone formation and resorption. *Bone* **2006**, *38*, S10–S14.
23. Brown, E.M. Is the calcium receptor a molecular target for the actions of strontium on bone? *Osteoporos. Int.* **2003**, *14* (Suppl 3), S25–S34.
24. Hurtel-Lemaire, A.S.; Mentaverri, R.; Caudrillier, A.; Cournarie, F.; Wattel, A.; Kamel, S.; Terwilliger, E.F.; Brown, E.M.; Brazier, M. The calcium-sensing receptor is involved in strontium ranelate-induced osteoclast apoptosis. New insights into the associated signaling pathways. *J. Biol. Chem.* **2009**, *284*, 575–584.
25. Yang, F.; Yang, D.; Tu, J.; Zheng, Q.; Cai, L.; Wang, L. Strontium enhances osteogenic differentiation of mesenchymal stem cells and *in vivo* bone formation by activating wnt/catenin signaling. *Stem Cells* **2011**, *29*, 981–991.
26. Benneker, L.M.; Gisep, A.; Krebs, J.; Boger, A.; Heini, P.F.; Boner, V. Development of an *in vivo* experimental model for percutaneous vertebroplasty in sheep. *Vet. Comp. Orthop. Traumatol.* **2012**, *25*, 173–177.
27. Krebs, J.; Ferguson, S.J.; Hoerstrup, S.P.; Goss, B.G.; Haeberli, A.; Aebli, N. Influence of bone marrow fat embolism on coagulation activation in an ovine model of vertebroplasty. *J. Bone Joint Surg. Am.* **2008**, *90*, 349–356.
28. Krebs, J.; Ferguson, S.J.; Nuss, K.; Leskosek, B.; Hoerstrup, S.P.; Goss, B.G.; Shaw, S.; Aebli, N. Plasma levels of endothelin-1 after a pulmonary embolism of bone marrow fat. *Acta Anaesthesiol. Scand.* **2007**, *51*, 1107–1114.
29. Aebli, N.; Krebs, J.; Schwenke, D.; Davis, G.; Theis, J.C. Cardiovascular changes during multiple vertebroplasty with and without vent-hole: An experimental study in sheep. *Spine (Phila Pa 1976)* **2003**, *28*, 1504–1511; discussion 1511–1512.
30. Boger, A.; Benneker, L.M.; Krebs, J.; Boner, V.; Heini, P.F.; Gisep, A. The effect of pulsed jet lavage in vertebroplasty on injection forces of pmma bone cement: An animal study. *Eur. Spine J.* **2009**, *18*, 1957–1962.
31. Measurements are not in the content of this paper and will be published elsewhere.
32. Data not shown here.
33. Robling, A.G.; Kedlaya, R.; Ellis, S.N.; Childress, P.J.; Bidwell, J.P.; Bellido, T.; Turner, C.H. Anabolic and catabolic regimens of human parathyroid hormone 1-34 elicit bone- and envelope-specific attenuation of skeletal effects in sost-deficient mice. *Endocrinology* **2011**, *152*, 2963–2975.

4 General Discussion and Outlook

This thesis presents two novel *in vivo* animal models for augmentation of cancellous bone in sheep while also investigating new bioactive and biodegradable materials for prophylactic augmentation of bones at risk for osteoporotic fractures. Metaphyseal regions like the proximal femur, proximal humerus, distal radius, and the vertebrae have the highest risk for fragility fractures in humans [9]. In our animal models presented, the proximal tibia and distal femur of both hind limbs (first animal model) and three cervical vertebrae (second animal model) were chosen as augmentation sites. Similarly to common fragility fracture regions in humans, the selected anatomical sites in our animal models consist of high proportions of cancellous bone. The lower muscle mass present at the injection sites, however, constitute a marked advantage in our models, when compared to the human clinical situation. Indeed, our model favors an easier and safer access to the bone. With a total of four augmentation sites for the tibia and the femur model and three for the cervical model, the total number of animals could be reduced. For each model, a customized aiming device was developed to ensure high reproducibility and accuracy of biomaterial distribution within the inter-trabecular spacing of the intact bones. Minimal invasive surgical techniques further reduce pain and suffering of study animals recruited. The standardized harvesting methods produced comparable bone samples of cement loaded bone regions and therefore, assured a highly standardized evaluation.

Both animal models have proven to be suitable to evaluate biocompatibility, biodegradability, and osteoconductive properties of new biomaterials intended for prophylactic augmentation of cancellous bone. In addition, these models have proven to be adequate for studying the consequences of extravasation of bone marrow and fat cells as well as augmentation material into surrounding tissue and the circulation. Extravasation may cause serious complications in both, humans and study animals, such as severe neurological deficits with paraplegia or pulmonary embolism with subsequent cardiovascular complications. Asymptomatic material extravasation in the studies presented here seemed more frequent than in human clinical cases.

Reasons for this higher frequency may be, firstly, the presence of normal dense trabecular bone in the non-osteoporotic sheep model as opposed to the diminished

structural properties of osteoporotic trabecular bone and massive bone loss typically found in menopausal women. Due to the dense trabecular structure in sheep, higher injection pressures are required for interosseus deposit and may lead to increased extravasation of bone marrow fat and/or material. Secondly, it is possible that the material itself, under the given circumstances, favors extravasation. Indeed, Bohner *et al.* considered the frequency of extravasation to be influenced by several parameters: Bone permeability, bone marrow and cement viscosity, bone porosity and pore size, size of injection cavity, diameter of extravasation path, and injected cement volume [61]. Material xtravasation has been associated mostly with low viscosity materials and is therefore not considered a primary factor in our model where a high viscosity material was used. Thirdly, in most asymptomatic clinical patients following vertebroplasties, no routine chest radiographs or CTs are performed and therefore regional or systemic cement leakage and pulmonary cement emboli may often not be detected [101,106,174].

Although the tested biomaterials are intended for prophylactic augmentation of osteoporotic bone with low BMD and change in trabecular bone architecture, we did not use osteopenic or osteoporotic animals. In our opinion, to date there is no true osteoporotic large animal model available. Some research groups have used ovariectomized sheep, but even in those animals a marked bone loss could not be detected [154,160]. A combination of ovariectomy, glucocorticoid treatment and highly anionic diet has shown to induce a more prominent loss of BMD and trabecular thickness in sheep [156-159]. However, such a combined bone loss induction model does present with rather significant difficulties:

1) Pathogenesis of osteoporosis in postmenopausal women has a different underlying cellular mechanism. However, postmenopausal women represent the largest patient group in humans [175].

2) Glucocorticoid administration may lead to infections due to immunosuppression, as well as joint pain with lameness, and therefore ethical considerations compromise acceptance of the model.

3) The glucocorticoids may influence the bioactivity of test materials and therefore bias the study outcome.

The tibia and femur augmentation model proved suitable for testing different biomaterials with the advantage to reduce the total number of animals und the suffering of each individual animal. Whereas the tibia and femur augmentation model with four easily accessible augmentation sites per animal, is a suitable model for preliminary screening studies of different material formulations, the cervical augmentation model reveals to be technically more challenging, but is topographically closer to the human situation. The cervical augmentation model was also closer to clinical reality with a more severe and a higher number of cardiovascular complications. Although for both animal models material as well as fat extravasation were detected (using fluoroscopy during augmentation and a postoperative thorax CT), the clinical complications of the cervical augmentation model were more severe. Two of seventeen animals in the cervical augmentation study died intraoperatively (11.76%) with 29.4% of the animals showing mild symptoms of pulmonary embolism. The exact reasons for these higher complication rates is unknown, it might be though due to the high vascularization of the vertebral body in the relatively high volume of injected material into healthy, physiologically dense bone. In humans the detected complications are fewer, but similar in nature and thus, the cervical augmentation model may in the future well serve to study and possibly reduce severe cardiovascular complications.

5 Bibliography

1. Johnell, O.; Kanis, J.A. An estimate of the worldwide prevalence and disability associated with osteoporotic fractures. *Osteoporosis international : a journal established as result of cooperation between the European Foundation for Osteoporosis and the National Osteoporosis Foundation of the USA* **2006**, *17*, 1726-1733.
2. Gomberg, B.F.; Gruen, G.S.; Smith, W.R.; Spott, M. Outcomes in acute orthopaedic trauma: A review of 130,506 patients by age. *Injury* **1999**, *30*, 431-437.
3. Riggs, B.L.; Melton, L.J., 3rd. The worldwide problem of osteoporosis: Insights afforded by epidemiology. *Bone* **1995**, *17*, 505S-511S.
4. Cummings, S.R.; Melton, L.J. Epidemiology and outcomes of osteoporotic fractures. *Lancet* **2002**, *359*, 1761-1767.
5. Bonnaire, F.; Zenker, H.; Lill, C.; Weber, A.T.; Linke, B. Treatment strategies for proximal femur fractures in osteoporotic patients. *Osteoporosis international : a journal established as result of cooperation between the European Foundation for Osteoporosis and the National Osteoporosis Foundation of the USA* **2005**, *16 Suppl 2*, S93-S102.
6. Gruber, R.; Koch, H.; Doll, B.A.; Tegtmeier, F.; Einhorn, T.A.; Hollinger, J.O. Fracture healing in the elderly patient. *Experimental gerontology* **2006**, *41*, 1080-1093.
7. Gosch, M.; Kammerlander, C.; Roth, T.; Luger, T.; Blauth, M. [geriatric traumatology: Interdisciplinary management of patients with fragility fractures]. *Deutsche medizinische Wochenschrift* **2014**, *139*, 1207-1210.
8. Heini, P.F.; Franz, T.; Fankhauser, C.; Gasser, B.; Ganz, R. Femoroplasty-augmentation of mechanical properties in the osteoporotic proximal femur: A biomechanical investigation of pmma reinforcement in cadaver bones. *Clinical biomechanics* **2004**, *19*, 506-512.
9. Cornell, C.N. Internal fracture fixation in patients with osteoporosis. *The Journal of the American Academy of Orthopaedic Surgeons* **2003**, *11*, 109-119.
10. Barrios, C.; Brostrom, L.A.; Stark, A.; Walheim, G. Healing complications after internal fixation of trochanteric hip fractures: The prognostic value of osteoporosis. *Journal of orthopaedic trauma* **1993**, *7*, 438-442.
11. Halvorson, T.L.; Kelley, L.A.; Thomas, K.A.; Whitecloud, T.S., 3rd; Cook, S.D. Effects of bone mineral density on pedicle screw fixation. *Spine* **1994**, *19*, 2415-2420.
12. Soshi, S.; Shiba, R.; Kondo, H.; Murota, K. An experimental study on transpedicular screw fixation in relation to osteoporosis of the lumbar spine. *Spine* **1991**, *16*, 1335-1341.
13. Frankel, B.M.; Jones, T.; Wang, C. Segmental polymethylmethacrylate-augmented pedicle screw fixation in patients with bone softening caused

by osteoporosis and metastatic tumor involvement: A clinical evaluation. *Neurosurgery* **2007**, *61*, 531-537; discussion 537-538.

14. Brunner, F.; Sommer, C.; Bahrs, C.; Heuwinkel, R.; Hafner, C.; Rillmann, P.; Kohut, G.; Ekelund, A.; Muller, M.; Audige, L., *et al.* Open reduction and internal fixation of proximal humerus fractures using a proximal humeral locked plate: A prospective multicenter analysis. *Journal of orthopaedic trauma* **2009**, *23*, 163-172.
15. Krappinger, D.; Bizzotto, N.; Riedmann, S.; Kammerlander, C.; Hengg, C.; Kralinger, F.S. Predicting failure after surgical fixation of proximal humerus fractures. *Injury* **2011**, *42*, 1283-1288.
16. Friedman, S.M.; Mendelson, D.A.; Bingham, K.W.; Kates, S.L. Impact of a comanaged geriatric fracture center on short-term hip fracture outcomes. *Archives of internal medicine* **2009**, *169*, 1712-1717.
17. Kammerlander, C.; Erhart, S.; Doshi, H.; Gosch, M.; Blauth, M. Principles of osteoporotic fracture treatment. *Best practice & research. Clinical rheumatology* **2013**, *27*, 757-769.
18. Kammerlander, C.; Zegg, M.; Schmid, R.; Gosch, M.; Luger, T.J.; Blauth, M. Fragility fractures requiring special consideration: Vertebral fractures. *Clinics in geriatric medicine* **2014**, *30*, 361-372.
19. Abrahamsen, B.; van Staa, T.; Ariely, R.; Olson, M.; Cooper, C. Excess mortality following hip fracture: A systematic epidemiological review. *Osteoporosis international : a journal established as result of cooperation between the European Foundation for Osteoporosis and the National Osteoporosis Foundation of the USA* **2009**, *20*, 1633-1650.
20. Kammerlander, C.; Gosch, M.; Kammerlander-Knauer, U.; Luger, T.J.; Blauth, M.; Roth, T. Long-term functional outcome in geriatric hip fracture patients. *Archives of orthopaedic and trauma surgery* **2011**, *131*, 1435-1444.
21. Lindner, T.; Kanakaris, N.K.; Marx, B.; Cockbain, A.; Kontakis, G.; Giannoudis, P.V. Fractures of the hip and osteoporosis: The role of bone substitutes. *The Journal of bone and joint surgery. British volume* **2009**, *91*, 294-303.
22. Erhart, S.; Kammerlander, C.; El-Attal, R.; Schmoelz, W. Is augmentation a possible salvage procedure after lateral migration of the proximal femur nail antirotation? *Archives of orthopaedic and trauma surgery* **2012**, *132*, 1577-1581.
23. Deckelmann, S.; Schwyn, R.; Van der Pol, B.; Windolf, M.; Heini, P.F.; Benneker, L.M. Densiprobe spine: A novel instrument for intraoperative measurement of bone density in transpedicular screw fixation. *Spine* **2010**, *35*, 607-612.
24. Suhm, N.; Haenni, M.; Schwyn, R.; Hirschmann, M.; Muller, A.M. Quantification of bone strength by intraoperative torque measurement:

A technical note. *Archives of orthopaedic and trauma surgery* **2008**, *128*, 613-620.

25. Brianza, S.; Roderer, G.; Schiuma, D.; Schwyn, R.; Scola, A.; Gebhard, F.; Tami, A.E. Where do locking screws purchase in the humeral head? *Injury* **2012**, *43*, 850-855.
26. Frankel, B.M.; D'Agostino, S.; Wang, C. A biomechanical cadaveric analysis of polymethylmethacrylate-augmented pedicle screw fixation. *Journal of neurosurgery. Spine* **2007**, *7*, 47-53.
27. Chen, L.H.; Tai, C.L.; Lai, P.L.; Lee, D.M.; Tsai, T.T.; Fu, T.S.; Niu, C.C.; Chen, W.J. Pullout strength for cannulated pedicle screws with bone cement augmentation in severely osteoporotic bone: Influences of radial hole and pilot hole tapping. *Clinical biomechanics* **2009**, *24*, 613-618.
28. Unger, S.; Erhart, S.; Kralinger, F.; Blauth, M.; Schmoelz, W. The effect of in situ augmentation on implant anchorage in proximal humeral head fractures. *Injury* **2012**, *43*, 1759-1763.
29. Erhart, S.; Schmoelz, W.; Blauth, M.; Lenich, A. Biomechanical effect of bone cement augmentation on rotational stability and pull-out strength of the proximal femur nail antirotation. *Injury* **2011**, *42*, 1322-1327.
30. Sermon, A.; Boner, V.; Boger, A.; Schwieger, K.; Boonen, S.; Broos, P.L.; Richards, R.G.; Windolf, M. Potential of polymethylmethacrylate cement-augmented helical proximal femoral nail antirotation blades to improve implant stability--a biomechanical investigation in human cadaveric femoral heads. *The journal of trauma and acute care surgery* **2012**, *72*, E54-59.
31. Fliri, L.; Lenz, M.; Boger, A.; Windolf, M. Ex vivo evaluation of the polymerization temperatures during cement augmentation of proximal femoral nail antirotation blades. *The journal of trauma and acute care surgery* **2012**, *72*, 1098-1101.
32. Kammerlander, C.; Gebhard, F.; Meier, C.; Lenich, A.; Linhart, W.; Clasbrummel, B.; Neubauer-Gartzke, T.; Garcia-Alonso, M.; Pavelka, T.; Blauth, M. Standardised cement augmentation of the pfna using a perforated blade: A new technique and preliminary clinical results. A prospective multicentre trial. *Injury* **2011**, *42*, 1484-1490.
33. Roderer, G.; Scola, A.; Schmolz, W.; Gebhard, F.; Windolf, M.; Hofmann-Fliri, L. Biomechanical in vitro assessment of screw augmentation in locked plating of proximal humerus fractures. *Injury* **2013**, *44*, 1327-1332.
34. Becker, S.; Chavanne, A.; Spitaler, R.; Kropik, K.; Aigner, N.; Ogon, M.; Redl, H. Assessment of different screw augmentation techniques and screw designs in osteoporotic spines. *European spine journal : official publication of the European Spine Society, the European Spinal Deformity Society, and the European Section of the Cervical Spine Research Society* **2008**, *17*, 1462-1469.

35. Burval, D.J.; McLain, R.F.; Milks, R.; Inceoglu, S. Primary pedicle screw augmentation in osteoporotic lumbar vertebrae: Biomechanical analysis of pedicle fixation strength. *Spine* **2007**, *32*, 1077-1083.
36. Krappinger, D.; Kastenberger, T.J.; Schmid, R. [augmented posterior instrumentation for the treatment of osteoporotic vertebral body fractures]. *Operative Orthopadie und Traumatologie* **2012**, *24*, 4-12.
37. Simmermacher, R.K.; Ljungqvist, J.; Bail, H.; Hockertz, T.; Vochteloo, A.J.; Ochs, U.; Werken, C.; studygroup, A.P. The new proximal femoral nail antirotation (pfna) in daily practice: Results of a multicentre clinical study. *Injury* **2008**, *39*, 932-939.
38. Kathrein, S.; Kralinger, F.; Blauth, M.; Schmoelz, W. Biomechanical comparison of an angular stable plate with augmented and non-augmented screws in a newly developed shoulder test bench. *Clinical biomechanics* **2013**, *28*, 273-277.
39. Bajammal, S.S.; Zlowodzki, M.; Lelwica, A.; Tornetta, P., 3rd; Einhorn, T.A.; Buckley, R.; Leighton, R.; Russell, T.A.; Larsson, S.; Bhandari, M. The use of calcium phosphate bone cement in fracture treatment. A meta-analysis of randomized trials. *The Journal of bone and joint surgery. American volume* **2008**, *90*, 1186-1196.
40. Moore, W.R.; Graves, S.E.; Bain, G.I. Synthetic bone graft substitutes. *ANZ journal of surgery* **2001**, *71*, 354-361.
41. Arrington, E.D.; Smith, W.J.; Chambers, H.G.; Bucknell, A.L.; Davino, N.A. Complications of iliac crest bone graft harvesting. *Clinical orthopaedics and related research* **1996**, 300-309.
42. Silber, J.S.; Anderson, D.G.; Daffner, S.D.; Brislin, B.T.; Leland, J.M.; Hilibrand, A.S.; Vaccaro, A.R.; Albert, T.J. Donor site morbidity after anterior iliac crest bone harvest for single-level anterior cervical discectomy and fusion. *Spine* **2003**, *28*, 134-139.
43. Russell, T.A.; Leighton, R.K.; Alpha, B.S.M.T.P.F.S.G. Comparison of autogenous bone graft and endothermic calcium phosphate cement for defect augmentation in tibial plateau fractures. A multicenter, prospective, randomized study. *The Journal of bone and joint surgery. American volume* **2008**, *90*, 2057-2061.
44. Keating, J.F.; Hajducka, C.L.; Harper, J. Minimal internal fixation and calcium-phosphate cement in the treatment of fractures of the tibial plateau. A pilot study. *The Journal of bone and joint surgery. British volume* **2003**, *85*, 68-73.
45. Lobenhoffer, P.; Gerich, T.; Witte, F.; Tscherne, H. Use of an injectable calcium phosphate bone cement in the treatment of tibial plateau fractures: A prospective study of twenty-six cases with twenty-month mean follow-up. *Journal of orthopaedic trauma* **2002**, *16*, 143-149.
46. Schildhauer, T.A.; Bauer, T.W.; Josten, C.; Muhr, G. Open reduction and augmentation of internal fixation with an injectable skeletal cement for

the treatment of complex calcaneal fractures. *Journal of orthopaedic trauma* **2000**, *14*, 309-317.

47. Thordarson, D.B.; Bollinger, M. Srs cancellous bone cement augmentation of calcaneal fracture fixation. *Foot & ankle international* **2005**, *26*, 347-352.
48. Barr, J.D.; Barr, M.S.; Lemley, T.J.; McCann, R.M. Percutaneous vertebroplasty for pain relief and spinal stabilization. *Spine* **2000**, *25*, 923-928.
49. Deramond, H.; Depriester, C.; Galibert, P.; Le Gars, D. Percutaneous vertebroplasty with polymethylmethacrylate. Technique, indications, and results. *Radiologic clinics of North America* **1998**, *36*, 533-546.
50. Garfin, S.R.; Yuan, H.A.; Reiley, M.A. New technologies in spine: Kyphoplasty and vertebroplasty for the treatment of painful osteoporotic compression fractures. *Spine* **2001**, *26*, 1511-1515.
51. Lieberman, I.H.; Dudeney, S.; Reinhardt, M.K.; Bell, G. Initial outcome and efficacy of "kyphoplasty" in the treatment of painful osteoporotic vertebral compression fractures. *Spine* **2001**, *26*, 1631-1638.
52. Fourney, D.R.; Schomer, D.F.; Nader, R.; Chlan-Fourney, J.; Suki, D.; Ahrar, K.; Rhines, L.D.; Gokaslan, Z.L. Percutaneous vertebroplasty and kyphoplasty for painful vertebral body fractures in cancer patients. *Journal of neurosurgery* **2003**, *98*, 21-30.
53. Weill, A.; Chiras, J.; Simon, J.M.; Rose, M.; Sola-Martinez, T.; Enkaoua, E. Spinal metastases: Indications for and results of percutaneous injection of acrylic surgical cement. *Radiology* **1996**, *199*, 241-247.
54. Mathis, J.M.; Barr, J.D.; Belkoff, S.M.; Barr, M.S.; Jensen, M.E.; Deramond, H. Percutaneous vertebroplasty: A developing standard of care for vertebral compression fractures. *AJNR. American journal of neuroradiology* **2001**, *22*, 373-381.
55. Lieberman, I.; Reinhardt, M.K. Vertebroplasty and kyphoplasty for osteolytic vertebral collapse. *Clinical orthopaedics and related research* **2003**, S176-186.
56. Galibert, P.; Deramond, H.; Rosat, P.; Le Gars, D. [preliminary note on the treatment of vertebral angioma by percutaneous acrylic vertebroplasty]. *Neuro-Chirurgie* **1987**, *33*, 166-168.
57. Heini, P.F.; Walchli, B.; Berlemann, U. Percutaneous transpedicular vertebroplasty with pmma: Operative technique and early results. A prospective study for the treatment of osteoporotic compression fractures. *European spine journal : official publication of the European Spine Society, the European Spinal Deformity Society, and the European Section of the Cervical Spine Research Society* **2000**, *9*, 445-450.
58. Tohmeh, A.G.; Mathis, J.M.; Fenton, D.C.; Levine, A.M.; Belkoff, S.M. Biomechanical efficacy of unipedicular versus bipedicular vertebroplasty

for the management of osteoporotic compression fractures. *Spine* **1999**, *24*, 1772-1776.

59. Lewis, G. Percutaneous vertebroplasty and kyphoplasty for the stand-alone augmentation of osteoporosis-induced vertebral compression fractures: Present status and future directions. *Journal of biomedical materials research. Part B, Applied biomaterials* **2007**, *81*, 371-386.
60. Heini, P.F.; Orler, R. [vertebroplasty in severe osteoporosis. Technique and experience with multi-segment injection]. *Der Orthopade* **2004**, *33*, 22-30.
61. Bohner, M.; Gasser, B.; Baroud, G.; Heini, P. Theoretical and experimental model to describe the injection of a polymethylmethacrylate cement into a porous structure. *Biomaterials* **2003**, *24*, 2721-2730.
62. Breusch, S.; Heisel, C.; Muller, J.; Borchers, T.; Mau, H. Influence of cement viscosity on cement interdigitation and venous fat content under in vivo conditions: A bilateral study of 13 sheep. *Acta orthopaedica Scandinavica* **2002**, *73*, 409-415.
63. Phillips, F.M.; Todd Wetzel, F.; Lieberman, I.; Campbell-Hupp, M. An in vivo comparison of the potential for extravertebral cement leak after vertebroplasty and kyphoplasty. *Spine* **2002**, *27*, 2173-2178; discussion 2178-2179.
64. Weisskopf, M.; Ohnsorge, J.A.; Niethard, F.U. Intravertebral pressure during vertebroplasty and balloon kyphoplasty: An in vitro study. *Spine* **2008**, *33*, 178-182.
65. Bostrom, M.P.; Lane, J.M. Future directions. Augmentation of osteoporotic vertebral bodies. *Spine* **1997**, *22*, 38S-42S.
66. Voggenreiter, G. Balloon kyphoplasty is effective in deformity correction of osteoporotic vertebral compression fractures. *Spine* **2005**, *30*, 2806-2812.
67. Gaitanis, I.N.; Hadjipavlou, A.G.; Katonis, P.G.; Tzermiadianos, M.N.; Pasku, D.S.; Patwardhan, A.G. Balloon kyphoplasty for the treatment of pathological vertebral compressive fractures. *European spine journal : official publication of the European Spine Society, the European Spinal Deformity Society, and the European Section of the Cervical Spine Research Society* **2005**, *14*, 250-260.
68. Kobayashi, N.; Numaguchi, Y.; Fuwa, S.; Uemura, A.; Matsusako, M.; Okajima, Y.; Ishiyama, M.; Takahashi, O. Prophylactic vertebroplasty: Cement injection into non-fractured vertebral bodies during percutaneous vertebroplasty. *Academic radiology* **2009**, *16*, 136-143.
69. Pneumaticos, S.G.; Triantafyllopoulos, G.K.; Evangelopoulos, D.S.; Hipp, J.A.; Heggeness, M.H. Effect of vertebroplasty on the compressive strength of vertebral bodies. *The spine journal : official journal of the North American Spine Society* **2013**, *13*, 1921-1927.

70. Tancioni, F.; Lorenzetti, M.; Navarria, P.; Nozza, A.; Castagna, L.; Gaetani, P.; Aimar, E.; Levi, D.; Di Ieva, A.; Pisano, P., *et al.* Vertebroplasty for pain relief and spinal stabilization in multiple myeloma. *Neurological sciences : official journal of the Italian Neurological Society and of the Italian Society of Clinical Neurophysiology* **2010**, *31*, 151-157.
71. Kebaish, K.M.; Martin, C.T.; O'Brien, J.R.; LaMotta, I.E.; Voros, G.D.; Belkoff, S.M. Use of vertebroplasty to prevent proximal junctional fractures in adult deformity surgery: A biomechanical cadaveric study. *The spine journal : official journal of the North American Spine Society* **2013**, *13*, 1897-1903.
72. Lewis, G. Injectable bone cements for use in vertebroplasty and kyphoplasty: State-of-the-art review. *Journal of biomedical materials research. Part B, Applied biomaterials* **2006**, *76*, 456-468.
73. Lewis, G. Viscoelastic properties of injectable bone cements for orthopaedic applications: State-of-the-art review. *Journal of biomedical materials research. Part B, Applied biomaterials* **2011**, *98*, 171-191.
74. Jaeblon, T. Polymethylmethacrylate: Properties and contemporary uses in orthopaedics. *The Journal of the American Academy of Orthopaedic Surgeons* **2010**, *18*, 297-305.
75. Kuehn, K.D.; Ege, W.; Gopp, U. Acrylic bone cements: Mechanical and physical properties. *The Orthopedic clinics of North America* **2005**, *36*, 29-39, v-vi.
76. Boger, A.; Bohner, M.; Heini, P.; Verrier, S.; Schneider, E. Properties of an injectable low modulus pmma bone cement for osteoporotic bone. *Journal of biomedical materials research. Part B, Applied biomaterials* **2008**, *86*, 474-482.
77. Harper, E.J.; Bonfield, W. Tensile characteristics of ten commercial acrylic bone cements. *Journal of biomedical materials research* **2000**, *53*, 605-616.
78. Lieberman, I.H.; Togawa, D.; Kayanja, M.M. Vertebroplasty and kyphoplasty: Filler materials. *The spine journal : official journal of the North American Spine Society* **2005**, *5*, 305S-316S.
79. Uppin, A.A.; Hirsch, J.A.; Centenera, L.V.; Pfiefer, B.A.; Pazianos, A.G.; Choi, I.S. Occurrence of new vertebral body fracture after percutaneous vertebroplasty in patients with osteoporosis. *Radiology* **2003**, *226*, 119-124.
80. Trout, A.T.; Kallmes, D.F.; Kaufmann, T.J. New fractures after vertebroplasty: Adjacent fractures occur significantly sooner. *AJNR. American journal of neuroradiology* **2006**, *27*, 217-223.
81. Li, S.; Chien, S.; Branemark, P.I. Heat shock-induced necrosis and apoptosis in osteoblasts. *Journal of orthopaedic research : official publication of the Orthopaedic Research Society* **1999**, *17*, 891-899.

82. Deramond, H.; Wright, N.T.; Belkoff, S.M. Temperature elevation caused by bone cement polymerization during vertebroplasty. *Bone* **1999**, *25*, 17S-21S.
83. Gough, J.E.; Downes, S. Osteoblast cell death on methacrylate polymers involves apoptosis. *Journal of biomedical materials research* **2001**, *57*, 497-505.
84. Boger, A.; Bohner, M.; Heini, P.; Schwieger, K.; Schneider, E. Performance of vertebral cancellous bone augmented with compliant pmma under dynamic loads. *Acta biomaterialia* **2008**, *4*, 1688-1693.
85. Hernandez, L.; Gurruchaga, M.; Goni, I. Injectable acrylic bone cements for vertebroplasty based on a radiopaque hydroxyapatite. Formulation and rheological behaviour. *Journal of materials science. Materials in medicine* **2009**, *20*, 89-97.
86. Hernandez, L.; Parra, J.; Vazquez, B.; Bravo, A.L.; Collia, F.; Goni, I.; Gurruchaga, M.; San Roman, J. Injectable acrylic bone cements for vertebroplasty based on a radiopaque hydroxyapatite. Bioactivity and biocompatibility. *Journal of biomedical materials research. Part B, Applied biomaterials* **2009**, *88*, 103-114.
87. Gorst, N.J.; Perrie, Y.; Gbureck, U.; Hutton, A.L.; Hofmann, M.P.; Grover, L.M.; Barralet, J.E. Effects of fibre reinforcement on the mechanical properties of brushite cement. *Acta biomaterialia* **2006**, *2*, 95-102.
88. Buchanan, F.; Gallagher, L.; Jack, V.; Dunne, N. Short-fibre reinforcement of calcium phosphate bone cement. *Proceedings of the Institution of Mechanical Engineers. Part H, Journal of engineering in medicine* **2007**, *221*, 203-211.
89. Cassidy, C.; Jupiter, J.B.; Cohen, M.; Delli-Santi, M.; Fennell, C.; Leinberry, C.; Husband, J.; Ladd, A.; Seitz, W.R.; Constanz, B. Norian srs cement compared with conventional fixation in distal radial fractures. A randomized study. *The Journal of bone and joint surgery. American volume* **2003**, *85-A*, 2127-2137.
90. Robinson, C.M.; Page, R.S. Severely impacted valgus proximal humeral fractures. *The Journal of bone and joint surgery. American volume* **2004**, *86-A Suppl 1*, 143-155.
91. Peltier, L.F.; Bickel, E.Y.; Lillo, R.; Thein, M.S. The use of plaster of paris to fill defects in bone. *Annals of surgery* **1957**, *146*, 61-69.
92. Coetzee, A.S. Regeneration of bone in the presence of calcium sulfate. *Archives of otolaryngology* **1980**, *106*, 405-409.
93. Bell, W.H. Resorption characteristics of bone and bone substitutes. *Oral surgery, oral medicine, and oral pathology* **1964**, *17*, 650-657.
94. Peltier, L.F.; Jones, R.H. Treatment of unicameral bone cysts by curettage and packing with plaster-of-paris pellets. *The Journal of bone and joint surgery. American volume* **1978**, *60*, 820-822.

95. Kelly, C.M.; Wilkins, R.M.; Gitelis, S.; Hartjen, C.; Watson, J.T.; Kim, P.T. The use of a surgical grade calcium sulfate as a bone graft substitute: Results of a multicenter trial. *Clinical orthopaedics and related research* **2001**, 42-50.
96. Beuerlein, M.J.; McKee, M.D. Calcium sulfates: What is the evidence? *Journal of orthopaedic trauma* **2010**, *24 Suppl 1*, S46-51.
97. Sermon, A.; Hofmann-Fliri, L.; Richards, R.G.; Flamaing, J.; Windolf, M. Cement augmentation of hip implants in osteoporotic bone: How much cement is needed and where should it go? *Journal of orthopaedic research : official publication of the Orthopaedic Research Society* **2014**, *32*, 362-368.
98. Heini, P.F.; Berlemann, U. Bone substitutes in vertebroplasty. *European spine journal : official publication of the European Spine Society, the European Spinal Deformity Society, and the European Section of the Cervical Spine Research Society* **2001**, *10 Suppl 2*, S205-213.
99. Baroud, G.; Heini, P.; Nemes, J.; Bohner, M.; Ferguson, S.; Steffen, T. Biomechanical explanation of adjacent fractures following vertebroplasty. *Radiology* **2003**, *229*, 606-607; author reply 607-608.
100. Schmidt, R.; Cakir, B.; Mattes, T.; Wegener, M.; Puhl, W.; Richter, M. Cement leakage during vertebroplasty: An underestimated problem? *European spine journal : official publication of the European Spine Society, the European Spinal Deformity Society, and the European Section of the Cervical Spine Research Society* **2005**, *14*, 466-473.
101. Yeom, J.S.; Kim, W.J.; Choy, W.S.; Lee, C.K.; Chang, B.S.; Kang, J.W. Leakage of cement in percutaneous transpedicular vertebroplasty for painful osteoporotic compression fractures. *The Journal of bone and joint surgery. British volume* **2003**, *85*, 83-89.
102. Jang, J.S.; Lee, S.H.; Jung, S.K. Pulmonary embolism of polymethylmethacrylate after percutaneous vertebroplasty: A report of three cases. *Spine* **2002**, *27*, E416-418.
103. Yoo, K.Y.; Jeong, S.W.; Yoon, W.; Lee, J. Acute respiratory distress syndrome associated with pulmonary cement embolism following percutaneous vertebroplasty with polymethylmethacrylate. *Spine* **2004**, *29*, E294-297.
104. Harrington, K.D. Major neurological complications following percutaneous vertebroplasty with polymethylmethacrylate : A case report. *The Journal of bone and joint surgery. American volume* **2001**, *83-A*, 1070-1073.
105. Ratliff, J.; Nguyen, T.; Heiss, J. Root and spinal cord compression from methylmethacrylate vertebroplasty. *Spine* **2001**, *26*, E300-302.
106. Hulme, P.A.; Krebs, J.; Ferguson, S.J.; Berlemann, U. Vertebroplasty and kyphoplasty: A systematic review of 69 clinical studies. *Spine* **2006**, *31*, 1983-2001.

107. Herndon, J.H.; Bechtol, C.O.; Crickenberger, D.P. Fat embolism during total hip replacement. A prospective study. *The Journal of bone and joint surgery. American volume* **1974**, *56*, 1350-1362.
108. Fahmy, N.R.; Chandler, H.P.; Danylchuk, K.; Matta, E.B.; Sunder, N.; Siliski, J.M. Blood-gas and circulatory changes during total knee replacement. Role of the intramedullary alignment rod. *The Journal of bone and joint surgery. American volume* **1990**, *72*, 19-26.
109. Pell, A.C.; Christie, J.; Keating, J.F.; Sutherland, G.R. The detection of fat embolism by transoesophageal echocardiography during reamed intramedullary nailing. A study of 24 patients with femoral and tibial fractures. *The Journal of bone and joint surgery. British volume* **1993**, *75*, 921-925.
110. Takahashi, S.; Kitagawa, H.; Ishii, T. Intraoperative pulmonary embolism during spinal instrumentation surgery. A prospective study using transoesophageal echocardiography. *The Journal of bone and joint surgery. British volume* **2003**, *85*, 90-94.
111. Syed, M.I.; Jan, S.; Patel, N.A.; Shaikh, A.; Marsh, R.A.; Stewart, R.V. Fatal fat embolism after vertebroplasty: Identification of the high-risk patient. *AJNR. American journal of neuroradiology* **2006**, *27*, 343-345.
112. Chen, H.L.; Wong, C.S.; Ho, S.T.; Chang, F.L.; Hsu, C.H.; Wu, C.T. A lethal pulmonary embolism during percutaneous vertebroplasty. *Anesth Analg* **2002**, *95*, 1060-1062, table of contents.
113. Murphy, P.; Edelist, G.; Byrick, R.J.; Kay, J.C.; Mullen, J.B. Relationship of fat embolism to haemodynamic and echocardiographic changes during cemented arthroplasty. *Canadian journal of anaesthesia = Journal canadien d'anesthesie* **1997**, *44*, 1293-1300.
114. Aebli, N.; Schwenke, D.; Davis, G.; Hii, T.; Theis, J.C.; Krebs, J. Polymethylmethacrylate causes prolonged pulmonary hypertension during fat embolism: A study in sheep. *Acta orthopaedica* **2005**, *76*, 904-911.
115. Colonna, D.M.; Kilgus, D.; Brown, W.; Challa, V.; Stump, D.A.; Moody, D.M. Acute brain fat embolization occurring after total hip arthroplasty in the absence of a patent foramen ovale. *Anesthesiology* **2002**, *96*, 1027-1029.
116. Lewis, G. Properties of acrylic bone cement: State of the art review. *Journal of biomedical materials research* **1997**, *38*, 155-182.
117. Boner, V.; Kuhn, P.; Mendel, T.; Gisep, A. Temperature evaluation during pmma screw augmentation in osteoporotic bone--an in vitro study about the risk of thermal necrosis in human femoral heads. *Journal of biomedical materials research. Part B, Applied biomaterials* **2009**, *90*, 842-848.

118. Granchi, D.; Stea, S.; Ciapetti, G.; Savarino, L.; Cavedagna, D.; Pizzoferrato, A. In vitro effects of bone cements on the cell cycle of osteoblast-like cells. *Biomaterials* **1995**, *16*, 1187-1192.
119. Lu, J.X.; Huang, Z.W.; Tropiano, P.; Clouet D'Orval, B.; Remusat, M.; Dejou, J.; Proust, J.P.; Poitout, D. Human biological reactions at the interface between bone tissue and polymethylmethacrylate cement. *Journal of materials science. Materials in medicine* **2002**, *13*, 803-809.
120. Nussbaum, D.A.; Gailloud, P.; Murphy, K. A review of complications associated with vertebroplasty and kyphoplasty as reported to the food and drug administration medical device related web site. *Journal of vascular and interventional radiology : JVIR* **2004**, *15*, 1185-1192.
121. Kalteis, T.; Luring, C.; Gugler, G.; Zysk, S.; Caro, W.; Handel, M.; Grifka, J. [acute tissue toxicity of pmma bone cements]. *Zeitschrift fur Orthopadie und ihre Grenzgebiete* **2004**, *142*, 666-672.
122. Lunt, M.; O'Neill, T.W.; Felsenberg, D.; Reeve, J.; Kanis, J.A.; Cooper, C.; Silman, A.J.; European Prospective Osteoporosis Study, G. Characteristics of a prevalent vertebral deformity predict subsequent vertebral fracture: Results from the european prospective osteoporosis study (epos). *Bone* **2003**, *33*, 505-513.
123. Kulcsar, Z.; Marosfoi, M.; Berentei, Z.; Veres, R.; Nyary, I.; Szikora, I. [frequency of adjacent vertebral fractures following percutaneous vertebroplasty]. *Orvosi hetilap* **2009**, *150*, 1744-1748.
124. Baroud, G.; Nemes, J.; Ferguson, S.J.; Steffen, T. Material changes in osteoporotic human cancellous bone following infiltration with acrylic bone cement for a vertebral cement augmentation. *Computer methods in biomechanics and biomedical engineering* **2003**, *6*, 133-139.
125. Baroud, G.; Nemes, J.; Heini, P.; Steffen, T. Load shift of the intervertebral disc after a vertebroplasty: A finite-element study. *European spine journal : official publication of the European Spine Society, the European Spinal Deformity Society, and the European Section of the Cervical Spine Research Society* **2003**, *12*, 421-426.
126. Davidson, M.K.; Lindsey, J.R.; Davis, J.K. Requirements and selection of an animal model. *Israel journal of medical sciences* **1987**, *23*, 551-555.
127. Beamer, W.G.; Donahue, L.R.; Rosen, C.J.; Baylink, D.J. Genetic variability in adult bone density among inbred strains of mice. *Bone* **1996**, *18*, 397-403.
128. Newman, E.; Turner, A.S.; Wark, J.D. The potential of sheep for the study of osteopenia: Current status and comparison with other animal models. *Bone* **1995**, *16*, 277S-284S.
129. Turner, R.T.; Maran, A.; Lotinun, S.; Hefferan, T.; Evans, G.L.; Zhang, M.; Sibonga, J.D. Animal models for osteoporosis. *Rev Endocr Metab Disord* **2001**, *2*, 117-127.

130. Kalu, D.N. The ovariectomized rat model of postmenopausal bone loss. *Bone and mineral* **1991**, *15*, 175-191.
131. Namkung-Matthai, H.; Appleyard, R.; Jansen, J.; Hao Lin, J.; Maastricht, S.; Swain, M.; Mason, R.S.; Murrell, G.A.; Diwan, A.D.; Diamond, T. Osteoporosis influences the early period of fracture healing in a rat osteoporotic model. *Bone* **2001**, *28*, 80-86.
132. Velasco, O.; James, A.W.; Asatrian, G.; Ajalat, M.; Pritchard, T.; Novshadian, S.; Murthy, A.; Bayani, G.; Zhang, X.; Ting, K.*, et al.* High resolution x-ray: A reliable approach for quantifying osteoporosis in a rodent model. *BioResearch open access* **2014**, *3*, 192-196.
133. Gallagher, A.; Chambers, T.J.; Tobias, J.H. The estrogen antagonist ici 182,780 reduces cancellous bone volume in female rats. *Endocrinology* **1993**, *133*, 2787-2791.
134. Turner, R.T.; Bell, N.H. The effects of immobilization on bone histomorphometry in rats. *Journal of bone and mineral research : the official journal of the American Society for Bone and Mineral Research* **1986**, *1*, 399-407.
135. Thompson, D.D.; Rodan, G.A. Indomethacin inhibition of tenotomy-induced bone resorption in rats. *Journal of bone and mineral research : the official journal of the American Society for Bone and Mineral Research* **1988**, *3*, 409-414.
136. Morey, E.R.; Baylink, D.J. Inhibition of bone formation during space flight. *Science* **1978**, *201*, 1138-1141.
137. Sampson, H.W.; Perks, N.; Champney, T.H.; DeFee, B., 2nd. Alcohol consumption inhibits bone growth and development in young actively growing rats. *Alcoholism, clinical and experimental research* **1996**, *20*, 1375-1384.
138. Wronski, T.J.; Dann, L.M.; Scott, K.S.; Cintron, M. Long-term effects of ovariectomy and aging on the rat skeleton. *Calcified tissue international* **1989**, *45*, 360-366.
139. Aerssens, J.; Boonen, S.; Lowet, G.; Dequeker, J. Interspecies differences in bone composition, density, and quality: Potential implications for in vivo bone research. *Endocrinology* **1998**, *139*, 663-670.
140. Bloebaum, R.D.; Ota, D.T.; Skedros, J.G.; Mantas, J.P. Comparison of human and canine external femoral morphologies in the context of total hip replacement. *Journal of biomedical materials research* **1993**, *27*, 1149-1159.
141. Stulberg, B.N.; Watson, J.T.; Stulberg, S.D.; Bauer, T.W.; Manley, M.T. A new model to assess tibial fixation in knee arthroplasty. I. Histologic and roentgenographic results. *Clinical orthopaedics and related research* **1991**, 288-302.
142. Yamaura, M.; Nakamura, T.; Nagai, Y.; Yoshihara, A.; Suzuki, K. Reduced mechanical competence of bone by ovariectomy and its

preservation with 24r,25-dihydroxyvitamin d3 administration in beagles. *Calcified tissue international* **1993**, *52*, 49-56.

143. Pearce, A.I.; Richards, R.G.; Milz, S.; Schneider, E.; Pearce, S.G. Animal models for implant biomaterial research in bone: A review. *European cells & materials* **2007**, *13*, 1-10.
144. Turner, A.S. Animal models of osteoporosis--necessity and limitations. *European cells & materials* **2001**, *1*, 66-81.
145. El-Warrak, A.O.; Olmstead, M.; Schneider, R.; Meinel, L.; Bettschart-Wolfisberger, R.; Akens, M.K.; Auer, J.; von Rechenberg, B. An experimental animal model of aseptic loosening of hip prostheses in sheep to study early biochemical changes at the interface membrane. *BMC musculoskeletal disorders* **2004**, *5*, 7.
146. Nuss, K.M.; Auer, J.A.; Boos, A.; von Rechenberg, B. An animal model in sheep for biocompatibility testing of biomaterials in cancellous bones. *BMC musculoskeletal disorders* **2006**, *7*, 67.
147. Plecko, M.; Sievert, C.; Andermatt, D.; Frigg, R.; Kronen, P.; Klein, K.; Stubinger, S.; Nuss, K.; Burki, A.; Ferguson, S., *et al.* Osseointegration and biocompatibility of different metal implants--a comparative experimental investigation in sheep. *BMC musculoskeletal disorders* **2012**, *13*, 32.
148. Ernst, S.; Stubinger, S.; Schupbach, P.; Sidler, M.; Klein, K.; Ferguson, S.J.; von Rechenberg, B. Comparison of two dental implant surface modifications on implants with same macrodesign: An experimental study in the pelvic sheep model. *Clinical oral implants research* **2014**.
149. Plecko, M.; Lagerpusch, N.; Andermatt, D.; Frigg, R.; Koch, R.; Sidler, M.; Kronen, P.; Klein, K.; Nuss, K.; Burki, A., *et al.* The dynamisation of locking plate osteosynthesis by means of dynamic locking screws (dls)-an experimental study in sheep. *Injury* **2013**, *44*, 1346-1357.
150. Siebenrock, K.A.; Fiechter, R.; Tannast, M.; Mamisch, T.C.; von Rechenberg, B. Experimentally induced cam impingement in the sheep hip. *Journal of orthopaedic research : official publication of the Orthopaedic Research Society* **2013**, *31*, 580-587.
151. Gerber, C.; Meyer, D.C.; Von Rechenberg, B.; Hoppeler, H.; Frigg, R.; Farshad, M. Rotator cuff muscles lose responsiveness to anabolic steroids after tendon tear and musculotendinous retraction: An experimental study in sheep. *The American journal of sports medicine* **2012**, *40*, 2454-2461.
152. Wieser, K.; Farshad, M.; Meyer, D.C.; Conze, P.; von Rechenberg, B.; Gerber, C. Tendon response to pharmaco-mechanical stimulation of the chronically retracted rotator cuff in sheep. *Knee surgery, sports traumatology, arthroscopy : official journal of the ESSKA* **2014**.
153. Newton, B.I.; Cooper, R.C.; Gilbert, J.A.; Johnson, R.B.; Zardiackas, L.D. The ovariectomized sheep as a model for human bone loss. *Journal of comparative pathology* **2004**, *130*, 323-326.

154. Augat, P.; Schorlemmer, S.; Gohl, C.; Iwabu, S.; Ignatius, A.; Claes, L. Glucocorticoid-treated sheep as a model for osteopenic trabecular bone in biomaterials research. *Journal of biomedical materials research. Part A* **2003**, *66*, 457-462.
155. Macleay, J.M.; Olson, J.D.; Turner, A.S. Effect of dietary-induced metabolic acidosis and ovariectomy on bone mineral density and markers of bone turnover. *Journal of bone and mineral metabolism* **2004**, *22*, 561-568.
156. Lill, C.A.; Fluegel, A.K.; Schneider, E. Effect of ovariectomy, malnutrition and glucocorticoid application on bone properties in sheep: A pilot study. *Osteoporosis international : a journal established as result of cooperation between the European Foundation for Osteoporosis and the National Osteoporosis Foundation of the USA* **2002**, *13*, 480-486.
157. Schorlemmer, S.; Gohl, C.; Iwabu, S.; Ignatius, A.; Claes, L.; Augat, P. Glucocorticoid treatment of ovariectomized sheep affects mineral density, structure, and mechanical properties of cancellous bone. *Journal of bone and mineral research : the official journal of the American Society for Bone and Mineral Research* **2003**, *18*, 2010-2015.
158. Zarrinkalam, M.R.; Beard, H.; Schultz, C.G.; Moore, R.J. Validation of the sheep as a large animal model for the study of vertebral osteoporosis. *European spine journal : official publication of the European Spine Society, the European Spinal Deformity Society, and the European Section of the Cervical Spine Research Society* **2009**, *18*, 244-253.
159. Ding, M.; Cheng, L.; Bollen, P.; Schwarz, P.; Overgaard, S. Glucocorticoid induced osteopenia in cancellous bone of sheep: Validation of large animal model for spine fusion and biomaterial research. *Spine* **2010**, *35*, 363-370.
160. Sigrist, I.M.; Gerhardt, C.; Alini, M.; Schneider, E.; Egermann, M. The long-term effects of ovariectomy on bone metabolism in sheep. *Journal of bone and mineral metabolism* **2007**, *25*, 28-35.
161. Chavassieux, P.; Pastoureau, P.; Boivin, G.; Chapuy, M.C.; Delmas, P.D.; Meunier, P.J. Dose effects on ewe bone remodeling of short-term sodium fluoride administration--a histomorphometric and biochemical study. *Bone* **1991**, *12*, 421-427.
162. Turner, A.S.; Alvis, M.; Myers, W.; Stevens, M.L.; Lundy, M.W. Changes in bone mineral density and bone-specific alkaline phosphatase in ovariectomized ewes. *Bone* **1995**, *17*, 395S-402S.
163. Klein, K.; Zamparo, E.; Kronen, P.W.; Kampf, K.; Makara, M.; Steffen, T.; von Rechenberg, B. Bone augmentation for cancellous bone-development of a new animal model. *BMC musculoskeletal disorders* **2013**, *14*, 200.
164. Klein, K.; Schense, J.; Kronen, P.; Fouche, N.; Makara, M.; Kämpf, K.; Steffen, T.; von Rechenberg, B. Feasibility study of a standardized novel

animal model for cervical vertebral augmentation in sheep using a pth derivate bioactive material. *Veterinary Sciences* **2014**, *1*, 96-120.

165. Aebli, N.; Krebs, J.; Davis, G.; Walton, M.; Williams, M.J.; Theis, J.C. Fat embolism and acute hypotension during vertebroplasty: An experimental study in sheep. *Spine* **2002**, *27*, 460-466.
166. Benneker, L.M.; Gisep, A.; Krebs, J.; Boger, A.; Heini, P.F.; Boner, V. Development of an in vivo experimental model for percutaneous vertebroplasty in sheep. *Vet Comp Orthop Traumatol* **2012**, *25*, 173-177.
167. Krebs, J.; Ferguson, S.J.; Hoerstrup, S.P.; Goss, B.G.; Haeberli, A.; Aebli, N. Influence of bone marrow fat embolism on coagulation activation in an ovine model of vertebroplasty. *The Journal of bone and joint surgery. American volume* **2008**, *90*, 349-356.
168. Krebs, J.; Ferguson, S.J.; Nuss, K.; Leskosek, B.; Hoerstrup, S.P.; Goss, B.G.; Shaw, S.; Aebli, N. Plasma levels of endothelin-1 after a pulmonary embolism of bone marrow fat. *Acta Anaesthesiol Scand* **2007**, *51*, 1107-1114.
169. Aebli, N.; Krebs, J.; Schwenke, D.; Davis, G.; Theis, J.C. Cardiovascular changes during multiple vertebroplasty with and without vent-hole: An experimental study in sheep. *Spine* **2003**, *28*, 1504-1511; discussion 1511-1502.
170. Turner, A.S. The sheep as a model for osteoporosis in humans. *Veterinary journal* **2002**, *163*, 232-239.
171. Galovich, L.A.; Perez-Higueras, A.; Altonaga, J.R.; Orden, J.M.; Barba, M.L.; Morillo, M.T. Biomechanical, histological and histomorphometric analyses of calcium phosphate cement compared to pmma for vertebral augmentation in a validated animal model. *European spine journal : official publication of the European Spine Society, the European Spinal Deformity Society, and the European Section of the Cervical Spine Research Society* **2011**, *20 Suppl 3*, 376-382.
172. Wilke, H.J.; Kettler, A.; Claes, L.E. Are sheep spines a valid biomechanical model for human spines? *Spine* **1997**, *22*, 2365-2374.
173. Wilke, H.J.; Kettler, A.; Wenger, K.H.; Claes, L.E. Anatomy of the sheep spine and its comparison to the human spine. *Anat Rec* **1997**, *247*, 542-555.
174. Schmidt, R.; Cakir, B.; Mattes, T.; Wegener, M.; Puhl, W.; Richter, M. Cement leakage during vertebroplasty: An underestimated problem? *European spine journal : official publication of the European Spine Society, the European Spinal Deformity Society, and the European Section of the Cervical Spine Research Society* **2005**, *14*, 466-473.
175. Manolagas, S.C. Birth and death of bone cells: Basic regulatory mechanisms and implications for the pathogenesis and treatment of osteoporosis. *Endocrine reviews* **2000**, *21*, 115-137.

CV and Publications

Personal/Contact Information

Name:	Karina Klein
Date/Place of Birth:	March 23, 1978 in Siegen, Germany
Nationality:	German
Address (office):	Musculoskeletal Research Unit, Vetsuisse Faculty University of Zurich Winterthurerstrasse 260, CH-8057 Zurich
Phone (office):	+41 44 63 58 864
E-Mail:	kklein@vetclinics.uzh.ch

Professional Experience

Apr 2009 – Sep 2014	PhD studies in the Musculoskeletal Research Unit, Vetsuisse Faculty, University of Zurich, Switzerland;
Aug 2006 – Jun 2008	Postgraduate Research in the Musculoskeletal Research Unit, Vetsuisse Faculty, University of Zurich, Switzerland; research on a comparative in vivo study of different hydrogels with variable pore structure (doctoral thesis)
Apr 2003 – Jul 2006	Medical assistant in small animal clinic, Dr. G. Winkler, Lohmar, Germany

Education

June 2008	Doctoral degree in Veterinary Medicine
March 2003	Diploma in Veterinary Medicine
Oct 1997 – Feb 2003	Studies in Veterinary Medicine
June 1997	German Matriculation Certificate (“Abitur”)

Publications

Ouellet JA, Fernand CE, Racloz G, **Klein K,** Richter H, Steffen T, Rechenberg BV. (2015). Evaluation of the modern Luque Trolley Construct for Treatment of Early Onset Scoliosis Using a Gliding Implant in an Immature Animal Model. J Spinal Disord. Tech. 2015 Feb 25 [epub ahead of print]

Richter H, Plecko M, Andermatt D, Frigg R, Kronen PW, **Klein K**, Nuss K, Fergusson SJ, Stöckle U, von Rechenberg B. (2015). Dynamization at the near cortex in locking plate osteosynthesis by means of dynamic locking screws: an experimental study of transverse tibial osteotomies in sheep. J Bine Joint Surg Am. 2915 Feb 4;97(3):208-15. Doi:10.2106/JBJS.M.00529.

Von Salis-Soglio M, Stübinger S, Sidler M, **Klein K**, Ferguson SJ, Kämpf K, Zlinszky K, Buchini S, Curno R, Péchy P, Aronsson BO, von Rechenberg B. (2014). A novel multi-phosphonate surface treatment of titanium dental implants: a study in sheep. *J Funct Biomater.* 2014 Sep 11;5(3):135-57. doi: 10.3390/jfb5030135.

Klein K, Schense J, Kronen PW, Fouche N, Makara m, Kämpf K, Steffen T, von Rechenberg B (2014). Feasibility Study of a Standardized Novel Animal Model for Cervical Vertebral Augmentation in Sheep Using a PTH Derivate Bioactive Material. *Vet. Sci.* 2014, *1*, 96-120; doi: 10.3390/vetsci1020096.

Sizarov A, de Bakker BS, **Klein K**, Ohlerth S (2014). Building foundations for transcatheter intervascular anastomoses: 3D anatomy oft he great vessels in large experimental animals. *Interact Cardiovasc Thorac Surg*. 2014 Jul 3. pii: ivu210.

Stübinger S, Waser J, Hefti T, Drechsler A, Sidler M, **Klein K**, von Rechenberg B, Schlottig F (2014). Evaluation of local cancellous bone amelioration by poly-l-dl-lactide copolymers to improve primary stability of dental implants: a biomechanical study in sheep. *Clin Oral Implants Res.* 2014 Jul 2. doi: 10.1111/clr.12445.

Ernst S, Stübinger S, Schüpbach P, Sidler M, **Klein K**, Ferguson SJ, von Rechenberg B (2014). Comparison of two dental implant surface modifications on implants with same macrodesign: an experimental study in the pelvic sheep model. *Clin Oral Implants Res.* 2014 May 21. doi: 10.1111/clr.12411.

Mallik AS, Nuss K, Kronen PW, **Klein K**, Karol A, von Rechenberg B, Rüfenacht DA, Wanke I, Kulcsár Z (2014). A new-generation, low-permeability flow diverting device for treatment of saccular aneurysms. *Eur Radiol.* 2014 Jan;24(1):12-8. doi: 10.1007/s00330-013-2970-3.

Klein K, Zamparo E, Kronen PW, Kämpf K, Makara M, Steffen T, von Rechenberg B (2013). Bone augmentation for cancellous bone- development of a new animal model. *BMC Musculoskelet Disord.* 2013 Jul 2;14:200. doi: 10.1186/1471-2474-14-200.

Stübinger S, Mosch I, Robotti P, Sidler M, **Klein K**, Ferguson SJ, von Rechenberg B (2013). Histological and biomechanical analysis of porous additive manufactured implants made by direct metal laser sintering: a pilot study in sheep. *J Biomed Mater Res B Appl Biomater*. 2013 Oct;101(7):1154-63. doi: 10.1002/jbm.b.32925.

Plecko M, Lagerpusch N, Andermatt D, Frigg R, Koch R, Sidler M, Kronen P, **Klein K**, Nuss K, Bürki A, Ferguson SJ, Stoeckle U, Auer JA, von Rechenberg B (2013). The dynamisation of locking plate osteosynthesis by means of dynamic locking screws (DLS)-an experimental study in sheep. *Injury.* 2013 Oct;44(10):1346-57. doi: 10.1016/j.injury.2012.10.022.

Plecko M, Sievert C, Andermatt D, Frigg R, Kronen P, **Klein K**, Stübinger S, Nuss K, Bürki A, Ferguson S, Stoeckle U, von Rechenberg B (2012). Osseointegration and biocompatibility of different metal implants--a comparative experimental investigation in sheep. *BMC Musculoskelet Disord.* 2012 Mar 8;13:32. doi: 10.1186/1471-2474-13-32.

Plecko M, Lagerpusch N, Pegel B, Andermatt D, Frigg R, Koch R, Sidler M, Kronen P, **Klein K**, Nuss K, Gedet P, Bürki A, Ferguson SJ, Stoeckle U, Auer JA, von Rechenberg B (2012). The influence of different osteosynthesis configurations with locking compression plates (LCP) on stability and fracture healing after an oblique 45° angle osteotomy. *Injury.* 2012 Jul;43(7):1041-51. doi: 10.1016/j.injury.2011.12.016.

von Plocki SC, Armbruster D, **Klein K**, Kämpf K, Zlinszky K, Hilbe M, Kronen P, Gruskin E, von Rechenberg B (2012). Biodegradable sleeves for metal implants to prevent implant-associated infection: an experimental in vivo study in sheep. *Vet Surg.* 2012 Apr;41(3):410-21. doi: 10.1111/j.1532-950X.2011.00943.x.

Schneider OD, Mohn D, Fuhrer R, **Klein K**, Kämpf K, Nuss KM, Sidler M, Zlinszky K, von Rechenberg B, Stark WJ (2011). Biocompatibility and Bone Formation of Flexible, Cotton Wool-like PLGA/Calcium Phosphate Nanocomposites in Sheep. *Open Orthop J.* 2011 Mar 16;5:63-71. doi: 10.2174/1874325001105010063.

Templin C, Meyer M, Müller MF, Djonov V, Hlushchuk R, Dimova I, Flueckiger S, Kronen P, Sidler M, **Klein K**, Nicholls F, Ghadri JR, Weber K, Paunovic D, Corti R, Hoerstrup SP, Lüscher TF, Landmesser U (2010). Coronary optical frequency domain imaging (OFDI) for in vivo evaluation of stent healing: comparison with light and electron microscopy. *Eur Heart J.* 2010 Jul;31(14):1792-801. doi: 10.1093/eurheartj/ehq168.

Conference presentations

January 2011	5th Graduate School Symposium, Bern, Switzerland "Bone augmentation for cancellous bone- development of a new animal model" (Poster)
February 2012	6th Graduate School Symposium, Bern, Switzerland "Bone augmentation for cancellous bone- using biomaterial composites as biomimetic agents" (Talk)

Declaration of Orginality

Last name, first name: Klein, Karina

Matriculation number: 06-728-299

I hereby declare that this thesis represents my original work and that I have used no other sources except as noted by citations.

All data, tables, figures and text citations, which have been reproduced from any other source, including the Internet, have been explicitly acknowledged as such.

I am aware that in case of non-compliance, the Senate is entitled to withdraw the doctorate degree awarded to me on the basis of the present thesis, in accordance with the "Statut der Universität Bern (Universitätsstatut; UniSt)", Art. 69, of 7 June 2011.

Place, date Zürich, 28.05.2015

Signature K. Kl